

IN SEARCH OF BIOMARKERS FOR COMPLEX 3D MICROTISSUE PHYSIOLOGY IN
VITRO – THE CASE FOR CYTOKINES

by

AMISH ASTHANA

(Under the Direction of William S. Kisaalita)

ABSTRACT

This study has been carried out to determine how the 3D microenvironment affects the complex functionality of the cells growing in it. The effect has been quantified in terms of albumin secretion from hepatic cells in this particular case to find which out of the three environmental cues (spatial, biophysical and biochemical) is the most dominant and which are redundant, if any. Inclusion of just the minimal essential cues would simplify the platform architecture making it cost effective and increasing its adaptability to the high throughput screening (HTS) format. Another objective is to find a biomarker associated with this physiological relevance which can act as an early indicator and diagnose if the tissue is on a trajectory toward physiological relevance or not. Equipped with the knowledge of the optimum microenvironment composition, one can engineer a 3D model that closely emulates the native tissue and would provide more predictive outcomes during the drug discovery and screening process.

INDEX WORDS: 3D cell culture, Microtissue, Drug discovery, Microenvironment, Polymer Scaffold, Biomaterials, Tissue engineering

IN SEARCH OF BIOMARKERS FOR COMPLEX 3D MICROTISSUE PHYSIOLOGY IN
VITRO – THE CASE FOR CYTOKINES

by

AMISH ASTHANA

B.TECH., Vellore Institute of Technology, India, 2008

A Dissertation Submitted to the Graduate Faculty of The University of Georgia in Partial
Fulfillment of the Requirements for the Degree

DOCTOR OF PHILOSOPHY

ATHENS, GEORGIA

2014

© 2014

Amish Asthana

All Rights Reserved

IN SEARCH OF BIOMARKERS FOR COMPLEX 3D MICROTISSUE PHYSIOLOGY IN
VITRO – THE CASE FOR CYTOKINES

by

AMISH ASTHANA

Major Professor:	William Kisaalita
Committee:	Jaroslava Halper
	David Blum
	Leidong Mao

Electronic Version Approved:

Julie Coffield
Interim Dean of the Graduate School
The University of Georgia
August 2014

TABLE OF CONTENTS

CHAPTER	Page
1 INTRODUCTION	1
1.1 The 3D Microenvironment	1
1.2 Complex Physiological Relevance and Three-Dimensionality Biomarkers.....	3
1.3 Specific Objectives	4
1.4 References.....	6
2 LITERATURE REVIEW: IN SEARCH OF BIOMARKERS FOR COMPLEX 3D MICROTISSUE PHYSIOLOGY IN VITRO – THE CASE FOR CYTOKINES	7
2.1 Abstract	8
2.2 Introduction.....	8
2.3 CPR and screening studies timing	11
2.4 Cohesivity: Microtissue formation and cytokine production.....	12
2.5 2D/3D culture comparative transcriptomic/proteomic up-regulation of cytokines	15
2.6 Intercellular crosstalk in 3D culture: Integrin-FN interaction	18
2.7 The link between the microenvironment and gene expression.....	21
2.8 Conclusion	28
2.9 References.....	29

3	CALCIUM OSCILLATION FREQUENCY IS A FUNCTIONAL COMPLEX PHYSIOLOGICAL RELEVANCE INDICATOR FOR A NEUROBLASTOMA BASED 3D (SPHEROID) CULTURE MODEL.....	49
3.1	Abstract.....	50
3.2	Introduction.....	50
3.3	Materials and Methods.....	52
3.4	Results and Discussion	55
3.5	Conclusion	58
3.6	References.....	59
4	THE EFFECT OF 3D MICROENVIRONEMT ON STRUCTURE AND FUNCTION OF HEPG2 MICROTISSUES	65
4.1	Abstract.....	66
4.2	Introduction.....	66
4.3	Materials and Methods.....	68
4.4	Results and Discussion	73
4.5	Conclusion	79
4.6	References.....	81
5	CYTOKINE UPREGULATION IN 3D HEPG2 CULTURES.....	91
5.1	Abstract.....	92
5.2	Introduction.....	92
5.3	Materials and Methods.....	95
5.4	Results and Discussion	98
5.5	Conclusion	102

5.6 References.....	104
6 CONCLUDING REMARKS AND FUTURE STUDIES	111
APPENDIX	
A PUBLISHED WORK	113

CHAPTER 1

INTRODUCTION

1.1 The 3D Microenvironment

With extensive research and recent developments in the field, 3D cell culture is being defined as platform that provides a comprehensive or an in vivo-like microenvironment for the cells to grow in, which elicits complex physiologically relevant (CPR) phenomenon from the microtissue formed in a manner not seen in traditional 2D monolayers. The microenvironment can be broadly classified into three factors (MEFs) or “three-dimensions” namely, 1) chemical or biochemical composition, 2) spatial (geometric 3D) dimensions, and 3) force and substrate physical properties^{1,2}, with the commercially available 3D platforms providing varying degrees of these exogenous MEFs. However, till now the optimum composition of the microenvironment that is required for the cells to provide a physiologically relevant response has remained elusive. In order to engineer a physiologically relevant 3D tissue model, the microenvironment first needs to be deconstructed so that effect of each individual factor and then their combinatorial or synergistic effects on cell behavior can be determined. However, it should be noted that cells are a dynamic entity and there exists a bidirectional signaling between the cells and their microenvironment. This means that it is not just the microenvironmental cues that have a profound effect on the behavior of cells but the cells also have the capacity to modulate their environment which in time can render the exogenously incorporated MEFs less significant. It is intuitively known that certain initial cues might be required to initiate microtissue formation but after cell adaptation, time emerges as the master controller of the all the other factors. This

switch from microenvironmental regulation of cells to cell modulation of the microenvironment might be the stepping stone towards the generation of a fully functional and structurally similar autonomous 3D microtissue. However, when this transition takes place is not clearly known which makes it important to analyze cell behavior in 3D in a time dependent manner as this might provide a design principle which would lead to the development of a construct with the most simplistic architecture. Once the optimum configuration of the three cues has been established, the microenvironment can be reconstructed to yield a microtissue model that is more similar to *in vivo*.

Finally, it should be taken into consideration that different applications might require different 3D models that are tailor made to satisfy their specific demands. As such, a certain set of optimized microenvironmental conditions should not be treated as a gold standard as it may depend on the application. For instance, in the field of regenerative medicine, circumventing hypoxia to produce larger tissues with higher viability for implantation *in vivo* is relentlessly pursued, on the contrary, the field of drug discovery might benefit from incorporating hypoxia in platform design as hypoxia is a very physiologically relevant phenomenon and is important for many *in-vivo* processes like development and tumor progression. Such a realization is important in rational design and/or choice of a 3D platform, where the need for strict control of the microenvironment is balanced against the need for flexibility to alter it to better emulate the *in vivo* conditions. The role of hypoxia in 3D and the need for its inclusion or exclusion to generate more physiologically relevant microtissue models has been further discussed by Asthana and Kisaalita (2012; Appendix)³. In the end, the main aim is to establish the most simplistic architecture that yields the most complex physiologically relevant outcomes to keep the model

cost effective and adaptable to the current high throughput (HTS) drug discovery platforms as elaborated by Lai et al (2011; Appendix)⁴.

1.2 Complex Physiological Relevance and Three-Dimensionality Biomarkers

In the past decade, the problem with the many emerging 3D platforms is that whenever 2D/3D culture differences are observed, “more physiological relevance” is claimed with no “gold standard” to substantiate the claims. Apart from the concept of “three-dimensional matrix adhesion,” originally proposed by Curkieman et al. (2001)⁵ as a possible indication for a culture state of three-dimensionality, the field of tissue engineering has not provided knowledge on the basis of which a consensus for three-dimensionality and the associated complex physiological relevance could be established. Future development of 3D cell culture platforms should be driven by the brief that is the responses generated by the cells growing in a 3D format are not just “different,” but are physiologically more relevant, when compared to cells cultured on traditional 2D surfaces. It is necessary to conclusively show that these responses produced in 3D formats are emulations of those that are seen in-vivo. To be meaningful, these physiologically relevant outcomes (structural or functional) that are also known in vivo should be absent in 2D formats and such outcomes (CPRs) should be established for cells derived from the for major tissue types. These outcomes can serve as a standard for determining how close a 3D culture is to its native tissue or which out of a given number of 3D platforms is better suited for a given application. The well-established or provisional CPR outcomes for cells derived from the three tissue types of most interest in pre-clinical drug discovery (epithelial, neuronal and cardiac) have been discussed in detail by Asthana and Kisaalita (2013; Appendix)⁶.

Even though structural and/or functional CPR outcomes can be used to establish and validate three-dimensionality, there are additional questions or drawbacks beyond the late-in-culture expression that is mentioned already. For example, a CPR outcome can be considered an end-point measurement, suggesting that once expressed, the culture has been on a trajectory, prior to this point, toward this desired in vivo emulation state. A natural question to ask is when is the most appropriate time to use the microtissue in screening studies; before, after, or at this point? It is well known that the viability of microtissues in vitro has a limited time, which raises the question of how long after observing CPR outcomes is the microtissue suitable for screening studies? Assuming, a cytokine expression profile early in culture accurately predicts CPR outcomes expressed later in culture, does this mean that for such a culture, resulting microtissues are suitable for screening studies before CPR outcomes expression? Answers to these questions are critical to the development and utilization of complex physiologically relevant 3D cell-based assays. To answer these questions or to establish the optimal performance time for a microtissue, with respect to meaningful assay results, biomarkers of three-dimensionality that reliably predicts CPR outcomes and are expressed early in culture are a must-have.

1.3 Specific Objectives

Taken together, the subfield or field of 3D culture needs validated biomarkers. In chapter 2 we have brought together evidence from transcriptomic, proteomic, inflammation and oncology-related pathways, as well as cellular functional studies that strongly point to cytokines and related chemical species as the most likely compounds to provide the badly needed biomarkers. As a first step towards conclusively confirming or ruling out this possibility, our specific objectives are follows:

1. To establish calcium oscillation frequency as a functional complex physiologically relevant (CPR) phenomenon for cells of neural origin in order to develop a relevant 3D culture. The results are presented in chapter 3.
2. To determine the optimal microenvironmental composition for culturing hepatic cells, based on CPR outcomes and designing a 3D HTS platform that provides such a microenvironment. The results from this study are presented in chapter 4
3. To determine the cytokine production time-profiles for hepatic cultures growing in different 3D platforms and establish their correlation with CPR outcomes and to determine the role of Ras/Raf/ERK pathway in the upregulation of cytokines in 3D. The results are presented in chapter 5.

If cytokines are validated as biomarkers of physiologically relevant three-dimensionality then a consensus for various natural hydrogel-forming (alginate, agarose, chitosan, fibrin, and hyaluronan) and synthetic (poly ethylene oxide, poly vinyl alcohol, poly acrylic acid, poly propylene fumarate-co-ethylene glycol, to name a few) constructs that claim to provide an in vitro tissue mimicking cell growth microenvironment can be established. This will lead to advances in tissue engineering, regenerative medicine, drug screening, tumor & developmental biology and also in the study of cell-cell and cell-material surface interactions and will take the field a step closer towards understanding and thus engineering 'in vivo-like' cell culture microenvironments.

1.4 References

1. Griffith, L.G. and Swartz, M.A. Capturing complex 3D tissue physiology in vitro. *Nat. Rev. Mol. Cell Biol.* **7**, 211, 2006.
2. Kisaalita WS. 3D Cell-Based Biosensors in Drug Discovery Programs: Microtissue Engineering for High Throughput Screening, Boca Raton, FL: Taylor and Francis, 2010.
3. Asthana, A., & Kisaalita, W. S. Microtissue size and hypoxia in HTS with 3D cultures. *Drug Discov Today*, **17**, 810, 2012.
4. Lai Y, Asthana A and Kisaalita WS. Biomarkers for simplifying HTS 3D cell culture platforms for drug discovery: the case for cytokines. *Drug Discovery Today* 2011, 16(7-8):293-7.
5. Cukierman, E.; Pankov, R.; Stevens, D.R.; Yamada, K. (2001) Taking cell-matrix adhesions to the third dimension. *Science* 294:1708-1712.
6. Asthana, A., & Kisaalita, W. S. (2013). Biophysical microenvironment and 3D culture physiological relevance. *Drug discovery today*, 18(11), 533-540.

CHAPTER 2
LITERATURE REVIEW:
IN SEARCH OF BIOMARKERS FOR COMPLEX 3D MICROTISSUE PHYSIOLOGY IN
VITRO – THE CASE FOR CYTOKINES¹

¹ Asthana A and Kisaalita WS. To be submitted to Tissue Engineering: Part B

2.1 Abstract

Claims of “physiologically more relevant” are readily made for cells cultured on any surface on in a scaffold that provides loosely defined 3D geometry. A set of tools to more accurately measure culture “3Dness” are needed. Such tools should find applications in fields ranging from high throughput identification of substrates for tissue engineering and regenerative medicine to cell-based screening of drug candidates. Up until now, these fields have not provided a consensus for the most promising place to initiate the search. Here we review recent advances in transcriptomic, proteomic, inflammation and oncology-related pathways, as well as functional studies that strongly point to cytokines as the most likely compounds to form the missing consensus. Validated biomarkers for complex 3D microtissue physiology in vitro should be a powerful tool in establishing cell-cell and cell-material interactions in microenvironments that support physiologically more relevant microtissue formation.

2.2 Introduction

The definition of three-dimensionality in cell culture has recently been extended from simple spatial organization to providing a complete microenvironment that leads to the formation of a “complex” physiologically relevant microtissue, which can be translated into better emulation of in vivo-like functional competence in a way not achievable in monolayer cultures¹. Interestingly, the critical components of this microenvironment can be expressed in a 3D Cartesian coordinate system (Figure 1), with the following three groups or microenvironmental factors (MEFs) or “three-dimensions” of: 1) biochemical or chemical configuration, 2) temporal dimensions and spatial (geometric 3D) architecture and 3) force and substrate physical properties. The three MEFs are well supported by recent literature¹⁻³. In the following four

paragraphs, before proceeding, we provide four compelling reasons why searching for three-dimensionality biomarkers is needed.

First, as long as the resulting phenotypes are different between cells growing in 2D and those cultured on any platform that provides a loosely defined 3D architecture, either at the nano or micro scale or their combinations, they are deemed to be “physiologically more relevant”. Apart from the concept of “three-dimensional matrix adhesion,” initially proposed by Curkieman et al.⁴ as a possible “diagnosis” or indicator for the three-dimensionality of a culture, the area of tissue engineering has not provided the know-how based on which these claims could be validated, as such a consensus for the three-dimensional state of a culture and the complex physiological relevance associated with it should be established.

Second, “hit materials” can be rapidly screened for future development via high throughput combinatorial approaches to generate libraries of polymers or other scaffolding substrates^{5,6}, useful in tissue engineering or cell-based drug discovery applications, provided three-dimensional assays are available. The advancement of these assays or biosensors can potentially be governed by a cell-substrate interaction outcome⁷. As previously pointed out, “three-dimensionality biomarkers would provide the intellectual basis for material discovery platform development,” where interactions with a substrate that produce cells that mimic *in vivo*-like competence are desired⁷. Figure 2.2 shows an illustration of a theoretical framework in which scaffold substrate discovery can be carried out in a high throughput screening (HTS)⁷ format. As shown in Figure 2.2a and b, poly (desaminotyrosyl-tyrosine ethyl ester carbonate (pDTEc) and poly (desaminotyrosyl-tryrosine octyl ester carbonate (pDTOc) have a structurally similar backbone, but different side chains (ethyl on pDTEc and octyl of pDTOc). Due to this, they show different properties which lead to variations in cells grown on films (2D) of the

polymers and their composites. When cultured on pDTEc, cells displayed enhanced adhesion, spreading and proliferation in comparison to pDToC^{8,9}. If a balance between differentiation and proliferation is needed, then an optimum polymeric composition that satisfies the requirement might exist and readily be found using HTS with a polymer blend combinatorial scaffold-library. The library can be constructed using a fluid handling instrument represented by a dual syringe pump system in Figure 2c, that would generate arrays of porogen-leached scaffolds of varying polymeric blends (Figure 2.2d). In the proof-of-concept study of the system shown in Figure 2.2, Yang et al.^{6,7} used Fourier transform infrared spectroscopy (FTIR) to verify scaffold polymer mixtures. Extending such a study to the question of how well the polymer blends support the three-dimensionality of cultures within, requires biomarkers measurable in HTS readouts.

Third, it is essential to reduce the costs associated with 3D platforms to increase their accessibility for high throughput applications; simplification of the platform without affecting the physiologically relevant behavior of the cells can only be achieved with validated biomarkers. In recent work, the definition of three-dimensionality in cell culture has been extended to providing a complete microenvironment that leads to the formation of a “complex” physiologically relevant microtissue or better emulation of *in vivo*-like functional competence in a way not achievable in monolayer cultures¹. – see Figure 2.3 for more detailed illustration. The platform simplification can be achieved easily if the physiologically relevant outcome can be measured in terms of three-dimensionality biomarkers, as elaborated by Lai et al.¹⁰ As the architecture of the platform is simplified, it will be feasible, using validated biomarkers, to know when the trajectory toward CPR outcomes is being affected.

Fourth, since CPR is a phenomenon that is generally expressed late in culture and is often associated with a combination of structural and functional attributes that are not quantitative, a

biomarker, that may be quantitative, expressed early in culture can act as an early indicator of the a trajectory toward CPR outcomes. Additionally, different techniques are typically employed to detect CPR in different tissue types and they are often incompatible with HTS. Therefore, a ubiquitous biomarker expressed early in culture would provide a single assay with which to predict CPR outcomes in cells derived from many tissue types.

Taken together, the field of 3D culture requires validated biomarkers. The “elephant in the room” is whether such a thing exists. In this review, we bring together evidence from transcriptomic, proteomic, inflammation and oncology-related pathways, as well as cellular functional studies that strongly point to cytokines as the most likely entity to provide the badly needed biomarkers.

2.3 CPR and screening studies timing

Differences in resulting cell phenotypes between 2D and 3D platforms are necessary but not sufficient for suggesting complex physiological relevance (CPR). It is therefore necessary to conclusively show that functional and/or structural outcomes from cells cultured on 3D platforms are emulating those observed in-vivo. The well-established or provisional CPR outcomes for cells belonging to the three types of tissues of major interest in pre-clinical drug discovery (epithelial, cardiac and neuronal) have been discussed in detail by Asthana and Kisaalita¹¹. Even though structural and/or functional CPR outcomes can be used to establish and validate three-dimensionality, there are additional questions or drawbacks beyond the late-in-culture expression that is mentioned already. For example, a CPR outcome can be considered an end-point measurement, suggesting that once expressed, the culture has been on a trajectory, prior to this point, toward this desired in vivo emulation state. A natural question to ask is when is the most

appropriate time to use the microtissue in screening studies; before, after, or at this point? It is well known that the viability of microtissues in vitro has a limited time, which raises the question of how long after observing CPR outcomes is the microtissue suitable for screening studies? Assuming, a cytokine expression profile early in culture accurately predicts CPR outcomes expressed later in culture, does this mean that for such a culture, resulting microtissues are suitable for screening studies before CPR outcomes expression? Answers to the above questions are critical to the advancement and utilization of complex physiologically relevant 3D cell-based assays. To answer these questions or to establish the optimal performance time for a microtissue, with respect to meaningful assay results, biomarkers of three-dimensionality that reliably predicts CPR outcomes and are expressed early in culture are a must-have.

2.4 Cohesivity: Microtissue formation and cytokine production

Living organisms have the ability to perceive their environment and respond to changes in it. Cells, being the building unit of an organism are also endowed with this power. Their surrounding, being comparable to their own size, is termed the microenvironment and cells are affected by changes in it. If the cells are transitioned from a monolayer culture to a 3D environment, how do they perceive this change? They find themselves in the vicinity of homotypic neighbors leading to the formation of a loosely bound aggregate. A similar scenario is encountered in vivo during avascular tumor progression, early stages of inflammatory wound healing and development. These phenomena are quite similar in nature and are controlled by the same molecules – Cytokines¹². So in vitro, depending upon their nature – malignant, primary or stem, the cells grown in 3D relate to any of these models, respectively, and therefore an increase in their cytokine expression is physiologically justified. Cytokines are soluble low molecular

weight extracellular protein mediators that typically act at short range between neighboring cells. They play important roles in intercellular regulation and mobilization of cells engaged in innate and adaptive inflammatory host defenses, cell growth and death, differentiation, angiogenesis, development and repair processes¹³. They have been studied extensively for their role in inflammation, tumor progression and normal development¹²⁻¹⁴. As cytokines and their associated receptors provide major signals for essential processes, abnormalities associated with them, their receptors or the signaling pathways they affect, are involved in a wide array of diseases, particularly by promoting and perpetuating inflammation. Based on the structural homologies of their receptors, Cytokines have been assigned to various family groups and can be broadly classified into: Colony Stimulating Factors, Interleukins, Interferons, TGF (transforming growth factor) family, TNF (tumor necrosis factor) superfamily, PDGF (platelet-derived growth factor) family and Chemokines. They act on cells expressing complementary receptors, in both autocrine and paracrine manner¹⁵. They can control their own production as well as that of the others by initiating a feedback loop¹⁶⁻¹⁸. Cytokine production and function is generally governed by transcription factors NF- κ B (Nuclear factor kappa-light-chain-enhancer of activated B cells)¹⁹ and AP-1(Activator protein 1)²⁰ as they have binding sites in the promoter region of most of the cytokine genes. The ERK (Extracellular-signal-regulated kinases)²¹ and the JAK-STAT (Janus kinase/signal transducers and activators of transcription)^{22, 23} pathways have also been widely implicated in their regulation.

Along with the down regulation of cytokines, another intriguing absence in the case of 2D monolayers is that of cell adhesion molecules (CAMs). This is substantiated by the microarray analysis done on many established cell lines and tissue derived cells in which cell adhesion molecules were found to be down regulated in conventional cultures²⁴. CAMs are

transmembrane receptors found on the surface of the cell and are composed of three domains: an extracellular domain that enables interactions either with similar CAMs (homophilic binding) or with different CAMs or the extracellular matrix (heterophilic binding), an intracellular domain which facilitates interactions with the cytoskeleton and a transmembrane domain. Cell adhesion molecules can be classified into five protein families: Ig (immunoglobulin) superfamily (IgSF CAMs), integrins, cadherins, the selectins and the lymphocyte homing receptor. Their structure and function have been reviewed in detail elsewhere²⁵. In 3D cultures, formation of aggregates or microtissues is brought about by cell-to-cell and cell to ECM (Extracellular Matrix) interaction through CAMs²⁶. Traditionally, integrins have been associated with cell to substrate adhesion while cadherins form cell to cell adherens junction²⁵. However recent studies carried out on CHO (Chinese Hamster Ovary) cells²⁷ and fibroblasts²⁸ have shown that integrins play a part in forming cohesive bonds between the cells in a 3D microenvironment leading to the formation of a microtissue. Cohesivity seems to be brought about by integrin binding to the Fibronectin (FN) matrix assembly²⁹ present in the ECM of 3D cultures, but absent in monolayers. Cellular crosstalk mediated by integrins and the subsequent intracellular pathways that they invoke might be related to the upregulation of cytokines in 3D. This is the main premise behind, “cytokines as the most likely family of compounds to provide the missing three-dimensionality biomarker consensus.” In the rest of this review, we provide more detailed experimental evidence to support this proposition. We have organized our presentation along 1) 2D/3D comparative transcriptomic and proteomic studies, 2) integrin-fibronectin studies, and 3) signaling pathways involved as an overarching view that integrates the other experimental evidence.

2.5 2D/3D culture comparative transcriptomic/proteomic up-regulation of cytokines

Recently many studies have shown that when cells are grown in a 3D culture their cytokine levels are elevated as compared to the traditional monolayer cultures (Table 2.1). We compared neural progenitor (NP) cells cultured on 2D substrates, 3D porous polystyrene scaffolds, and as 3D neurospheres (in vivo surrogate) with respect to transcriptomic expression, using the Human Whole Genome U133 plus 2.0 GeneChip Expression Analysis (Affymetrix, Santa Clara, CA)¹⁴. The expression data available on the GEO site as Series GSE13715. An increase in the expression of cytokines as a group in 3D and neurospheres was observed. The number of probesets that were up-regulated in 3D and neurospheroid culture conditions was forty and ninety-one, respectively. The difference in the number of upregulated probesets might be due to inability to regulate the size of neurospheres. Many neurospheres were observed to be bigger than the pore size of the 3D scaffolds (e.g., three times the maximum pore diameter of 100 μm)³⁰. The core of the cellular aggregate may experience hypoxia in large neurospheres, to the extent that genes not observed in 3D are up-regulated. For example, *MIP-2* gene (Macrophage inflammatory protein-2), induced by hypoxia³¹, was found to be up-regulated in neurospheroids but not in 3D conditions in our study. A group of 13 cytokines including ANGTL7/CDT6 (Angiopoietin-like 7), ARMET/MANF (Mesencephalic astrocyte-derived neurotrophic factor), BMP8B/OP2 (Bone morphogenetic protein 8b/Osteogenic protein 2), CCL13/MCP-4 (Monocyte chemotactic protein-4), FGF5 (Fibroblast growth factor 5), GHRL (ghrelin/obestatin), IL-11 (Interleukin-11), IL-1B/IL-1F2 (Interleukin 1B), NOV/IBP-9 (nephroblastoma overexpressed), PDGFB (Platelet-derived growth factor subunit B), STC1 (Stanniocalcin-1), TGFA (Transforming growth factor alpha), and VEGF-A (Vascular endothelial growth factor A) were commonly up-regulated in cells cultured in polystyrene scaffolds and

neurospheres. As such, any or a combination from this list has potential to serve as three-dimensionality biomarkers.

We particularly focused on the above genes because there was less likelihood of them being up-regulated due to hypoxic conditions that may be present in NS (neurospheroids) but not in 3D conditions. The functional classification of these cytokines suggested an underlying theme of development which is physiologically relevant as progenitor cells in a 3D culture in vitro try to emulate embryonic development. The result of this study is in agreement with many other transcriptomic and proteomic studies where cytokines have been shown to be upregulated in 3D cultures. These studies have been conducted on many different cell lines spanning various cell types including primary cells, fibroblasts, multi and pluripotent stem cells and cancer cells grown on different 3D platforms. The results are summarized in Table 2.1. As shown, despite the fact that there are no neural cells in the studies cited in Table 2.1, identical (IL-11) or related (ANGTL7, IL1-B, and VEGF-A) cytokine up-regulation from our study have been reported by others from different cell types. In a recent review, on how cells know where they are, Lander³² has emphasized the importance of morphogen diffusion gradients. Since many cytokines (e.g., BMP8B, PDGFB) are well known morphogens, upregulation of cytokines, which would change the diffusion gradient, must convey information to cells that result in different decisions in comparison to those made by cells in 2D cultures. Taken together, this shows that cytokines have the potential to validate the 3D platforms with respect to emulating the in-vivo microenvironment. The fact that they are secreted in the culture media and as such quantifiable without lysing the cells by Enzyme-linked immunosorbent assay (ELISA)³³, makes cytokines convenient as suitable as biomarkers. This will not be the first instance for the proposed usage of cytokines as biomarkers. Due to their robustness and versatility, cytokines have been proposed

extensively to be used as markers for early detection of head, neck³⁴ and ovarian cancers³⁵ Alzheimer's disease³⁶, heart diseases³⁷, prostatitis³⁸, determining the potential activity of drugs early in clinical development³⁹ and many more scenarios.

Hypoxia is another physiologically relevant characteristic of 3D microenvironments both in vivo and in vitro⁴⁰. In tissues, the concentration of oxygen is dependent on the balance between oxygen supplied and consumed. This balance is well controlled in vivo, by evenly distributed capillary networks, which are lacking in vitro. Therefore the core of a homotypic 3D microtissue might become hypoxic as the size of the tissue increases. This event can cause induction of chemical signals (cytokines) from the cells for angiogenesis, which is similar to the way normal tissues respond to hypoxia where balanced signaling mechanisms lead to angioadaptation and vascular remodeling until the concentration of oxygen in tissue is back within its normal range⁴¹. Hypoxia inducible transcription factors (HIFs) are the molecular mediators of physiological hypoxia and the cellular response. Under hypoxic condition, HIF-1 α and HIF-1 β translocate to the nucleus⁴², where their dimerization takes place and they subsequently bind to target gene motifs called hypoxia responsive elements (HREs) resulting in altered gene expression⁴³. HIF-1 α seems to regulate the production of VEGF as its suppression has been shown to cause transcriptional inhibition of VEGF⁴⁴ and reduced vascular density⁴⁵. Hypoxic conditions have also been shown to trigger AP-1⁴⁶ and NF- κ B⁴⁷ which affect the production of a myriad of cytokines (Supplementary Table 1). The effect of hypoxia on cytokine production was further established by a study which showed higher levels of cytokines produced by hypoxic 3D co-cultures of CD34 and HUVEC (human umbilical vein endothelial cells) than normal cultures⁴⁸. In another study, by Fischbach et al.⁴⁹, hypoxia was found to be associated with increased cytokine secretion in 3D tumors. However, comparing monolayer cultures under

reduced oxygen concentration with 3D cultures indicated that the sole contribution of hypoxia is comparably small and that the joint effect of hypoxia and 3D microenvironment is necessary to elicit increased expression of cytokines, particularly IL-8⁴⁹.

2.6 Intercellular crosstalk in 3D culture: Integrin-FN interaction

Integrin $\alpha 5\beta 1$ is the only integrin that naturally assembles fibronectin (FN) into a matrix and this can lead to the formation of an endogenous matrix. Fibronectin is a multifunctional component of the Extracellular matrix which exists in a dimeric state, with the two chains attached through disulfide bonds at the C-terminus⁵⁰. Every FN chain has a single cell binding domain having an RGD (Arginine-Glycine-Aspartic acid) sequence to which $\alpha 5\beta 1$ integrin specifically binds⁵¹. FN matrix assembly structural make-up includes FN's dimeric structure, the N-terminal assembly domain and FN-binding sites in the first two type III repeats^{52, 53} and integrin binding to the RGD sequence in the cell-binding domain⁵⁴. Interaction of integrin with FN promotes intermolecular association between the FN dimers, leading to the formation of fibrils which further increases cell adhesion and cohesivity. This is consistent with the fact that monomers of fibronectin could not lead to aggregate formation²⁷ and this substantiates the notion that FN matrix assembly may support aggregate cohesivity by forming a scaffold, or an organized 3D matrix, which leads to a functional linkage between cells. Using $\alpha 5$, αV and $\beta 1$ integrin blocking antibodies²⁸ caused a reduction in the amount of FN produced in fibroblast spheroids, suggesting that these integrins are involved in the expression of FN in spheroids but that the formation of tight compact spheroids is mediated through the $\alpha 5\beta 1$ integrin only.

Integrin $\alpha 4$, $\alpha 5$ and $\beta 1$ subunits are important for embryonic development *in vivo*, as their absence has been shown to be lethal to mouse embryos⁵⁵. It has also been observed that there

exists a perfect correlation between the cohesivity of the germ layers in amphibian gastrulae and the spatial position of these integrins⁵⁶. Moreover, injecting RGD peptide into amphibian blastulae has been shown to disrupt cell interactions with FN causing blockage of gastrulation and preventing formation of FN fibril meshwork involved in migration⁵⁷. If the interaction between integrin $\alpha 5\beta 1$ and FN is indeed responsible for the cohesivity of tissues, particularly very early in development when embryos are essentially aggregate-like, then it is possible that this particular interaction also has the capacity to provide cohesive forces to cells within a microtissue in vitro.

Compaction mediated by fibronectin has also been shown to be of importance in the later stages of development. A correlation has been found between FN production and pre-cartilage mesenchymal condensation during the development of wings and leg bud in chick embryos⁵⁸, with higher FN expression correlating with compaction of tissues. The interaction between integrin $\alpha 5\beta 1$ and FN has also been shown to generate the tractional force which is essential for retraction of 3D FN-fibrin clot matrices⁵⁹. This retraction process is crucial for early wound healing and tissue remodeling. It has been proposed that this intercellular cohesivity also contributes to clot retraction, akin to the apparent 'retraction' or compaction observed for CHO aggregates in response to increased concentrations of FN. Ergo, this cell to cell cohesivity produced by integrin engagement with FN is probably responsible for triggering the intracellular signaling pathways that lead to the difference in cytokine production seen in 2D monolayer and 3D microtissues. These pathways and their key molecular regulators have been elaborated in the following Section. Evidence in support of involvement of integrin mediated cell adhesion to FN in the production of cytokines has been provided by a study where microarray analysis done on myeloma cells growing on FN showed upregulation of many NF- κ B regulated genes⁶⁰. NF- κ B

controls the expression of many growth factors and cytokines as discussed in the following Section. Some of the cytokines that were found to be upregulated, compared to control suspended cells, included TNFaIP2, CCL4, IL-6 and IL-8. Another study by Fischbach et al.⁶¹ showed how transition from a monolayer to a 3D environment lead to an increase in the production of IL-8 and VEGF by breast cancer, glioblastoma and oral carcinoma cells, both in vitro and in vivo in a SCID mouse model. The results from this study⁶¹ suggest that the 3D microenvironment plays a vital role in regulating the secretion of IL-8 but that the combined effects of the 3D microenvironment, 3D cell morphology, and 3D integrin (particularly $\alpha 5\beta 1$) engagement are required to fully regulate the production of IL-8 by tumor cells. Interestingly, engagement of integrins in 2D and spread morphology of cells in a 3D space lead to a higher IL-8 production than a conventional monolayer but less than 3D cultures, further emphasizing that spatial cues along with cell-ECM interactions and morphology of the cell regulate its cytokine secretion. Also, cell morphology is an often neglected but an important parameter as alterations in morphology cause actin cytoskeleton remodeling that can lead to differential NF- κ B signaling⁸⁹ which controls cytokine production.

Integrin mediated adhesion regulates many important intracellular signaling cascades. These pathways are most likely aberrantly regulated in 2D cultures due to the absence of an endogenous extracellular matrix assembly or cell to cell interactions. However in a more physiologically relevant microenvironment, they can relay signals through a variety of adapter proteins that are localized at their cytoplasmic tails forming the focal adhesion complexes. Integrin signaling is mediated through FAK (Focal adhesion kinase), Src (Rous sarcoma oncogene cellular homolog), Shc (Adapter protein involved in oncogenesis) and Grb2 (Growth factor receptor-bound protein 2) to downstream kinases. Ras/Raf/ERK pathway is one of the

most important pathways regulated by integrin mediated adhesion. ERK activates several transcription factors in the nucleus like NF- κ B, AP-1, CREB (cAMP response element-binding protein) and Ets-1 (E26 AMV virus oncogene cellular homolog) which control the production of cytokines and survival and growth factors important for the cell. Therefore, through proper activation of the ERK pathway, integrins can indirectly regulate the production of cytokines, provided they interact with a tissue mimicking environment having optimum spatial, biophysical and biochemical cues.

2.7 The link between the microenvironment and gene expression

2.7.1 Focal Adhesion Kinase

Focal-adhesion kinase (FAK) is a type of non-receptor tyrosine kinase that affects the dynamics of integrin associated adhesions and the actin cytoskeleton that is coupled to it, through various molecular interactions. Being a component of the focal-adhesion ‘scaffolding’, it performs protein–protein interaction adaptor functions at the loci of cell adhesion to the ECM and also relays adhesion and growth factor dependent cues into the cell body. Many reports have linked upregulated FAK expression with tumorous growth^{62, 63}. The *FAK* gene locus at 8q23-q24 has also been shown to be a target of gene amplification during tumor progression⁶⁵. However, as far as cytokine production is concerned, the gene is controlled by FAK through the Ras/Raf/ERK signaling pathway and activation of its downstream transcription factors NF- κ B and AP-1. FAK signaling has been directly implicated in VEGF production by avascular tumors in vivo⁶⁶. FAK expression and its catalytic activity due to Y925 phosphorylation promotes the ERK pathway which leads to increased VEGF expression resulting in tumor neo-vascularization without any significant alteration in cell proliferation or anchorage-independent survival. Inhibition of FAK activity by stable FRNK (FAK C-terminal domain) expression lead to reduced

secretion of VEGF compared to control, in 4T1 breast carcinoma cells⁶⁶. Cells expressing FRNK showed formation of small tumors that were avascular, without exhibiting differences in tumor associated apoptosis. It was observed that FRNK lead to the inhibition of a FAK-Grb2-MAPK-signaling linkage controlling VEGF production, which was further supported by point-mutations that affected FAK catalytic activity or Y925 phosphorylation disrupting the ability of FAK to promote ERK and VEGF associated tumor growth. Reduction in VEGF expression was also observed when FAK expression was inhibited in prostate, breast and neuroblastoma cells. Furthermore, a point mutation (FRNK S-1034), which inactivates FRNK by disrupting its co-localization with integrins, leads to the restoration of FAK activity and VEGF production⁶⁷. Another major factor that activates VEGF expression is the development of hypoxia within the core of the proliferating tumor⁶⁸. Interestingly, hypoxia has also been found to increase FAK tyrosine phosphorylation and bolster the linkage between FAK and Grb2 in cardiac myocytes in vitro⁶⁹. FAK overexpression has also been shown to facilitate neovascularization of retina in a mouse model of hypoxia-induced retinal angiogenesis⁷⁰. Further evidence of FAK involvement in VEGF production is presented in the studies where overexpression of FAK in vascular endothelial cells lead to angiogenesis in transgenic mice⁷¹ and FAK expression was found to be upregulated, in angiogenic blood vessels within astrocytic-associated tumor stroma, in comparison to normal brain endothelial cells⁷². Also, expression of FAK within endothelial cells is essential for vasculogenesis during development⁷³.

2.7.2 The pathway to cytokine upregulation: Ras/Raf/ERK signaling and transcription factors

The extracellular signals are relayed from the integrin via FAK and Src, leading to the activation of several intracellular signaling pathways, mainly the Ras/Raf/ERK pathway (Figure 2.3). In the context of cytokine production, Raf activity has been implicated in many studies. Transformation of hematopoietic cells by activated Raf genes has often been shown to result in the expression of granulocyte macrophage-colony stimulating factor (GM-CSF), which acts as an autocrine growth factor^{74,75}. NIH-3T3 cells expressing activated Raf have shown increased secretion of heparin binding epidermal growth factor (hbEGF)⁷⁶. Kaposi's sarcoma transformed B cells that exhibit elevated expression of B-Raf also show an increased production of VEGF⁷⁷. It has been shown recently that the infectivity of Kaposi's Sarcoma Virus is increased by B-Raf expression⁷⁸ and induction of VEGF production by B-Raf might be a mechanism for this elevation in viral infection⁷⁹. Moreover, Raf activity leads to the subsequent activation of Mitogen-activated protein kinase/ERK kinase (MEK1) that activates downstream ERK which regulates the activation of transcription factors like NF- κ B and AP-1 (Figure 2.4) that have been directly implicated in the expression of cytokines, mitogens and cell survival factors (Supplementary Table 2.1). The involvement of these transcription factors is discussed in details in the following subsection. The activity of Raf is regulated positively through phosphorylation on S residues in its catalytic domain. All three members of the Raf family (B-Raf, Raf-1, and A-Raf) have the capability to phosphorylate and activate MEK with different biochemical efficiencies⁸⁰. This step is also adhesion dependent and is brought about by activation of endogenous PAK (p21-activated kinase) by small GTPase Rac induced by integrin mediated adhesion to FN. Also, B-Raf which directly activates MEK1, independently of Raf-1 is also activated by integrin bound focal adhesion complexes. However, Raf-1 can also activate NF- κ B

through a mechanism independent of MEK1/ERK by degradation of its inhibitor I κ B via MEKK-1 (MEK kinase 1)⁸¹ (Figure 2.4).

ERKs (1 and 2) activities are regulated positively through phosphorylation mediated by MEK1 and MEK2 and can directly activate many transcription factors like Ets-1, AP-1 and c-Myc. ERKs can also control the phosphorylation and activation of the 90 kDa ribosomal S6 kinase (p90Rsk or RSK1), which in turn regulates the activation of the transcription factor CREB⁸². Moreover, it has also been observed that p90Rsk can lead to the activation of NF- κ B by phosphorylating its inhibitor I κ B α at Ser32 causing its ubiquitination⁸³ (Figure 2.4). The localization of activated ERK is quite important in determining the cellular fate. To carry out the phosphorylation of its downstream transcription factors, ERK needs to be translocated from the cytoplasm to the nucleus. This is an adhesion dependent step and is brought about by PAK activation by small GTPase Rac, induced by integrin mediated adhesion to FN. In cells lacking adhesion cues (suspended cells), ERK activation can be achieved by overexpressing active Raf (22W Raf) or MEK (MEK1- Δ ED) mutants, but still the signal is transmitted poorly to the nucleus as activated ERK cannot translocate to the nucleus and fully activate its downstream transcription factors⁸⁴. Most of the cytokines and growth factors are the target genes of NF- κ B, AP-1 and ETS (Supplementary Table 1) which are in turn regulated by ERK or other components of the MAPK pathway (Raf and p90Rsk) and so proper control and activation of the pathway is essential for production and regulation of the cytokines⁸⁵.

2.7.2.1 NF- κ B

NF- κ B activation can be brought about by a variety of stimuli and thus far two different NF- κ B signaling mechanisms - classical and alternate have been described⁸⁶. The main NF- κ B

dimer that is activated through the classical pathway is p65:p50. Translocation of p65:p50 to the nucleus leads to the transcription of many proinflammatory targets, such as cytokines, chemokines, proangiogenic factors, adhesion molecules, antiapoptotic proteins and inducible enzymes. NF- κ B activity can be regulated either in an ERK independent fashion by Raf-1 via membrane shuttle kinase MEKK1 or in an ERK dependent manner by RSK1 (as discussed in the previous Section). The activation of both these pathways (Raf-1/MEKK1 or ERK/RSK) is dependent on integrin mediated adhesion to the ECM and so is regulated by the microenvironment and therefore requires physiologically relevant microenvironmental cues to be properly activated. NF- κ B was found to be upregulated in Hepatic Stellate Cells (HSC) in 3D collagen I gel cultures⁸⁷ and in mammary tumor cell spheroids, where its activation was also responsible for resistance to apoptosis⁸⁸. Many studies have also correlated NF- κ B activation with cytokine production in different 3D cultures. In most of these studies, cytokine production in control 2D monolayer cultures was either lacking or at basal levels. Fibroblasts, when grown in spheroids, have shown an inverse correlation between NF- κ B and I κ B at a time point just prior to cytokine secretion³¹. The degradation of I κ B leads to the activity of NF- κ B in spheroids, whereas monolayer levels remained unchanged and the correlation was further substantiated when the activity of NF- κ B was found to be higher in 3D than monolayers at the same time points³¹. Also, changes in cell morphology may lead to production of cytokines as changes in the actin cytoskeleton also lead to differential activation of NF- κ B⁸⁹. Such cytoskeletal changes are evident in transition from monolayer to a 3D culture platform⁶¹. Furthermore, it has been shown that FN is a potent activator of the NF- κ B signaling pathway⁹⁰ and α 5 β 1 integrin mediated formation of FN endogenous matrix assembly leading to cellular cohesivity in 3D cultures as

described earlier. Taken together, this suggests the basis for upregulation of cytokine production in 3D cultures in comparison to 2D or monolayer cultures.

2.7.2.2 AP-1

The AP-1 transcription factor is not a solitary protein; it is instead comprised of various dimeric basic region-leucine zipper (bZIP) proteins that belong to the Jun, Fos, Maf and ATF⁹¹ families. The activity of AP-1 is induced by various stimuli such as cytokines, growth factors, polypeptide hormones, neurotransmitters, bacterial and viral infections, cell–matrix interactions and many physical and chemical stresses. These stimuli lead to the activation of mitogen activated protein kinase (MAPK) signaling cascades⁹² that upregulate AP-1 activity through phosphorylation of distinct moieties. AP-1 activation controls the expression of several cytokines and cell adhesion molecules. In monolayers, AP-1 activity might be impaired as the ERK pathway is differentially regulated due to the lack of optimum microenvironmental factors. However in 3D cultures, in the presence of a physiologically relevant tissue mimicking microenvironment, AP-1 activity leads to cytokine production, depending on the cell type (malignant versus primary) and/or scenario (tumor progression or wound healing). This hypothesis is substantiated by the fact that recently AP-1 was found to be activated in spheroids of different cell types culminating in cytokine production. All three cell types tested - transformed Human Embryonic Kidney (HEK293)⁹³, primary Human Foreskin Fibroblasts (HFF-2) and carcinogenic Glioblastoma cell line (T98G)⁹⁴, showed activation of different pathways leading to spheroid formation, quiescence and survival but the signals converged to the activation of AP-1 resulting in higher cytokine production than control monolayer cultures. This shows that response to microenvironmental cues can be cell line specific in terms of pathways

but the final outcome (autocrine cytokine signaling and survival in this case) is dependent on the same transcription factor, further highlighting its importance. Furthermore, such autocrine and paracrine signaling is lacking in monolayer cultures due to lack of proximity between cells and absence of cell-cell interactions and crosstalk.

2.7.2.3 Ets

Ets is a family of transcription factors, which include Ets-1, Ets-2, Elk-1, SAP1, SAP2, E1AF, PEA3, PU1 and others⁹⁵. The Ets transcription factors regulate the expression of various other transcription factors like p53⁹⁶, c-Fos⁹⁷ and NF- κ B⁹⁸. Ets proteins usually activate their target genes through association with other transcription factors. For instance, Ets-1 regulates the expression of GM-CSF in Jurkat T cells⁹⁹ and mast cells, by coordinately regulating the GM-CSF promoter in partnership with NF- κ B and/or AP-1 factors¹⁰⁰. It has been shown that both Ets-1 and Ets-2 induce the expression of the IL-5 promoter reporter gene construct in Jurkat T cells on stimulation with PMA (phorbol ester) and ionomycin¹⁰¹. Ets-1 also bound to an IL-5 promoter reporter gene when transfected into the mouse D10.G4.1 Th2 T cell clone, where it strongly cooperated with an adjacent AP-1 binding motif¹⁰². Also, co-transfection of Ets-1 and AP-1 (Fos/Jun) proteins into D10.G4.1 cells was able to induce expression of the endogenous IL-5 gene in the absence of exogenous activator molecules like PMA or cAMP that normally induce IL-5 expression in these cells¹⁰². This cooperative activity is consistent with the production of cytokine in 3D cultures, where ERK cascade controlled AP-1 and Ets activation is induced due to presence of a physiologically relevant milieu and cellular crosstalk and synergistically drives cytokine production without the presence of any external induction molecule. Furthermore, Ets-1 binding sites have also been found in the promoters of many chemokines like CXCL4

(PF4)^{103,104}, CCL2 (MCP-1)¹⁰⁵ and CXCL8 (IL-8)¹⁰⁶ and Ets-1 knockout (Ets-1^{-/-}) or silencing (siRNA) has been shown to block the induction of these chemokines.

2.8 Conclusion

We have methodically built a case for cytokines' potential as biomarkers for three-dimensionality or 3D cultures. The fact that cytokines are secreted in media makes their detection easier, especially in HTS readouts. The fact that cytokines seem to be expressed in a wide range of cells from the four tissue types (muscle, connective, epithelial, and nerve), suggests their high potential for ubiquity as opposed to being cell- or tissue-specific. Also, their temporal expression suggests use of profiles as opposed to single-time measurements, increasing their robustness as biomarkers. For these reasons, cytokines are particularly attractive as biomarkers. As pointed out in Section 2, cytokines are broadly classified into seven subfamilies. In ongoing investigation in our and possibly other laboratories, the question of which subfamily is most suitable to target for follow-up validation studies is being addressed.

2.9 References

1. Kisaalita WS. 3D Cell-Based Biosensors in Drug Discovery Programs: Microtissue Engineering for High Throughput Screening, Boca Raton (CRC Press, Taylor and Francis Group), 2010.
2. Griffith, L.G. and Swartz, M.A. Capturing complex 3D tissue physiology in vitro. *Nat. Rev. Mol. Cell Biol.* **7**, 211, 2006.
3. Green, J.A. and Yamada, K.M. Three-dimensional microenvironments moderate fibroblast signaling responses. *Adv. Drug Delivery Rev.* **59**, 1293, 2007.
4. Cukierman, E., Pankov, R., Steven, D.R. and Yamada, K.M. Talking cell-matrix adhesion to the third dimension. *Science* **294**, 1708, 2001.
5. Simon Jr, C.G., Stephens, J.S., Dorsey, S.M., Beck, M.L. Fabrication of combinatorial polymer scaffolds libraries. *Rev. Sci. Instrum.* **78**, 0722071, 2007.
6. Yang, Y. et al. X-ray imaging optimization of 3D tissue engineering scaffolds via combinatorial fabrication methods. *Biomaterials* **29**, 1901, 2008b.
7. Yang, Y. et al. Combinatorial polymer scaffold libraries for screening cell-biomaterial interactions in 3D. *Adv. Mater.* **20**, 2037, 2008a.
8. Bailey L.O. et al. Cellular response to phase-separated blends of tyrosine-derived polycarbonates. *J. Biomed. Mater. Res. Part A* **76A**(3), 491, 2006.
9. Ertel, S.I. and Kohn, J. Evaluation of tyrosine-derived polycarbonates as degradable biomaterials. *J. Biomed Mater. Res.* **28**, 919, 1994.
10. Lai, Y., Asthana, A., Kisaalita, W.S. Biomarkers for simplifying HTS 3D cell culture platforms for drug discovery: the case for cytokines. *Drug Discov Today* **16**, 293, 2011.
11. Asthana, A., Kisaalita, W. S. (2012). Biophysical microenvironment and 3D culture physiological relevance. *Drug Discov Today* **18**, 533, 2012.
12. Coussens, L.M. and Werb, Z. Inflammation and cancer. *Nature* **420**, 860, 2002.
13. Oppenheim, J. J. Cytokines: past, present, and future. *Int. J. hematol.* **74**, 3, 2001.
14. Lai, Y., Asthana, A., Cheng, K., Kisaalita, W.S. Neural Cell 3D Microtissue Formation Is Marked by Cytokines' Up-Regulation. *PLoS ONE* **6**(10), e26821, 2011.
15. Lazar-Molnar, E., Hegyesi, H., Toth, S. and Falus, A. Autocrine and paracrine regulation by cytokines and growth factors in melanoma. *Cytokine* **12**, 547, 2000.

16. Freeman, M. Feedback control of intercellular signalling in development. *Nature* **408**, 313, 2000.
17. Ogura, H. et al. Interleukin-17 promotes autoimmunity by triggering a positive-feedback loop via interleukin-6 induction. *Immunity* **29**, 628, 2008.
18. Jimbo, K., Park, J.S., Yokosuka, K., Sato, K. and Nagata, K. Positive feedback loop of interleukin-1beta upregulating production of inflammatory mediators in human intervertebral disc cells in vitro. *J. Neurosurg. Spine* **2**, 589, 2005.
19. Blackwell, T.S., Christman, J.W. The role of nuclear factor kappa B in cytokine gene regulation. *Am. J. Respir. Cell Mol. Biol.* **17**, 3, 1997.
20. Foletta, V.C., Segal, D.H. and Cohen, D.R. Transcriptional regulation in the immune system: all roads lead to AP-1. *J. Leukoc. Biol.* **63**, 139, 1998.
21. Chang, F. et al. Signal transduction mediated by the Ras/Raf/MEK/ERK pathway from cytokine receptors to transcription factors: potential targeting for therapeutic intervention. *Leukemia* **17**, 1263, 2003.
22. Liu, K.D., Gaffen, S.L. and Goldsmith M.A. JAK/STAT signaling by cytokine receptors. *Curr. Opin. Immunol.* **10**, 271, 1998.
23. O'Shea, J.J., Gadina, M. and Schreiber, R.D. Cytokine signaling in 2002: New surprises in the Jak/Stat pathway. *Cell* **109**, (Suppl.) S121, 2002.
24. Sandberg, R. and Ernberg, I. The molecular portrait of in vitro growth by meta-analysis of gene-expression profiles. *Genome Biol.* **6**, R65, 2005.
25. Aplin, A.E., Howe, A., Alahari, S.K. and Juliano, R.L. Signal Transduction and Signal Modulation by Cell Adhesion Receptors: The Role of Integrins, Cadherins, Immunoglobulin-Cell Adhesion Molecules, and Selectins. *Pharmacol. Rev.* **50**, 197, 1998.
26. Lin, R.Z., & Chang, H.Y. Recent advances in three-dimensional multicellular spheroid culture for biomedical research. *Biotechnol. J.* **3**, 1172, 2008.
27. Robinson, E.E., Zazzali, K.M., Corbett, S.A. and Foty, R.A. $\alpha 5\beta 1$ Integrin mediates strong tissue cohesion. *J. Cell Sci.* **116**(2), 377, 2003.
28. Salmenperä P., et al. Formation and activation of fibroblast spheroids depend on fibronectin–integrin interaction, *Exp. Cell Res.* **314**, 3444, 2008.

29. Robinson, E.E., Foty, R.A. and Corbett, S.A. Fibronectin matrix assembly regulates alpha5beta1-mediated cell cohesion, *Mol. Biol. Cell* **15**, 973, 2004.
30. Cheng K, Lai Y and Kisaalita WS. Three-dimensional polymer scaffolds for high throughput cell-based assay systems. *Biomaterials*, **29**, 2802, 2008.
31. Zampetaki, A., Mitsialis, S.A., Pfeilschifter, J., Kourembanas, S. Hypoxia induces macrophage inflammatory protein-2 (MIP-2) gene expression in murine macrophages via NF- κ B: the prominent role of p42/p44 and PI3 kinase pathways. *FASEB J* **18**, U808, 2004.
32. Lander, A. D. How Cells Know Where They Are. *Science*, **339**, 923, 2013.
33. Enzerink A., Salmenperä, P., Kankuri, E. and Vaheri, A. Clustering of fibroblasts induces proinflammatory chemokine secretion promoting leukocyte migration. *Mol. Immunol.* **46**, 1787, 2009.
34. Linkov, F. *et al.*, Early detection of head and neck cancer: development of a novel screening tool using multiplexed immunobead-based biomarker profiling, *Cancer Epidemiol. Biomark. Prev.* **16**, 102, 2004.
35. Gorelick, E. *et al.* Multiplexed immunobead-based cytokine profiling for early detection of ovarian cancer. *CEBP* **14**, 981, 2005.
36. Guerreiro, R.J. *et al.* Peripheral inflammatory cytokines as biomarkers in Alzheimer's disease and mild cognitive impairment. *Neurodegener. Dis.* **4**, 406, 2007.
37. Petersen, J.W. and Felker, G.M. Inflammatory biomarkers in heart failure. *Congest. Heart Fail.* **12**, 324, 2006.
38. Penna, G. *et al.* Seminal plasma cytokines and chemokines in prostate inflammation: interleukin 8 as a predictive biomarker in chronic prostatitis/chronic pelvic pain syndrome and benign prostatic hyperplasia. *Eur. Urol.* **51**, 524, 2007.
39. Prabhakar, U., Eirikis, E. and Davis, H.M. Simultaneous quantification of proinflammatory cytokines in human plasma using the LabMAP assay. *J. Immunol. Methods* **260**, 207, 2002.
40. Asthana, A., & Kisaalita, W. S. Microtissue size and hypoxia in HTS with 3D cultures. *Drug Discov Today*, **17**, 810, 2012.

41. Pries, A.R., Reglin, B. and Secomb, T.W. Structural adaptation of microvascular networks: functional roles of adaptive responses. *Am. J. Physiol. Heart. Circ. Physiol.* **281**, H1015, 2001.
42. Jewell, U.R. et al. Induction of HIF-1alpha in response to hypoxia is instantaneous. *Faseb J.* **15**, 1312, 2001.
43. Semenza, G. Signal transduction to hypoxia-inducible factor 1. *Biochem. Pharmacol.* **64**, 993, 2002.
44. Blancher, C., Moore, J.W., Robertson, N. & Harris, A.L. Effects of ras and von Hippel-Lindau (VHL) gene mutations on hypoxia-inducible factor (HIF)-1alpha, HIF-2alpha, and vascular endothelial growth factor expression and their regulation by the phosphatidylinositol 3'-kinase/Akt signaling pathway. *Cancer Res.* **61**, 7349, 2001.
45. Zhang, X. et al. Enhancement of hypoxia-induced tumor cell death in vitro and radiation therapy in vivo by use of small interfering RNA targeted to hypoxia-inducible factor-1alpha. *Cancer Res.* **64**, 8139, 2004.
46. Michiels, C. et al. HIF-1 and AP-1 cooperate to increase gene expression in hypoxia: role of MAP kinases. *IUBMB Life* **52**, 49, 2001.
47. Cardenas-Navia, L.I., Richardson, R.A. and Dewhirst, M.W. Targeting the molecular effects of a hypoxic tumor microenvironment. *Front. Biosci.* **12**, 4061, 2007.
48. Scheubel, R.J. et al. Paracrine effects of CD34 progenitor cells on angiogenic endothelial sprouting. *Int. J. Cardiol.* **139**, 134, 2008.
49. Fischbach, C. et al. Engineering tumors with 3D scaffolds, *Nat Methods* **4**, 855, 2007.
50. Hynes, R. O. Integrins: versatility, modulation, and signaling in cell adhesion. *Cell* **69**, 11, 1992.
51. Akiyama, S. K. Integrins in cell adhesion and signaling. *Hum. Cell* **9**, 181, 1996.
52. Schwarzbauer, J.E. Identification of the fibronectin sequences required for assembly of a fibrillar matrix. *J. Cell Biol.* **113**, 1463, 1991.
53. Sechler, J.L. et al. A novel fibronectin binding site required for fibronectin fibril growth during matrix assembly. *J. Cell Biol.* **154**, 1081, 2001.
54. Sechler, J.L., Takada, Y. and Schwarzbauer, J.E. Altered rate of fibronectin matrix assembly by deletion of the first type III repeats. *J. Cell Biol.* **134**, 573, 1996.

55. Beauvais-Jouneau, A. and Thiery, J.P. Multiple roles for integrins during development. *Biol. Cell* **89**, 5, 1997.
56. Davis, G.S., Phillips, H.M. and Steinberg, M.S. Germ-layer surface tensions and “tissue affinities” in *Rana pipiens* gastrulae: quantitative measurements. *Dev. Biol.* **192**, 630, 1997.
57. Boucaut, J.C. et al. Biologically active synthetic peptides as probes of embryonic development: a competitive peptide inhibitor of fibronectin function inhibits gastrulation in amphibian embryos and neural crest cell migration in avian embryos. *J. Cell Biol.* **99**, 1822, 1984.
58. Downie, S.A. and Newman, S.A. Different roles for fibronectin in the generation of fore and hind limb pre cartilage condensations. *Dev. Biol.* **172**, 519, 1995.
59. Corbett, S.A. and Schwarzbauer, J.E. Requirements for alpha(5)beta(1) integrin-mediated retraction of fibronectin-fibrin matrices. *J. Biol. Chem.* **274**, 20943, 1999.
60. Landowski, T.H., Olashaw, N.E., Agrawal, D. and Dalton, W.S. Cell adhesion-mediated drug resistance (CAM-DR) is associated with activation of NF-kappa B (RelB/p50) in myeloma cells. *Oncogene* **22**, 2417, 2003.
61. Fischbach, C. et al. Cancer cell angiogenic capability is regulated by 3D culture and integrin engagement. *Proc. Natl. Acad. Sci. U S A* **106**(2), 399, 2009.
62. Lark, A. L. et al. Overexpression of focal adhesion kinase in primary colorectal carcinomas and colorectal liver metastases: immunohistochemistry and real-time PCR analyses. *Clin. Cancer Res.* **9**, 215, 2003.
63. Cance, W. G. et al. Immunohistochemical analyses of focal adhesion kinase expression in benign and malignant human breast and colon tissues: correlation with preinvasive and invasive phenotypes. *Clin. Cancer Res.* **6**, 2417, 2000.
64. McCormack, S.J., Brazinski, S.E., Moore, J.L. Jr, Werness, B.A. & Goldstein, D.J. Activation of the focal adhesion kinase signal transduction pathway in cervical carcinoma cell lines and human genital epithelial cells immortalized with human papillomavirus type 18. *Oncogene* **15**, 265, 1997.
65. Naylor, T.L. et al. High resolution genomic analysis of sporadic breast cancer using array-based comparative genomic hybridization. *Breast Cancer Res.* **7**, R1186, 2005.

66. Mitra, S.K. and Schlaepfer, D.D. Integrin-regulated FAK-Src signaling in normal and cancer cells. *Curr. Opin. Cell Biol.* **18**, 516, 2006.
67. Mitra, S.K. et al., Intrinsic FAK activity and Y925 phosphorylation facilitate an angiogenic switch in tumors. *Oncogene* **25**, 5969, 2006.
68. Pages, G. and Pouyssegur, J. Transcriptional regulation of the Vascular Endothelial Growth Factor gene-a concert of activating factors. *Cardiovasc. Res.* **65**, 564, 2005.
69. Seko, Y. et al. Hypoxia induces activation and subcellular translocation of focal adhesion kinase (p125(FAK)) in cultured rat cardiac myocytes. *Biochem. Biophys. Res. Commun.* **262**, 290, 1999.
70. Kornberg, L.J., Shaw, L.C., Spoerri, P.E., Caballero, S. and Grant, M.B. Focal adhesion kinase overexpression induces enhanced pathological retinal angiogenesis. *Invest. Ophthalmol. Vis. Sci.* **45**, 4463, 2004.
71. Peng, X. et al. Overexpression of focal adhesion kinase in vascular endothelial cells promotes angiogenesis in transgenic mice. *Cardiovasc. Res.* **64**, 421, 2004.
72. Haskell, H. et al. Focal adhesion kinase is expressed in the angiogenic blood vessels of malignant astrocytic tumors in vivo and promotes capillary tube formation of brain microvascular endothelial cells. *Clin. Cancer Res.* **9**, 2157, 2003.
73. Ilic, D. et al. Focal adhesion kinase is required for blood vessel morphogenesis. *Circ. Res.* **92**, 300, 2003.
74. McCubrey, J.A. et al. Differential abilities of activated Raf oncoproteins to abrogate cytokine-dependency, prevent apoptosis and induce autocrine growth factor synthesis in human hematopoietic cells. *Leukemia* **12**, 1903, 1998.
75. Shelton, J.G. et al. Differential effects of kinase cascade inhibitors on neoplastic and cytokine-mediated cell proliferation. *Leukemia* **17**, 1765, 2003.
76. McCarthy, S.A., Samuels, M.L., Pritchard, C.A., Abraham, J.A. and McMahon, M. Rapid induction of heparin-binding epidermal growth factor/diphtheria toxin receptor expression by Raf and Ras oncogenes. *Genes Dev.* **9**, 1953, 1995.
77. Akula, S.M. et al. B-Raf dependent expression of vascular endothelial growth factor-A in Kaposi's sarcoma-associated herpesvirus infected human B cells. *Blood* **105**, 4516, 2005.

78. Akula, S.M. et al. Raf promotes human herpesvirus-8 (HHV-8/KSHV) infection. *Oncogene*. **23**, 5227, 2004.
79. Hamden, K.E., Ford, P.W., Whitman, A.G., McCubrey, J.A. and Akula, S.M. Raf induced Vascular Endothelial Growth Factor Augments Kaposi's Sarcoma-Associated Herpesvirus (KSHV/HHV-8) Infection. *J. Virol.* **78**, 13381, 2004.
80. Alessi, D.R. et al. Identification of the sites in MAP kinase kinase-1 phosphorylated by p74raf-1. *EMBO J.* **13**, 1610, 1994.
81. Baumann, B. et al. Raf induces NF- κ B by membrane shuttle kinase MEKK1, a signaling pathway critical for transformation. *Proc. Natl. Acad. Sci. USA* **97**, 4615, 2000.
82. Steelman, L.S. et al. JAK/STAT, Raf/MEK/ERK, PI3K/Akt and BCR-ABL in cell cycle progression and leukemogenesis. *Leukemia* **18**, 189–218, 2004.
83. Schouten, G.J. et al. I κ B α is a target for the mitogen-activated 90 kDa ribosomal S6 kinase. *EMBO J.* **16**, 3133, 1997.
84. Aplin, A.E., Stewart, S.A., Assoian, R.K. and Juliano, R.L. Integrin-mediated adhesion regulates ERK nuclear translocation and phosphorylation of Elk-1. *J. Cell Biol.* **153**, 273, 2001.
85. Chang, F. et al. Signal transduction mediated by the Ras/Raf/MEK/ERK pathway from cytokine receptors to transcription factors: potential targeting for therapeutic intervention. *Leukemia* **17**, 1263, 2003.
86. Bonizzi, G. and Karin, M. The two NF-kappaB activation pathways and their role in innate and adaptive immunity. *Trends Immunol.* **25**, 280, 2004.
87. Takahra, T., Smart, D.E., Oakley, F. and Mann, D.A. Induction of myofibroblast MMP-9 transcription in three-dimensional collagen I gel cultures: regulation by NF-kappaB, AP-1 and Sp1. *Int. J. Biochem. Cell Biol.* **36**, 353, 2004.
88. Friedland, J.C. et al. alpha6beta4 integrin activates Rac-dependent p21-activated kinase 1 to drive NF-kappaB-dependent resistance to apoptosis in 3D mammary acini. *J. Cell Sci.* **120**, 3700, 2007.
89. Nemeth, Z.H. et al. Disruption of the actin cytoskeleton results in nuclear factor- κ B activation and inflammatory mediator production in cultured human intestinal epithelial cells. *J. Cell Physiol.* **200**, 71, 2004.

90. Kolachala, V.L. Epithelial-derived fibronectin expression, signaling, and function in intestinal inflammation. *J. Biol. Chem.* **282**, 32965, 2007.
91. Chimenov, Y. & Kerppola, T. K. Close encounters of many kinds: Fos–Jun interactions that mediate transcription regulatory specificity. *Oncogene* **6**, 533, 2001.
92. Chang, L. & Karin, M. Mammalian MAP kinase signalling cascades. *Nature* **410**, 37, 2001.
93. Jack, G.D. et al. Long term metabolic arrest and recovery of HEK293 spheroids involves NF- κ B signaling and sustained JNK activation. *J. Cell. Physiol.* **206**, 526, 2006.
94. Jack, G.D. et al. Activated stress response pathways within multicellular aggregates utilize an autocrine component. *Cell Signal.* **19**, 772, 2007.
95. Wasylyk, B., Hahn, S.L., Giovane, A. The Ets family of transcription factors. *Eur. J. Biochem.* **211**, 7, 1993.
96. Vananzoni, M.C., Robinson, L.R., Hodge, D.R., Kola, I. and Seth, A. ETS1 and ETS2 in p53 regulatin: spatial separation of ETS binding sites (EBS) modulate protein: DNA interaction. *Oncogene* **12**, 1199, 1996.
97. Liu, S.H., Ng, S.Y. Serum response factor associated ETS proteins: ternary complex factors and PEA3-binding factor. *Biochem. Biophys. Res. Commun.* **201**, 1406, 1994.
98. Lambert, P.E., Ludford-Menting, M.J., Deacon, N.J., Kola, I. and Doherty, R.R. The nfkb1 promoter is controlled by proteins of the Ets family. *Mol. Biol. Cell* **8**, 313, 1997.
99. Nimer S.D., Zhang W., Kwan K., Whang Y. and Zhang J. Adjacent, cooperative elements form a strong, constitutive enhancer in the human granulocyte-macrophage colony-stimulating factor gene. *Blood* **87**, 3694, 1996.
100. Thomas, R.S. et al. ETS1, NF kappaB and AP1 synergistically transactivate the human GM-CSF promoter. *Oncogene* **14**, 2845, 1997.
101. Blumenthal, S.G. et al. Regulation of the human interleukin-5 promoter by Ets transcription factors. Ets1 and Ets2, but not Elf-1, cooperate with GATA3 and HTLV-I Tax1. *J. Biol. Chem.* **274**, 12910, 1999.
102. Wang, J., Shannon, M.F. and Young, I.G. A role for Ets1, synergizing with AP-1 and GATA-3 in the regulation of IL-5 transcription in mouse Th2 lymphocytes. *Int. Immunol.* **18**, 313, 2006.

103. Minami, T., Tachibana, K., Imanishi, T. and Doi, T. Both Ets-1 and GATA-1 are essential for positive regulation of platelet factor 4 gene expression. *Eur. J. Biochem.* **258**, 879, 1998.
104. Lu, J., Pazin, M.J. and Ravid, K. Properties of ets-1 binding to chromatin and its effect on platelet factor 4 gene expression. *Mol. Cell Biol.* **24**, 428, 2004.
105. Zhan, Y. et al. Ets-1 is a critical regulator of Ang II-mediated vascular inflammation and remodeling. *J. Clin. Invest.* **115**, 2508, 2005.
106. Qiao, J., Kang, J.H., Cree, J., Evers, B.M. and Chung, D.H. Ets1 transcription factor mediates gastrin-releasing peptide-induced IL-8 regulation in neuroblastoma cells. *Neoplasia* **9**, 184, 2007.
107. Eckes, B. et al. Interleukin-6 expression by fibroblasts grown in three-dimensional gel cultures. *FEBS Lett.* **298**, 229, 1992.
108. Shweiki, D., Neeman, M., Itin, A., and Keshet, E. Induction of vascular endothelial growth factor expression by hypoxia and by glucose deficiency in multicell spheroids: Implications for tumor angiogenesis. *Proc Natl Acad Sci USA* **92**, 768, 1995.
109. Sonoda, T., Kobayashi, H., Kaku, T., Hirakawa, T., Nakano, H. Expression of angiogenesis factors in monolayer culture, multicellular spheroid and in vivo transplanted tumor by human ovarian cancer cell lines. *Cancer Lett* **196**, 229, 2003.
110. Klapperich, C.M. and Bertozzi, C.R. Global gene expression of cells attached to a tissue engineering scaffold. *Biomaterials* **25**, 5631, 2004.
111. Ghosh, S. et al., Three-dimensional culture of melanoma cells profoundly affects gene expression profile: a high density oligonucleotide array study. *J. Cell Physiol.* **204**, 522, 2005.
112. Trojani, C. et al., Three-dimensional culture and differentiation of human osteogenic cells in an injectable hydroxypropylmethylcellulose hydrogel. *Biomaterials* **26**, 5509, 2005.
113. Liu, H., Lin, J. and Roy, K. Effect of 3D scaffold and dynamic culture condition on the global gene expression profile of mouse embryonic stem cells. *Biomaterials* **27**, 5978, 2006.

114. Birgersdotter, A. et al. Three-dimensional culturing of the Hodgkin lymphoma cell-line L1236 induces a HL tissue-like gene expression pattern. *Leuk. Lymphoma* 48, 2042, 2007.
115. Ghosh S, Josh MB, Ivanov D, FederMengus C, Spagnoli GC, Martin I, Erne P, Resink T. Use of multicellular tumor spheroids to dissect endothelial cell-tumor cell interactions: A role for T-cadherin in tumor angiogenesis. *FEBS Lett* 581, 4523, 2007.
116. Bhatia, M. et al. Placenta Derived Adherent Cell (PDAC) Interaction and Response on Extracellular Matrix Isolated from Human Placenta. *Wounds* 20(2), 2008.
117. Kankuri, E., Babusikova, O., Hlubinova, K., Salmenpera, P., Boccaccio, C., Lubitz, W., Harjula, A., Bizik, J. Fibroblast nemoisis arrests growth and induces differentiation of human leukemia cells. *Int J Cancer* 122, 1243, 2008.
118. de Barros, A.N.D. et al. Osteoblasts and Bone Marrow Mesenchymal Stromal Cells Control Hematopoietic Stem Cell Migration and Proliferation in 3D *In Vitro* Model. *PLoS One*. 5(2): e9093, 2010.
119. Bartosh, T.J., Ylostalo, J.H., Mohammadipoor, A., Bazhanov, N., Coble, K., Claypool, K., Lee, R.H., Choi, H., Prockop, D.J. Aggregation of human mesenchymal stromal cells (MSCs) into 3D spheroids enhances their anti inflammatory properties. *Proc Natl Acad Sci USA* 107, 13724, 2010.
120. Ho, W. J., Pham, E. A., Kim, J. W., Ng, C. W., Kim, J. H., Kamei, D. T. and Wu, B. M. Incorporation of multicellular spheroids into 3-D polymeric scaffolds provides an improved tumor model for screening anticancer drugs. *Cancer Science* 101, 2637, 2010.
121. Leung, M., Kievit, F.M., Florczyk, S.J., et al . Chitosan-alginate scaffold culture system for hepatocellular carcinoma increases malignancy and drug resistance. *Pharmaceutical Research* 27, 1939, 2010.
122. Verbridge, S.S., Choi, N.W., Zheng, Y., Brooks, D.J., Stroock, A.D., Fischbach, C. Oxygen-controlled three-dimensional cultures to analyze tumor angiogenesis. *Tissue Eng Part A* 16, 2133, 2010.
123. Tan, P.H., Aung, K.Z., Toh, S.L., Goh, J.C. & Nathan, S.S. Three-dimensional porous silk tumor constructs in the approximation of in vivo osteosarcoma physiology. *Biomaterials* 32, 6131, 2011.

124. Talukdar, S. and Kundu, S. C. A Non-Mulberry Silk Fibroin Protein Based 3D In Vitro Tumor Model for Evaluation of Anticancer Drug Activity. *Adv. Funct. Mater.* 22, 4778, 2012.
125. Yamada, K. M., Pankov, R. and Cukierman, E. Dimensions and dynamics in integrin function. *Braz. J. Med. Biol. Res.* **36(8)**, 959, 2003.
126. Bierwolf, J., Lutgehetmann, M., Feng, K., Erbes, J., Deichmann, S., Toronyi, E., Stieglitz, C., Nashan, B., Ma, P.X., Pollok, J.M. Primary rat hepatocyte culture on 3D nanofibrous polymer scaffolds for toxicology and pharmaceutical research. *Biotechnol Bioeng* 108, 141, 2011.
127. Crawford, J.M., Mockel, G.M., Crawford, A.R., Hagen, S.J., Hatch, V.C., Barnes, S., Godleski, J.J. and Carey, M.C. Imaging biliary lipid secretion in the rat: ultrastructural evidence for vesiculation of the hepatocyte canalicular membrane. *J Lipid Res* 36, 2147, 1995.
128. Uygun, B.E., Soto-Gutierrez, A., Yagi, H., Izamis, M.L., Guzzardi, M.A., Shulman, C., et al. Organ reengineering through development of a transplantable recellularized liver graft using decellularized liver matrix. *Nat Med* 16, 814, 2010.

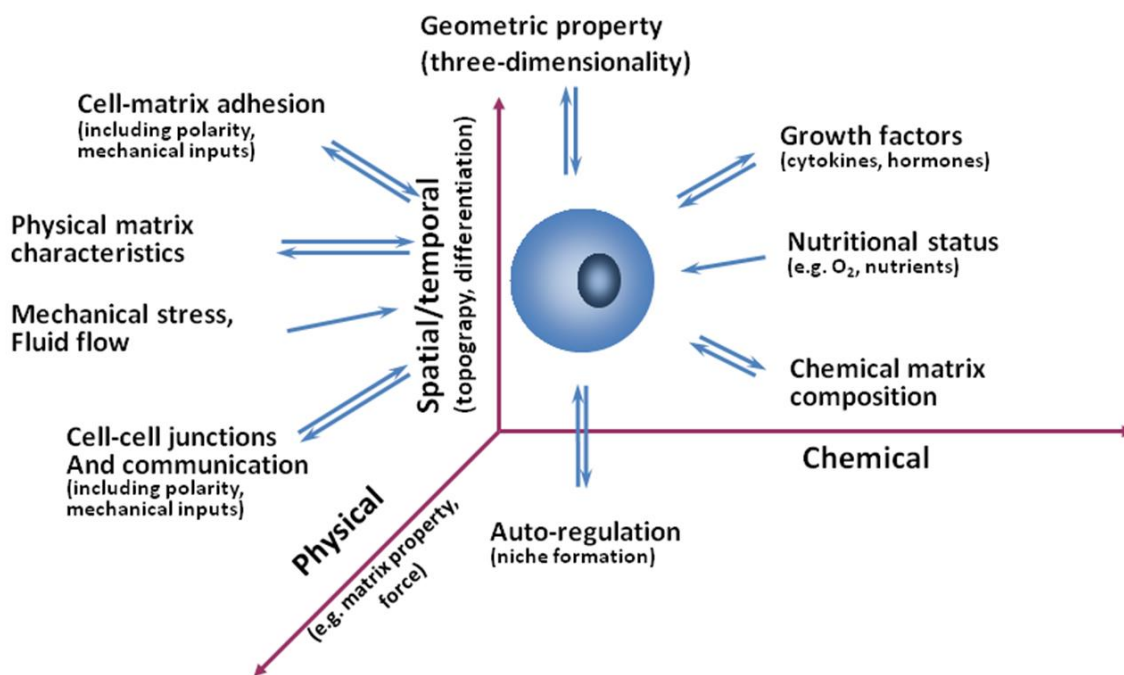


Figure 2.1. Microenvironment factors (MEFs) that regulate environmental cues to which cells respond resulting in specific cellular phenotype outcomes. The biochemical factor includes short range (e.g., substrate coatings) and long range (e.g., growth factors and nutrients) factors. The physical/force factor includes substrate material property (e.g., rigidity and mechanical inputs like stress). The spatial/temporal factor includes geometry (topography, aspect ratio, etc) and proliferation, migration, and differentiation. Adapted from Yamada et al.¹²⁵.

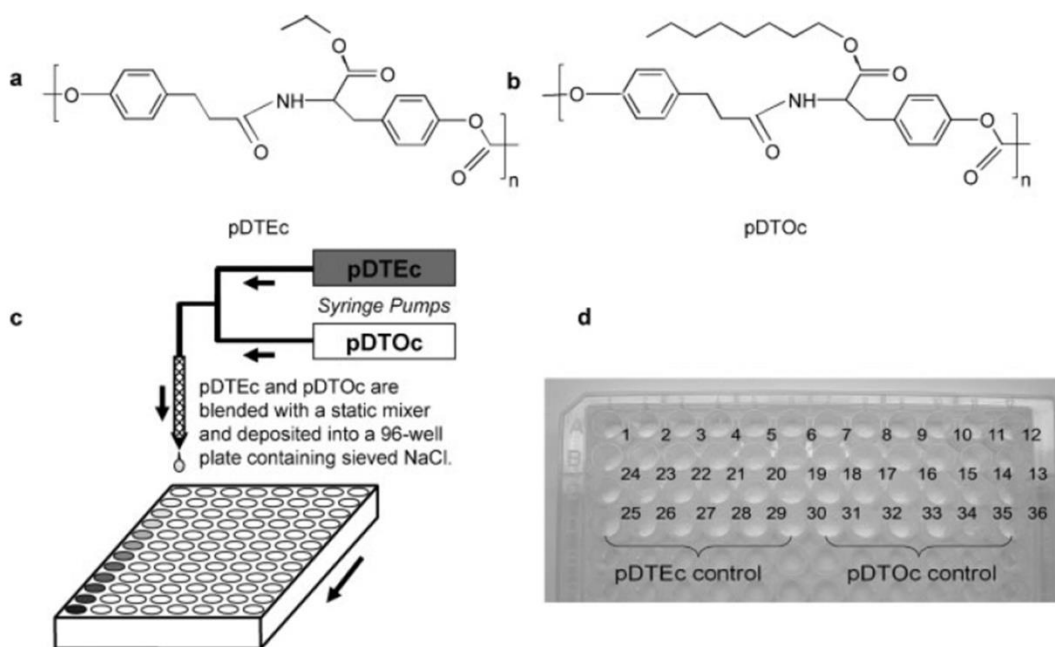


Figure 2.2. HTS scaffold material discovery conceptual framework. a) Chemical structure of pDTEc. b) Chemical structure of and pDTOc. c) Combinatorial fabrication of pPDTEc-pDTOc polymer blend scaffold library schematic. d) Porogen-leached and freeze-dried sample of scaffold library in a 96-well plate. With permission, from Kisaalita et al. (2010)¹.

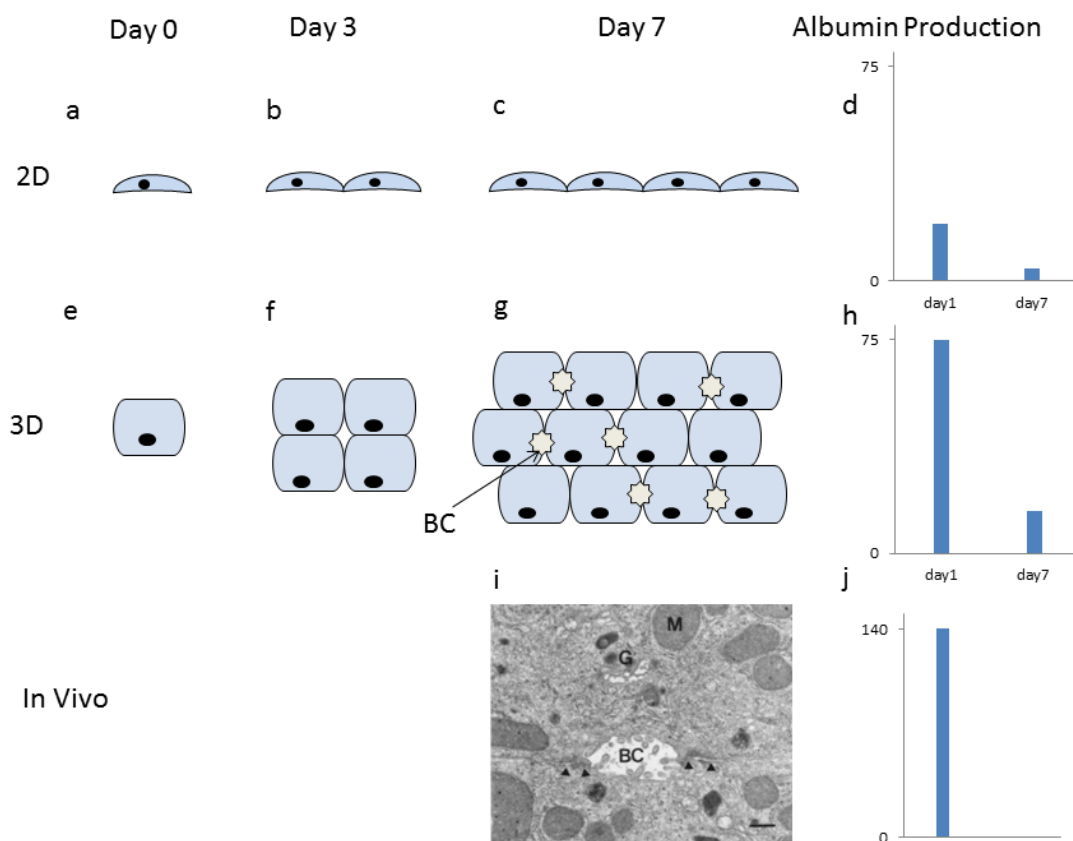


Figure 2.3. Complex physiological relevance (CPR) concept. A comparative structural gallery of 2D (abc), 3D (efg) and in vivo (i) hepatocyte cultures. In this illustration, unlike 2D, both the 3D and in vivo cultures express bile canaliculi. Additionally, the functional outcome of albumin secretion depicted in Figures d (2D), h (3D) and j (in vivo) show 3D closer to in vivo than to 2D. With such structural and functional outcomes, the 3D culture is considered to be expressing complex physiological relevance (CPR). Although preferred, it is however not necessary to have both structural and functional outcomes emulating the in vivo situation to have CPR. Data in d and h are in $\mu\text{g}/1 \times 10^6$ cells and were obtained from Bierwolf et al.¹²⁶. The micrograph in i was obtained from Crawford et al.¹²⁷ and data in j was calculated in $\mu\text{g}/1 \times 10^6$ cells from Uygun et

al.¹²⁸. The labeled components of i are the bile canaliculus (BC), mitochondria (M), Golgi apparatus (G) and tight junctional regions (arrowheads).

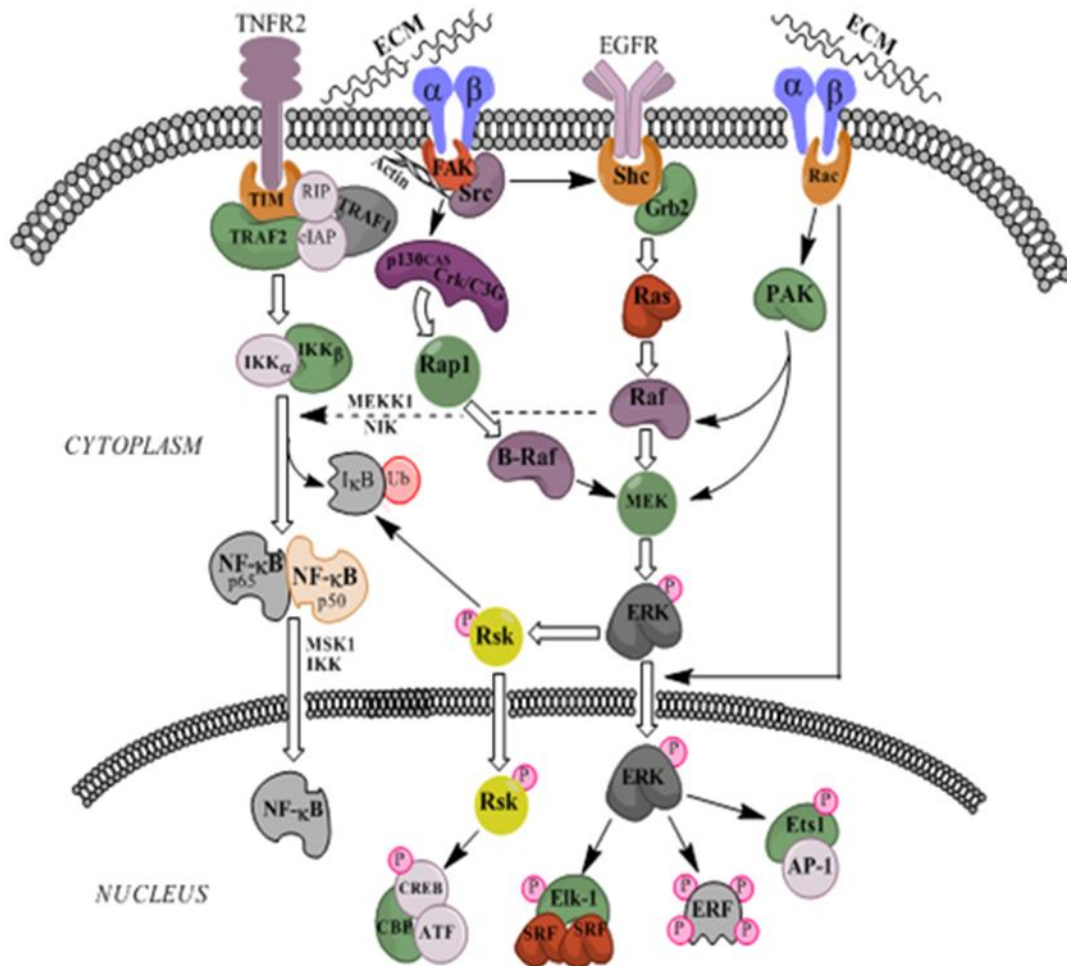


Figure 2.4. Erk and subsequent transcription factor activation via ECM-integrin binding.

Upstream events in the signaling cascade like integrin mediated adhesion to ECM lead to GTP loading of Ras in many ways like activation of Src and phosphorylation of Shc and Grb2.

Transmission of the signal to Raf and subsequently to MEK and ERK is mitigated in suspended cells as there exists an evident anchorage-dependent step between Ras and Raf. A similar anchorage dependent signal relay seems to be present between Raf and MEK. These two activation steps are regulated by integrin dependent PAKs. The activation of ERK can be achieved through heterologous expression of active upstream components like Raf (22W Raf) or

MEK1 (MEK1- Δ ED) in suspended cells but still the signal is transmitted poorly to the nucleus⁸⁴ as integrin activated Rac regulates ERK translocation to the nucleus along with controlling ERK activation through PAK. MEK activation is also controlled by B-Raf, which in turn is activated through engagement of FAK with the actin cytoskeleton and subsequent formation of focal complexes. There is also a close interplay between the ERK pathway and NF- κ B, with Rsk⁸³ and Raf⁸¹ regulating its activation. In the nucleus, ERK is involved in the activation of all the three sub classes of Ets family of transcription factors and formation of the ternary nucleoprotein complex between TCFs (Elk-1, Net and Sap-1) and Serum Response Factor (SRF) over the Serum Response Element (SRE) of the promoter. Activation of RSK in the cytoplasm and translocation to the nucleus further activates CREB⁸⁵.

Abbreviations: ECM-Extracellular matrix, EGFR-Epidermal growth factor receptor, FAK-Focal adhesion kinase, Src-Rous sarcoma oncogene cellular homolog, Shc – Adapter protein involved in oncogenesis, GRB2-Growth factor receptor-bound protein 2, PAK-p21-activated kinase, Crk/C3G-CT10 sarcoma oncogene cellular homolog/Guanine nucleotide-releasing factor 2, Rap1-Repressor activator protein 1, MEK-MAPK/ERK kinase, ERK-Extracellular signal-regulated kinase, Rsk-Ribosomal protein S6 kinase, TNFR2-Tumor necrosis factor Receptor 2, TIM – T cell immunoglobulin- and mucin-domain-containing molecule, RIP-Receptor-interacting protein, TRAF1-TNF receptor-associated factor 1, TRAF2-TNF receptor-associated factor 2, cIAP-Cellular inhibitor of apoptosis protein, IKK-I κ B kinase, Ub-Ubiquitin, NF- κ B-Nuclear factor κ B, I κ B-Inhibitor of NF- κ B, MEKK1-MAPK/Erk kinase kinase 1, NIK-NF- κ B-inducing kinase, MSK1-Mitogen and stress activated kinase 1, CREB-cAMP response element-binding protein, ATF-Activating transcription factor, CBP-CREB binding protein, SRF-Serum

Response Factor, ERF-ETS2 Repressor Factor, AP-1-Activator protein 1, Ets-E26 AMV virus
oncogene cellular homolog, Elk-Ets like transcription factor

Table 2.1. Transcriptomic/proteomic up-regulation of cytokines in 3D cultures.

Cell Line	Cell Type	3D Scaffold	Cytokines ¹	Ref
Fibroblasts	Primary (biopsy)	Collagen matrix	IL6	Eckes et al. ¹⁰⁷
C6	Rat glial tumor cell line	Spheroids	VEGF	Shweiki et al. ¹⁰⁸
MCAS, SKOV/MG	Ovarian cancer cell lines	Spheroids by liquid overlay	VEGF	Sonoda et al. ¹⁰⁹
IMR-90	Human fetal lung fibroblasts	Collagen – GAG matrix	IL-8, CXCL1, CXCL2, CXCL3, CXCL5, VEGF, LIF	Klapperich & Bertozzi ¹¹⁰
NA8	Melanoma	Spheroids on pHEMA plates	CXCL1, IL-8, MIP-3a , Angiopoetin like4, CXCL2,3	Ghosh et al. ¹¹¹
MG-63, SaOS-2	Human osteosarcoma	Si-HPMC polymer hydrogel	IL-6, GM-CSF	Trojani et al. ¹¹²
R1	Murine ES cells	Cytomatrix RW-spinner culture	BMP-4, IGF2	Liu et al. ¹¹³
L1236	Hodgkin-lymphoma derived cell line	RADA-oligopeptide matrix	CCL4, CCL5, CCL17, CCL22, IL-13, TNF, TNFS2, TNFS7, INHBA	Birgersdott er et al. ¹¹⁴
NA8	Melanoma	Spheroids on pHEMA plates	IL-8, VEGF, ANGPTL4	Ghosh et al. ¹¹⁵
PDAC	Pluripotent Progenitor Cell	pECM	IL-6, IL-8, MCP-1	Bhatia et al. ¹¹⁶
HFSF-132	Human foreskin fibroblasts	Spheroids	IL-1β, IL-6, IL-8, IL-11, GM-CSF, LIF	Kankuri et al. ¹¹⁷
HFSF, CRL-2088 HES HAL MRC-5	Human foreskin fibroblasts Embryonic skin fibroblasts Adult lung fibroblasts Embryonic lung fibroblasts	Spheroids on Agarose plates	CCL2-5, CXCL1-3, 8 CXCL8 CXCL8 CXCL8	Enzerink et al. ³¹
OSCC3 U87 MDA-MB231	Oral Squamous Carcinoma Glioblastoma Breast cancer	PLG, RGD alginate, Matrigel	IL8, VEGF	Fischbach et al. ³⁹
BMSC	Bone marrow derived mesenchymal stroma cells	Spheroids on Agarose plates	CXCL12, Wnt5a, KITLG	de Barros et al. ¹¹⁸

hMSC	Mesenchymal stem cells	Spheroids	IL-24, LIF, Stanniocalcin-1	Bartosh et al. ¹¹⁹
U251	Glioma cell line	Collagen coated PLGA 3D scaffolds	VEGF, bFGF	Ho et al. ¹²⁰
PLC, HepG2	Hepatocellular carcinoma	Chitosan- alginate	VEGF, bFGF, IL-8	Leung et al. ¹²¹
OSCC3 U87	Oral Squamous Carcinoma Glioblastoma	alginate	VEGF, IL-8	Verbridge et al. ¹²²
143.98.2	Osteosarcoma	Silk fibroin scaffold	VEGF, IL-8	Tan et al. ¹²³
MDA-MB- 231	Breast cancer	3D fibroin scaffold	VEGF, IL-8	Talukdar & Kundu ¹²⁴

¹Bold indicates protein results, other results are only transcriptomic.

CHAPTER 3

CALCIUM OSCILLATION FREQUENCY IS A FUNCTIONAL COMPLEX PHYSIOLOGICAL RELEVANCE INDICATOR FOR A NEUROBLASTOMA BASED 3D (SPHEROID) CULTURE MODEL²

²Asthana A, Mendez D, Cheng X and Kisaalita WS. To be submitted to Tissue Engineering:

3.1 Abstract

In vitro screening for drugs that affect neural function in vivo is still primitive. It primarily relies on single cellular responses from 2D monolayer cultures that have been shown to be exaggerations of the in vivo response. In order for the 3D model to be physiologically relevant it should express characteristics that not only differentiate it from 2D but also be similar to those seen in vivo. These complex physiologically relevant outcomes (CPR) can serve as a standard for determining how close a 3D culture is to its native tissue or which out of a given number of 3D platforms is better suited for a given application. In this study we try to establish calcium oscillation frequency as a potential functional CPR for neural cultures. It was found that calcium oscillation frequency is upregulated in traditional 2D cultures while it was found to be comparable to in vivo in our SH-SY5Y based spheroid 3D model. It was also found that cells in 3D proceeded towards a more differentiated state with time without the need for an exogenous differentiating agent.

3.2 Introduction

Neurodegenerative disorders are one of the most devastating illnesses and as such effective drug discovery against them is need. In the new target-driven drug discovery paradigm, genomic sciences and combinatorial chemistry are synergistically leading to the development of diverse molecular libraries. These libraries can yield promising drug candidates - hits that can be developed into leads, which demonstrate activity in animal models, if effectively screened¹⁻³. In order to quickly and efficiently identify potential hits from these libraries, application of cell based assays or biosensors together with automated high throughput screening (HTS) are the state of the art^{4,5}. SH-SY5Y, a neuroblastoma derived cell line, has been commonly used for

studying properties of neurotoxins, the pathogenesis of neurodegenerative diseases and development and screening of drugs against them⁶⁻⁹. However, in vitro screening for drugs that affect neural function in vivo is still primitive as current assays rely on single cellular responses from 2D monolayer cultures^{10, 11}. It has been hypothesized that cellular responses obtained from 2D platforms, such as SH-SY5Y calcium dynamics¹², are an exaggeration of the in vivo situation, which may partly explain the lack of noticeable differences in Investigational New Drug applications before and after the adoption of the aforementioned target-driven drug discovery paradigm by pharmaceutical and biotechnology industries¹³. It has been proposed that three-dimensional (3D) cell-based assays may yield “physiologically more relevant” results and thus have the potential to save time and cost by reducing drug candidate attrition through early fidelity matching of drug candidates and targets¹⁴.

In order for the 3D model to be physiologically relevant it should express characteristics that not only differentiate it from 2D but also be similar to those seen in vivo. These complex physiologically relevant outcomes (CPR) can serve as a standard for determining how close a 3D culture is to its native tissue or which out of a given number of 3D platforms is better suited for a given application. For instance, hepatic tissues have well defined CPR outcomes like albumin production, bile canaliculi formation and cytochrome p450 activity. Similarly, beat frequency and contraction force can be used to show physiological relevance of a culture¹⁵. However, the literature on cells of neuronal origin has not provided a consensus toward establishing a neuronal microtissue CPR; but several phenomena are more worthy of further exploration. For example, intracellular calcium oscillations are an innate characteristic of neural cells in vivo and play a pivotal

role in synaptic signal transmission. Although oscillatory calcium waves have been observed in both 2D and 3D nerve cell cultures, we submit that there should be differences in the nature of oscillations between the two cultures. The frequency of these oscillations found in 3D cultures is considerably lower (3.42/600s; brain slices¹⁶, 8/600s; NP cells derived from neurospheres¹⁷) than that found in 2D (60/600s¹⁸, 60/600s¹⁹) and is closer to in vivo (3.6/600s²⁰). In this study we show that the frequency of calcium oscillations is a promising CPR for SH-SY5Y neuroblastoma 3D (spheroid) model. Further studies with different cells of neural origin and/or platforms are needed to conclusively establish this neural CPR indicator.

3.3 Materials and Methods

3.3.1 Cell line and cell culture

SH-SY5Y human neuroblastoma cells were obtained from ATCC and routinely cultured in 75 cm² tissue culture flasks (Costar, Corning, NY) in Dulbecco's Modified Eagle Medium: Nutrient Mixture F-12 (DMEM/F12) (Life Technologies) containing 10% heat inactivated fetal bovine serum (FBS), 2.2 g/L sodium bicarbonate, 2 mM l-glutamine and 1 mM sodium pyruvate in 5% CO₂ at 37 °C. Medium was changed every 2 days. At 75% confluence, the cells were detached by using 0.25% Trypsin-EDTA (Gibco®) and re-suspended in growth medium for plating. For differentiating cells, a half medium change was performed every day with differentiation medium after the second day of plating, hereafter referred to as day 0 into differentiation. The differentiation medium was comprised of DMEM/F12 with 1% FBS, 2.2 g/L sodium bicarbonate, 2 mM l-glutamine, 1 mM sodium pyruvate and 10 μM Retinoic Acid (RA).

3.3.2 Spheroid culture and characterization

SH-SY5Y spheroids (500 cells/spheroid) were fabricated in AggreWell™400 plate according to the manufacturer's protocol. Briefly, the wells were first coated with 5% Pluronic F-127 to avoid attachment. Cells were counted using Millipore Scepter 2.0 handheld automated cell counter and 6×10^5 cells (in 2 ml medium) were seeded in each well followed by centrifugation at $150 \times g$ for 5 minutes. For non-differentiated cells half medium was changed twice daily. After 48 hours, for differentiating cells, a half medium change was performed every day with differentiation medium. After 72 hours of incubation the wells were triturated and the spheroids were resuspended in 100mm dishes coated with 5mg/ml Poly(2-hydroxyethyl methacrylate) (poly HEMA) to avoid attachment. Spheroid size distribution for differentiated and undifferentiated spheroids was determined using ImageJ software from phase contrast images of spheroids taken every day from 3-8 days.

3.3.3 Calcium imaging

Both differentiated and undifferentiated 2D and spheroid cultures were observed for $[Ca^{2+}]_i$ oscillations on days 3, 6 and 9. Fluo-4/AM, a Ca^{2+} -sensitive fluorescent dye (Invitrogen) was dissolved in DMSO to a concentration of 1 mM and used as a stock solution. This solution was diluted to a final concentration of 2 μ M with Hank's basal salt solution (HBSS; with calcium and magnesium) consisting of 20 mM HEPES buffer (pH 7.4). Finally, Probenecid and Pluronic-127 were added to a final concentration of 2.5 mM and 0.02%, respectively. The cells were incubated with the Fluo-4/AM solution at 37 °C for 60 min in MatTek® glass bottom Petri dishes (Cat#: P35G-0-10; well diameter: 10

mm). After washing out excess dye, 2 mL of HBSS solution was added to the plate and it was incubated at room temperature in dark for another 40 minutes. The cells were analyzed under Leica TCS SP2 confocal microscope. The changes in the intensity were measured by using Simple PCI image analysis software. To collect Fluo-4 fluorescence signals, regions of interest (ROI) were drawn electronically around individual cells in the recording field. The fluorescence intensities from the ROIs were digitized and changes in $[Ca^{2+}]_c$ were monitored as changes in the relative fluorescence of Fluo-4, where an increase in fluorescence intensity, measured in arbitrary fluorescence units (afu), reflected a proportional increase in $[Ca^{2+}]_c$ concentration. All measurements were performed at room temperature (22–24°C). The data was transferred to an excel file that was analyzed using a MatLab program that calculated the oscillation frequency of each cell per 600s.

3.3.4 Flow cytometry

Rabbit anti-NSE primary and Alexa 488 goat anti-rabbit secondary antibodies were bought from Abcam (MA, USA) and Invitrogen, respectively. For flow cytometry, standard protocol was followed. Briefly, 1×10^6 cells were fixed with 100 μ l of 4% paraformaldehyde and 0.1% Triton-X at room temperature for 20 minutes. After removal of fixative, cell were incubated with ice cold methanol for 30 minutes at -20°C. After centrifugation washing with 3% BSA in PBS, primary antibody was added (10 μ g/ml) and cells were incubated overnight at 4°C. After washing with the wash buffer, secondary antibody (1:500) was added and the cells were incubated for an hour at room temperature. After the final wash with wash buffer, cell were resuspended in 500 μ l PBS and taken for flow cytometry. The fluorescence was recorded by

collecting 20,000 events on a Cyan flow cytometer. The median fluorescence intensity was used for comparisons.

3.4 Results and Discussion

3.4.1 Characterization of SH-SY5Y spheroids

Spheroids were fabricated using AggreWell™ plates. The size/time profile of spheroids obtained from the analysis of phase contrast images taken every 24 hours over 8 days is shown in Figure 3.1c. Compact tissue-like spheroids cultures were observed at day 3-4 (Figure 3.1a). Over 8 days the size of the non-differentiated spheroids increased from 73 to 100 μm while the differentiated spheroids increased from 84 to 88 μm . However, the mean size for both was found to be not significantly different. The constant size of the RA differentiated spheroids is expected as the proliferation rate decreases when cells start differentiation. However, the undifferentiated spheroids being tumorous should have proliferated over time. This can be explained by the fact that cells growing in 3D tend to have lower growth rates than 2D cultures^{21, 22} as 3D by itself leads the cells towards a more differentiated state. Human neuroblastoma cells generally exhibit characteristics of de-differentiation where they have reentered S-phase of the cell cycle, and are highly resistant to apoptosis^{23, 24}. Amplification in the expression of the proto-oncogene N-myc has been correlated with cellular de-differentiation and increased resistance to apoptosis, and is believed to have a crucial role in maintenance of the cells' malignant phenotype^{25, 26}. However, it has been shown that 3D culture can lead to a reduction in the expression of N-myc which can contribute to an increase in cellular differentiation²¹ (Myers et al., 2008).

3.4.2 Analysis of calcium oscillations

It is a well-known fact that responses in 2D are exaggerated. We believe that the same might be true for intracellular calcium transients. It has already been shown in primary cultures that the frequency of these oscillations found in 3D cultures is considerably lower (3.42/600s; brain slices¹⁶, 8/600s; NP cells derived from neurospheres¹⁷) than that found in 2D (60/600s¹⁸, 60/600s¹⁹) and is closer to in vivo (3.6/600s²⁰). Here we report similar findings for SH-SY5Y cells. The median calcium oscillation frequencies for 2D differentiated, 3D differentiated and 3D undifferentiated on days 3, 6 and 9 are shown in Figure 3.2. The frequency for 2D differentiated and undifferentiated cultures increased with time while that for 3D cultures remained constant or showed slight increase. The higher frequency of 2D differentiated cells makes sense as it is a known fact that differentiated SH-SY5Y cells are more excitable and have higher membrane potential relative to undifferentiated cells²⁷. The frequency of the non-differentiated spheroid became comparable to the differentiated spheroid at later time points. This can be explained by the fact that it took 3 to 4 days for tissue compaction and only after that time the spheroid started exhibiting behavior similar to the native tissue. This also shows that with longer time in culture, the non-differentiated spheroid starts displaying behavior similar to the exogenously differentiated spheroid and this might render the use of a differentiation agent like RA redundant.

Recently, Lai et al. (2012)²⁸ showed that calcium increases in response to high K⁺ depolarization were similar for 3D cultured and freshly dissected mouse superior cervical ganglion (SCG) cells, but significantly higher for 2D cells. Their results indicated that the higher response in 2D might be due to differences in membrane architecture, specifically the co-localization of L-type VGCC and Caveolin1 (marker for lipid rafts); their distribution being

more punctuated in 2D and more diffused in 3D²⁸. As L-type VGCC facilitates calcium signaling, their being clustered in 2D might explain the high oscillation frequency in monolayer cultures.

3.4.2 Flow cytometric analysis of neuronal marker

Differentiated SH-SY5Y cells are morphologically, biochemically and electrophysiologically more similar to neurons. They express a variety of neuronal markers like growth-associated protein (GAP-43), neuron-specific enolase (NSE), neuronal nuclei (NeuN), receptors for neurotropic factors, neuropeptides vesicle proteins such as synaptophysin, and neuronal-specific cytoskeletal proteins, including microtubule associated protein (MAP)²⁷. SH-SY5Y cells can be differentiated by treatment with a variety of agents, including retinoic acid (RA), phorbol ester 12-O-tetradecanoylphorbol-13-acetate (TPA), brain derived neurotrophic factor (BDNF), dibutyryl cyclic AMP (dBcAMP) or staurosporine, with RA being one of the more commonly used agents. However, apart from cell differentiation, RA can trigger survival signaling in different cell types^{29, 30} which might alter the cellular response to neurotoxins. It has been shown that RA-differentiated cells are less susceptible to Parkinson mimetics than undifferentiated cells due to the upregulation of survival signaling (Akt and Erk1/2) that can protect differentiated SH-SY5Y cells from Parkinson mimicking agents^{31, 32}.

As stated earlier, we hypothesize that 3D can differentiate cells even in the absence of exogenous differentiating agents, thus eliminating the need to use RA along with its undesired effects. To determine the extent of differentiation in 2D differentiated and 3D undifferentiated cultures we used NSE as a neuronal marker and analyzed the

amount of NSE expressed using flow cytometry at three time points (Days 3, 6 and 9). The level of NSE in 3D undifferentiated cultures was found to be higher compared to 2D differentiated cells on all the three time points as shown in Figure 3.3 and also showed an increase with time in culture. 2D on the other hand, increased from day 3 to 6 but showed a decrease on day 9. This can be due to the fact that SH-SY5Y cells consist of two morphologically and biochemically distinct phenotypes: neuroblastic (N-type) and substrate adherent (S-type). Differentiation with RA exhibits proliferation control on the N-type population and it has been shown that after around 10 days of culture in the presence of RA, the percentage of S-type cells can progressively increase. In fact, long term treatments with RA have been shown to subsequently shift the proportion between the N-type and S-type phenotypes toward the S-type one³³. This provides another reason why differentiation with RA is not suitable.

3.5 Conclusion

Calcium oscillation frequency was found to be higher in 2D but lower and similar to in vivo in our 3D culture which substantiates that it has potential as a marker of complex functional physiological relevance. Additionally, it was also shown that cells in 3D can differentiate on their own without the need for an exogenous agent therefore removing the other undesirable effects of the differentiation agent.

3.6 References

1. Hogan Jr JC. Combinatorial chemistry in drug discovery. *Nature Biotechnology* 1997, 15:328-330.
2. Guild BC. Genomics, target selection, validation, and assay considerations in the development of antibacterial screens. *Annu. Rep. Med. Chem.* 1999, 34:227–236.

3. Debouck C and Metcalf B. The impact of genomics on drug discovery. *Annu. Rev. Pharmacol. Toxicol.* 2000, 40:193–208.
4. Drews J. Drug discovery: a historical perspective. *Science* 2000, 287(5460):1960-1964.
5. Boldt GE, Dickerson TJ, Janda KD. Emerging chemical and biological approaches for the preparation of discovery libraries. *Drug Discovery Today* 2006, 11:143-148.
6. Chang, R. C. C., Suen, K. C., Ma, C. H., Elyaman, W., Ng, H. K., & Hugon, J. (2002). Involvement of double-stranded RNA-dependent protein kinase and phosphorylation of eukaryotic initiation factor-2 α in neuronal degeneration. *Journal of neurochemistry*, 83(5), 1215-1225.
7. Xue, S., Jia, L., & Jia, J. (2006). Hypoxia and reoxygenation increased BACE1 mRNA and protein levels in human neuroblastoma SH-SY5Y cells. *Neuroscience letters*, 405(3), 231-235.
8. Zheng, L., Roberg, K., Jerhammar, F., Marcusson, J., & Terman, A. (2006). Autophagy of amyloid beta-protein in differentiated neuroblastoma cells exposed to oxidative stress. *Neuroscience letters*, 394(3), 184-189.
9. Levites, Y., Amit, T., Youdim, M. B., & Mandel, S. (2002). Involvement of protein kinase C activation and cell survival/cell cycle genes in green tea polyphenol (–)-epigallocatechin 3-gallate neuroprotective action. *Journal of Biological Chemistry*, 277(34), 30574-30580.
10. Gross GW, Harsch A, Rhoades BK, Gopel W. Odor, drug and toxin analysis with neuronal networks in vitro: extracellular array recording of network responses. *Biosensors & Bioelectronics* 1997, 12(5):373-393.
11. Gross GW, Rhoades BK, Azzazy HME, Wu MC. The use of neuronal networks on multielectrode arrays as biosensors. *Biosensors & Bioelectronics* 1995, 10:553-567.
12. Desai, A., Kisaalita, W. S., Keith, C., & Wu, Z. Z. (2006). Human neuroblastoma (SH-SY5Y) cell culture and differentiation in 3-D collagen hydrogels for cell-based biosensing. *Biosensors and Bioelectronics*, 21(8), 1483-1492.
13. DiMasi JA, Hansen RW, Grabowski HG. The price of innovation: new estimates of drug development costs. *Journal of Health Economics* 2003, 22:151–185.
14. Kunz-Schughart LA, Freyer JP, Hofstaedter F, Ebner R. The use of 3-D cultures for high-throughput screening: the multicellular spheroid model. *J. Biomol. Screen.* 2004, 9:273-285

15. Asthana, A., & Kisaalita, W. S. (2013). Biophysical microenvironment and 3D culture physiological relevance. *Drug discovery today*, 18(11), 533-540.
16. Kawamura, M. Jr., and Kawamura, M. 2011. Long-term facilitation of spontaneous calcium oscillations in astrocytes with endogenous adenosine in hippocampal slice cultures. *Cell Calcium* 49:249-258.
17. Striedinger, K., Meda, P., and Scemes, E. 2007. Exocytosis of ATP from astrocyte progenitors modulates spontaneous Ca²⁺ oscillations and cell migration. *Glia* 55:652-662.
18. Numakawa, T., Yamagishi, S., Adachi, N., Matsumoto, T., Yokomaku, D., Yamada, M., and Hatanaka, H. 2002. Brain-derived neurotrophic factor-induced potentiation of Ca(2+) oscillations in developing cortical neurons. *J Biol Chem* 277:6520-6529.
19. Hemstapat, K., Smith, M.T., and Monteith, G.R. 2004. Measurement of intracellular Ca²⁺ in cultured rat embryonic hippocampal neurons using a fluorescence microplate reader: potential application to biomolecular screening. *J Pharmacol Toxicol Methods* 49:81-87.
20. Kuribara, M., Eijssink, V.D., Roubos, E.W., Jenks, B.G., and Scheenen, W.J. 2010. BDNF stimulates Ca²⁺ oscillation frequency in melanotrope cells of *Xenopus laevis*: contribution of IP₃-receptor-mediated release of intracellular Ca²⁺ to gene expression. *Gen Comp Endocrinol* 169:123-129.
21. Myers, T. A., Nickerson, C. A., Kaushal, D., Ott, C. M., Höner zu Bentrup, K., Ramamurthy, R., & Philipp, M. T. (2008). Closing the phenotypic gap between transformed neuronal cell lines in culture and untransformed neurons. *Journal of neuroscience methods*, 174(1), 31-41.
22. dit Faute, M. A., Laurent, L., Ploton, D., Poupon, M. F., Jardillier, J. C., & Bobichon, H. (2002). Distinctive alterations of invasiveness, drug resistance and cell-cell organization in 3D-cultures of MCF-7, a human breast cancer cell line, and its multidrug resistant variant. *Clinical & experimental metastasis*, 19(2), 161-167.
23. Kang JH, Rychahou PG, Ishola TA, Qiao J, Evers BM, Chung DH. MYCN silencing induces differentiation and apoptosis in human neuroblastoma cells. *Biochemical and biophysical research communications*. 2006;351:192-7.
24. van Noesel MM, Pieters R, Voute PA, Versteeg R. The N-myc paradox: N-myc overexpression in neuroblastomas is associated with sensitivity as well as resistance to apoptosis. *Cancer letters*. 2003;197:165-72.

25. Grandinetti KB, Spengler BA, Biedler JL, Ross RA. Loss of one HuD allele on chromosome #1p selects for amplification of the N-myc proto-oncogene in human neuroblastoma cells. *Oncogene*. 2006;25:706–12.
26. van Golen CM, Soules ME, Grauman AR, Feldman EL. N-Myc overexpression leads to decreased beta1 integrin expression and increased apoptosis in human neuroblastoma cells. *Oncogene*. 2003;22:2664–73.
27. Xie, H. R., Hu, L. S., & Li, G. Y. (2010). SH-SY5Y human neuroblastoma cell line: in vitro cell model of dopaminergic neurons in Parkinson's disease. *Chin Med J (Engl)*, 123(8), 1086-1092.
28. Lai, Y., Cheng, K., & Kisaalita, W. (2012). Three dimensional neuronal cell cultures more accurately model voltage gated calcium channel functionality in freshly dissected nerve tissue. *PloS one*, 7(9), e45074.
29. Paillaud E, Costa S, Fages C, Plassat JL, Rochette-Egly C, Monville C, et al. Retinoic acid increases proliferation rate of GL-15 glioma cells, involving activation of STAT-3 transcription factor. *J Neurosci Res* 2002;67:670–9.
30. Lee, J. H., Shin, S. Y., Kim, S., Choo, J., & Lee, Y. H. Suppression of PTEN expression during aggregation with retinoic acid in P19 mouse embryonal carcinoma cells. *Biochem Biophys Res Commun* 2006;347:715–22.
31. Cheung, Y. T., Lau, W. K. W., Yu, M. S., Lai, C. S. W., Yeung, S. C., So, K. F., & Chang, R. C. C. (2009). Effects of all-trans-retinoic acid on human SH-SY5Y neuroblastoma as in vitro model in neurotoxicity research. *Neurotoxicology*, 30(1), 127-135.
32. Cavanaugh JE, Jaumotte JD, Lakoski JM, Zigmond MJ. Neuroprotective role of ERK1/2 and ERK5 in a dopaminergic cell line under basal conditions and in response to oxidative stress. *J Neurosci Res* 2006; 84:1367–75.
33. Encinas, M., Iglesias, M., Liu, Y., Wang, H., Muhaisen, A., Cena, V. & Comella, J. X. (2000). Sequential Treatment of SH-SY5Y Cells with Retinoic Acid and Brain-Derived Neurotrophic Factor Gives Rise to Fully Differentiated, Neurotrophic Factor-Dependent, Human Neuron-Like Cells. *Journal of neurochemistry*, 75(3), 991-1003.

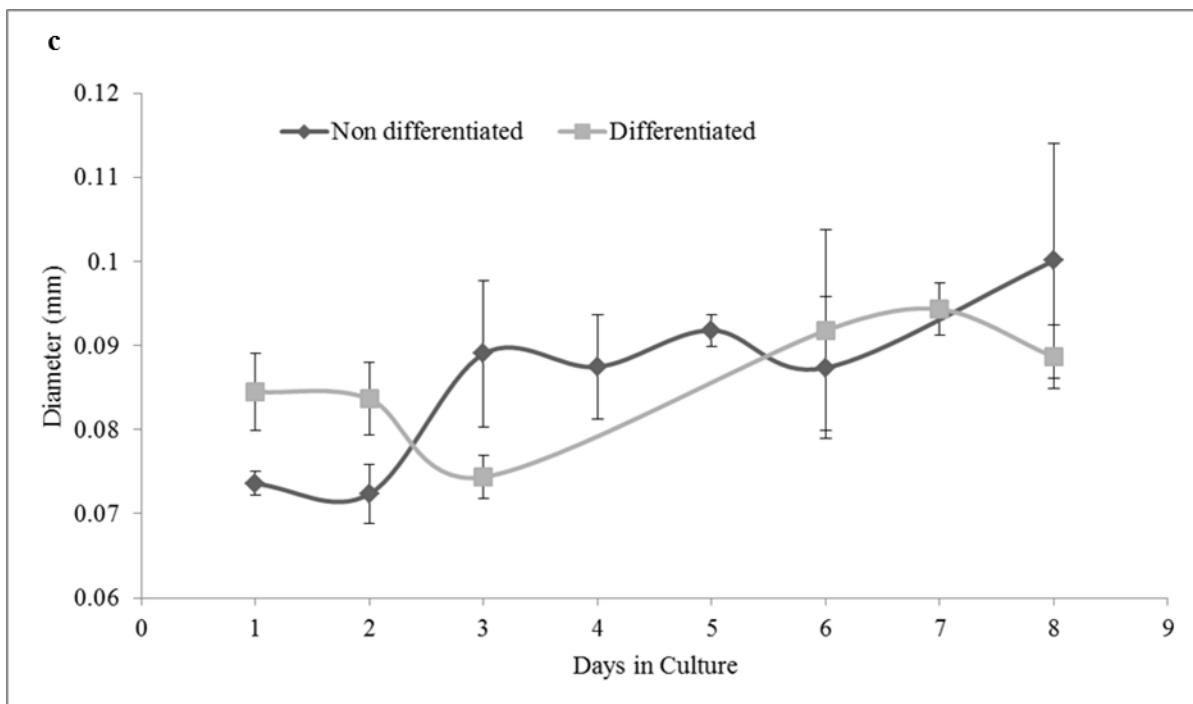
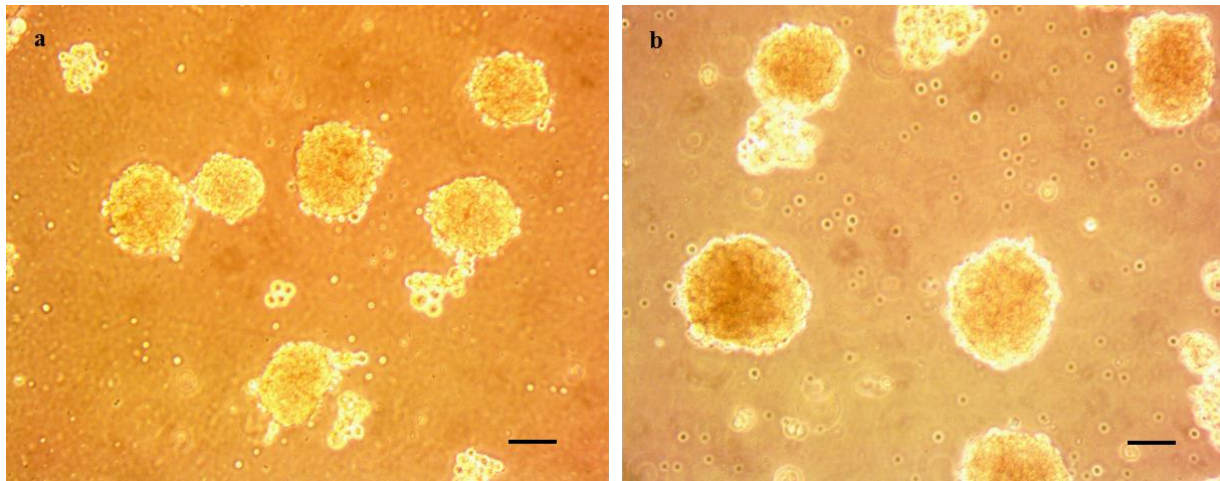


Figure 3.1. Phase contrast images show formation of compact spheroids on Day 4 of culture (a). The spheroids had grown slightly in size on day 8 (b). (c) Shows the size/time profile of neuroblastoma spheroids. Phase contrast images of spheroids were taken over 8 days of culture and analyzed to get the diameter. Each point shows the mean \pm SD (n>5). Bar is 100 μ m for (a) and (b).

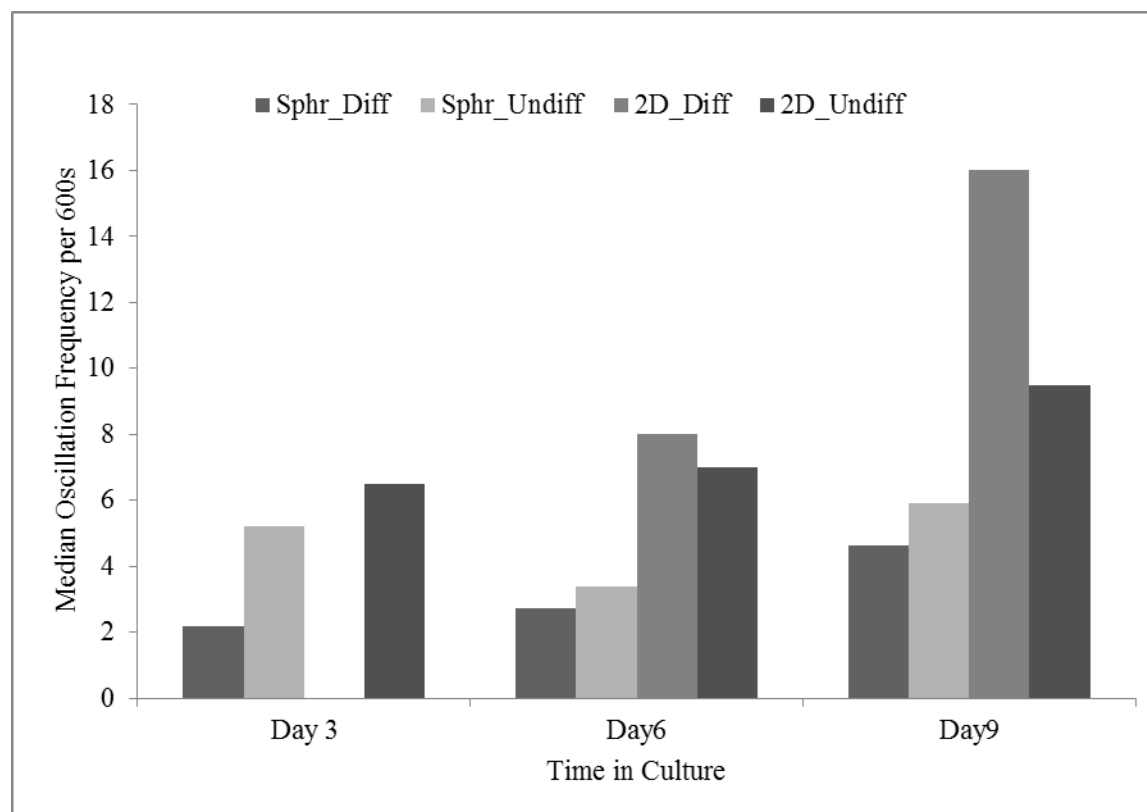


Figure 3.2. Variation of median calcium oscillation frequency with culture time. The median frequency was plotted for differentiated spheroid, undifferentiated spheroid, differentiated 2D and undifferentiated 2D on days 3, 6 and 9. The frequency was found to be higher for 2D compared to 3D on all the three time points.

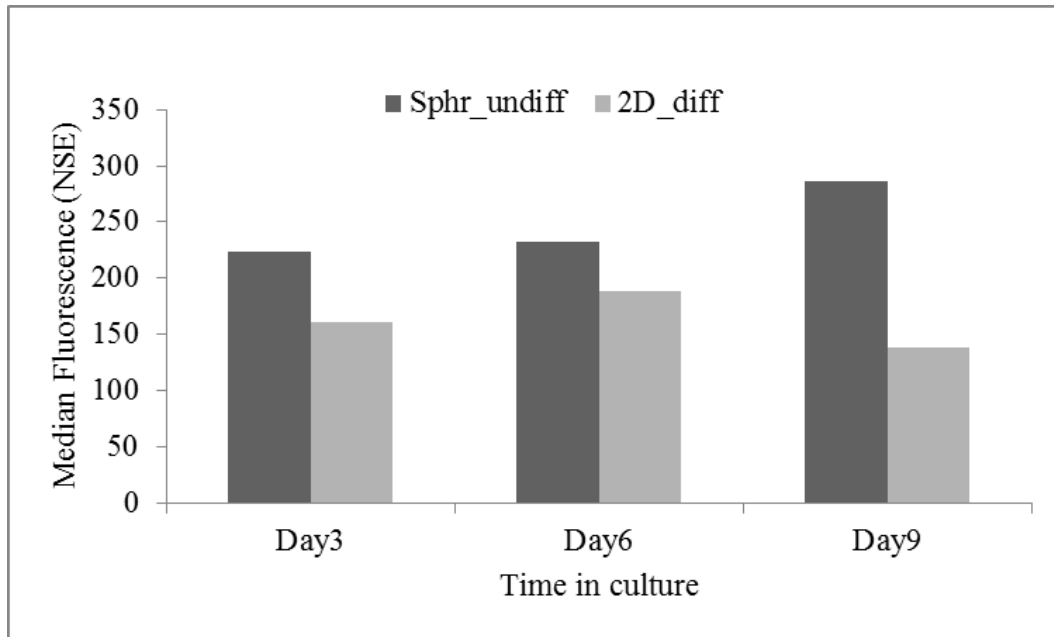


Figure 3.3. Neuron specific enolase (NSE) content of 2D differentiated cells was found to be lower than the 3D undifferentiated cells on all the three time points. The medians were calculated from the events versus log fluorescence intensity graphs obtained after flow cytometry.

CHAPTER 4
THE EFFECT OF 3D MICROENVIRONEMT ON STRUCTURE AND FUNCTION OF
HEPG2 MICROTISSUES³

³Asthana A, White C and Kisaalita WS. To be submitted to Biomaterials

4.1 Abstract

The effect of the three microenvironmental factors (spatial, physical and biochemical) on the formation of bile canaliculi like structures and the production of albumin in HepG2 cells was investigated in time to determine the optimal microenvironmental composition that produces a 3D in vitro model that is closest to the native tissue. Firstly, to find the effect of spatial cues on the complex functionality of the cells, four different cell seeding densities were chosen to form spheroids. Subsequently, the mean size of the least and most functional spheroids was selected and polymeric scaffolds having a similar pore size were fabricated to find out if the introduction of a substrate (physical factor) would lead to any significant difference in the functionality. Finally, biochemical signals were introduced by adding Fibronectin to the spheroids or coating it on the scaffold surfaces to find out if it altered the complex functionality of the cells. It was found that size or the spatial factor is most important out of the three, if it is too large, hypoxia can manifest in the core of the tissue thereby decreasing the hepatic functions. Also, the physical property of the substrate and exogenous chemical coatings did not significantly alter the behavior of the cells because they are rendered redundant as the tissue develops its own Extracellular matrix (ECM) with time. Therefore the microenvironment provided by the PLLA micro porous scaffold developed in this study was found to be most optimal for developing a hepatic model with structural integrity and complex functionality.

4.2 Introduction

The liver is responsible for many vital functions including bile acid synthesis, hepatobiliary circulation, drug metabolism and transport and producing a myriad of proteins that are critical to homeostasis. Drug-induced liver injury or hepatotoxicity is a problem of increasing

frequency and importance in the United States as it is a major deciding factor behind the approval, withdrawal or limitation in the usage of the drug by the Food and Drug Administration (FDA). There are over 900 drugs that have been implicated in causing liver injury after two years of marketing¹. The continuous increase in the number of compound failures and increasing costs associated with drug and substance development, call for the use of biologically more complex cell based assays and their physiological relevance is a key requirement to improve the predictive power of these models. Currently, hepatocellular carcinoma cells (HepG2) cultured in 2D monolayers are the most recognized hepatocyte-like cells routinely used for screening drugs against such hepatotoxicity. However, cells in this format entirely lack or express acutely low levels of many drug metabolizing enzymes (Cytochrome P450s - CYPs) and transporters found in hepatocytes *in vivo*². It has been demonstrated at mRNA and protein expression levels that HepG2 in general express lower amounts of drug metabolizing enzymes and many liver specific genes³ including CYPs.

In contrast, 3D hepatocyte-like cell cultures achieved in bioreactors have been shown to emulate *in vivo* characteristics to such a high degree that they can be utilized to fabricate a functional bioartificial organ for transplantation^{4,5}. Three dimensionality means providing a total microenvironment to the cells that supports the formation of a microtissue that exhibits “complex” physiological relevance (CPR) or better emulation of the *in vivo* functionality in a manner not possible in 2D cultures⁶. The critical components of this microenvironment or microenvironment factors (MEFs) or “three-dimensions” can be expressed as: 1) chemical or biochemical composition, 2) spatial (geometric 3D) and temporal dimensions, and 3) force and substrate physical properties⁶⁻⁸. The microenvironmental factors affect cell behavior and functionality and lead to responses that are not just “different,” but are physiologically more

relevant, when compared to cells cultured on traditional 2D surfaces. To be meaningful, it is necessary to conclusively show that these responses produced in 3D formats are emulations of those that are seen in-vivo and can serve as a standard for determining how close a 3D culture is to its native tissue or which out of a given number of 3D platforms is better suited for a given application.

Due to the vast amount of literature available, both structural and functional CPR responses for liver cells can be established easily and have been discussed in detail by Asthana and Kisaalita (2013)⁹. For the purpose of this study, formation of bile canaliculi like structures and production of albumin have been used as structural and functional CPR responses, respectively. The effect of the three microenvironmental factors (spatial, physical and biochemical) on CPR has been observed in time to determine the optimal microenvironmental composition that produces a 3D in vitro model that is closest to the native tissue.

4.3 Materials and Methods

4.3.1 Scaffold fabrication

The microporous polymer scaffold was fabricated using the salt leaching method routinely used in our laboratory¹⁰. Briefly, poly L-lactic acid (PLLA) was dissolved in chloroform and then sieved sodium carbonate decahydrate particles were added to the polymer solution and mixed thoroughly. The casting mixture was composed of 0.2 g PLLA, 2.5 g sodium carbonate decahydrate and 4 ml chloroform. The size of the salt particles used was in the range of 106-125 μm (Scaffold A) and 218-250 μm (Scaffold B). 140 μL of the solution was casted in MatTek® glass bottom Petri dishes (Cat#: P35G-0-10; well diameter: 10 mm). After casting, the plate was immediately covered to control the evaporation rate of chloroform. This step was

crucial as chloroform also served as an adhesive to “weld” the scaffold by partially dissolving the polystyrene wall of the well. After chloroform was completely evaporated, the dishes were leached with water overnight. Then the scaffold was treated with 0.2 M NaOH for 40 minutes at 40°C to make it hydrophilic. After washing with water thrice, the scaffold was sterilized in 70% ethanol (3 hours) and UV (30 mins). Finally, to increase cell adhesion, the scaffold was coated with fibronectin (8 µg in 150 µL PBS).

4.3.2 Scaffold characterization

4.3.2.1 Porosity measurement

The porosity of the polymer scaffolds was measured by a modified liquid displacement method¹¹. Ethanol was used as the displacement liquid as it penetrated easily into the pores and did not induce shrinkage or swelling. The scaffolds were carefully removed from the dishes with an ultra-sharp blade and then submerged in ethanol.

4.3.2.2 Surface energy and contact angle measurement

Contact Angle System OCA (Future Digital Scientific Corp.) with analysis software (SCA20) was used to determine the surface contact angles on the nanofibrous PLLA samples both before and after NaOH treatment. Distilled water was used as a contacting solvent. All data were obtained 5 s after placing the droplet on the surfaces under ambient conditions. The surface energy of the contacting surface (E_s) was calculated according to $E_s = E_{lv}\cos\theta$. E_{lv} is the surface energy between the water and air, which is 72.8 mJ/m² at 20°C for pure water; θ is the static contact angle¹².

4.3.2.3 Pore size distribution

The pore size distribution of the scaffolds was determined by analyzing SEM images using ImageJ software from collective SEM top view images of the sponges. Detailed protocol for SEM is described in the following section.

4.3.3 Scanning electron microscopy (SEM)

Cells on PLLA scaffolds or spheroids were fixed with 2.5% glutaraldehyde in 0.1 M sodium cacodylate buffer, pH 7.2 for 1 h before rinsing in cacodylate buffer (without glutaraldehyde) three times, 15 min each. This was followed by post-fixing with 1% OsO₄ in 0.1 M sodium cacodylate buffer for 1 h and rinsing in cacodylate buffer (without OsO₄) three times, 5 min each. The samples were then dehydrated successively in 30%, 50%, 70%, 80%, 95% and 100% ethanol for 10 min each and dried in a SAMDRI-780A critical point drier (Tousimis Research Corporation, Rockville, MD, USA). Patterns were sputter-coated with gold for 60 s to achieve a coating thickness of about 15.3 nm. SEM images were captured with a FEI Inspect-F scanning electron microscope (SEM) (FEI Company, OR). A similar protocol was followed for scaffold samples without cells, with the exception that the preparation started with sputter coating.

4.3.4 HepG2 cell culture

HepG2 human hepatocellular carcinoma cells (HB-8065) (ATCC, VA) were routinely cultured in 75 cm² tissue culture flasks (Costar, Corning, NY) in Dulbecco's Modified Eagle Medium (DMEM) (Life Technologies) containing 10% heat inactivated fetal bovine serum (FBS), 2.2 g/L sodium bicarbonate, 2 mM l-glutamine and 1 mM sodium pyruvate in 5% CO₂ at

37 °C. At 75% confluence, the cells were detached by using 0.25% Trypsin-EDTA (Gibco®) and re-suspended in growth medium for plating. For seeding on scaffolds, cells were counted using Millipore Scepter 2.0 handheld automated cell counter and 7×10^5 cells (in 140 μ l medium) were seeded on each scaffold. After allowing 4 hours for attachment, the medium was removed and 2 ml fresh growth medium was added to each plate. Control 2D cultures were plated in 48 well tissue culture plates in 500 μ l of medium.

4.3.5 Spheroid culture

HepG2 spheroids were fabricated in either AggreWell™400 (1000 cells/spheroid) or AggreWell™800 (2000 cells/spheroid, 5000 cells/spheroid) plates depending upon the cell number for each spheroid according to the manufacturer's protocol. Briefly, the wells were first coated with 5% Pluronic F-127 to avoid attachment and then cell solution of desired cell density was added and the plates were centrifuged for 5 minutes at 355 x g. After 24 hours of incubation the wells were triturated and the spheroids were resuspended in either 100 mm dishes or 48 well plates (one spheroid in each well; 500 μ l medium) coated with 5 mg/ml Poly(2-hydroxyethyl methacrylate) (poly HEMA) to avoid attachment.

4.3.6 Spheroid characterization

Spheroid size distribution was determined using ImageJ software from phase contrast images of spheroids taken every 24 hours for 8 days. SEM images were taken from spheroids fixed (protocol as described before) on days 3, 5 and 9 and analyzed for morphology and ECM deposition.

4.3.7 Functional and structural assessment

4.3.7.1 Transmission electron microscopy

Scaffolds and spheroids were fixed with 2.5% glutaraldehyde for 30 min and treated with 1% OsO₄ for 2 h at room temperature. Samples were subsequently dehydrated step-wise with ethanol (25%, 50%, 75%, 95% and 100%) for 10 min followed by 100% propylene oxide (PO) twice for 20 min each. Upon dehydration, samples were then treated with 1:1 ratio mixture of PO and Epon resin overnight at room temperature. On the following day, the samples were placed into Epon resin for 30 min at room temperature before transferring into a 40 °C oven for another 30 min. Resin was subsequently changed followed by 1 h treatments at 45 °C and 1 h at 50 °C. Lastly, the samples were embedded with Epon resin at 60 °C for 24 h. Ultrathin sections of 70–90 nm thickness were sliced using a Leica EM UC6 Ultramicrotome, collected onto 200-mesh copper grids and co-stained with uranyl acetate and lead citrate for 10 min each. Observation was undertaken with a Transmission Electron Microscope (TEM) (JEOL JEM-1010, Japan) at voltage 100 kV.

4.3.7.2 Biliary excretion of fluorescein dye

For monitoring the functional status of HepG2 cell polarization, the excretion of fluorescein dye via bile canaliculi was monitored. Spheroids were incubated with 15 µg/mL fluorescein diacetate (Molecular Probes, USA) in culture medium at 37 °C for 45 min at different time intervals (3 and 5 days) post-seeding. The cultures were then rinsed and fixed with 3.7% paraformaldehyde for 30 min before viewing with a 20× lens on a Zeiss Meta 510 upright confocal microscope.

4.3.7.3 Albumin Secretion

Albumin secretion from HepG2 cells in 2D, scaffolds and spheroids was quantified by a sandwich enzyme-linked immunosorbent assay (ELISA) using a human albumin ELISA kit (Bethyl Laboratories, Montgomery, TX), according to manufacturer's protocol. 500 μ l of culture medium was collected every 24 h and kept at -80°C until analysis. The data was normalized by the number of cells at the respective time point quantified using Pierce LDH Cytotoxicity Assay Kit (Thermo Fisher Scientific, IL, USA).

4.3.8 Statistical analysis

Statistical comparisons were undertaken using paired two-tailed Student t tests. Results were expressed as mean \pm standard error of the mean.

4.4 Results and Discussion

4.4.1 Fabrication and characterization of the 3D scaffold

The fabrication process is illustrated in Figure 4.1. As shown, a viscous polymer solution was prepared by dissolving PLLA chloroform solution with sodium carbonate decahydrate particles. Sived particles ranging in size from 106-125 μm (Scaffold A) and 218-250 μm (Scaffold B) were used. The solution mixture was then cast into the wells MatTek plates. After chloroform was completely evaporated, the dishes and plates were leached with water to remove the salt, creating a thin porous polymer scaffold. Figure 4.2 a and d show SEM images of the fabricated 3D cell culture scaffold A and B, respectively. The porosity of the 3D scaffolds was determined by liquid displacement method to be 89%. The average pore size was found by the analysis of SEM images to be 92 ± 16 and 157 ± 38 μm , respectively. The pore size range was a found to be

smaller than the size range of salt particles used. The two aforementioned pore size ranges were chosen with respect to the size of the cells seeded onto the scaffolds. Smaller pores prevented cell invasion, while bigger pores ($>200\mu\text{m}$) acted more identical to 2D surfaces¹³. As pointed out by Asthana and Kisaalita (2012)¹⁴, the major advantage of this type of scaffold is that they have a defined geometry and controllable pore sizes that provide a strict spatial control on the dimension of the microtissues and thereby, the development of hypoxia which might be detrimental to the functionality of the tissues. Also, they are better suited for incorporation in HTS state of the art instrumentation when compared to spheroids or hydrogels. The drawback of using PLLA is that the pliability of synthetic polymers is above the physiological range and so it is usually assumed that they fail to provide the optimum biophysical cues for the cells⁹. However, it should be noted that it is not just the material that affects the pliability but also the form in which it is presented. For example, polystyrene in its bulk state as used in tissue culture plates has a very high elastic modulus ($2 - 4 \text{ MPa}$ ¹⁵) but when used to fabricate salt leached microporous scaffolds, it exhibits a considerably lower modulus (77 kPa ¹⁶).

PLLA is hydrophobic in nature which is not suitable for cell culture. In order to alter the surface wettability, the scaffolds were treated with $0.2M$ NaOH. It has been shown that treatment of PLLA with NaOH increases material wettability and surface roughness at nanometer scale which in turn lead to improved cell adhesion¹⁷. Due to the treatment, the contact angle of PLLA film decreased from 116.4° to 46.4° and surface energy increased from -32.3 to 50.2 mJ/m^2 . After coating with Fibronectin (FN; $8 \mu\text{g/scaffold}$), 7×10^5 cells (in $140 \mu\text{l}$ medium) were seeded on each scaffold and tissue formation on both the scaffolds was observed by taking SEM images at different time points (days 3 and 7) during culture period (8 days) and the results are shown in Figure 4.2 (b,c) and 4.2 (e,f) for scaffold A and B, respectively. The round morphology of the

cells which is a characteristic of 3D culture is visually evident in the pores of both the scaffolds. Single cell surfaces can be seen on day 3 but are less evident on day 7 signifying compaction of tissues and production of Extracellular Matrix (ECM). By comparing parts b and e it can be concluded that ECM deposition started early in scaffold B which is totally embedded in ECM by day 7(f) and individual pores cannot be identified. As such the pore size of scaffold B seems to be more conducive for 3D cell culture.

4.4.2 Characterization of HepG2 spheroids

Spheroids starting with different cell numbers (1000, 2000 and 5000) were fabricated using AggreWell™ plates. The size/time profile of HepG2 spheroids obtained from the analysis of phase contrast images taken every 24 hours over 8 days is shown in Figure 4.3. Compact tissue-like spheroids cultures were observed at day 3-4 (Figure 4.4a). The spheroids became compact earlier than the tissues growing in scaffold A (day3; Figure 4.4a) probably due to centrifugation and the lack of adhesion with the substrate. At all the three cell numbers compact spheroids of reproducible diameters were produced. Moreover, cell proliferation was evident due to the continuously increasing spheroid sizes (Figure 4.3). This lack of control on tissue size is a major disadvantage while developing a hepatic model as the spheroids might become hypoxic as their size increases with time thereby reducing their functionality. In 1000 cells/spheroid (smallest) at day 8, the mean diameter was found to be 326 μm while that for 2000 and 5000 cells/spheroid was observed to be 390 and 490 μm , respectively. This might indicate manifestation of hypoxia in the core of the spheroids as oxygen is usually most readily depleted due to its relatively low solubility in culture medium (the diffusion coefficient of oxygen in culture medium is $2 \times 10^{-5} \text{ cm}^2/\text{s}$) compared to gradients in glucose and amino acids that are

almost negligible. It is known that oxygen can diffuse across 100-200 μm thickness of cells¹⁸ and therefore it is generally desired to control the size of the aggregates below 300 μm ¹⁹ and so a better control on tissue size is required. The size of the 1000 cells/spheroid and 1000 cells/spheroid with FN added to it were comparable. The mean size of the spheroids over the course of culture is represented in Figure 4.6a.

4.4.3 Structural and functional assessment of cells

One of the basic structural phenomena that distinguish liver cells in the native tissue from those cultured in 2D formats is polarity. While those in their natural environment possess structural and functional polarity^{20, 21}, the ones that are isolated and cultured on most flat non-porous surfaces do not^{22, 23}. Most hepatic functions like biliary excretion, albumin secretion and urea synthesis are thought to be dependent on the polarized phenotype of the cells. In their native conditions, hepatocytes maintain a cuboidal shape, with two to three basal surfaces facing the sinusoid. The lateral domain between adjacent cells is divided by a polygonal network of microvilli-lined bile canaliculi which is formed by membranes contributed from contiguous cells and comprises the apical domain of cells.

The ultra-structure of HepG2 cells cultured on scaffold A and as spheroids was examined by TEM. A time profile of bile canalicular network development in both spheroid (1000) and scaffold A is shown in Figure 4.5. Spheroids showed the presence of tight junctions and bile canaliculi like structures as early as day 3 (Figure 4.5b). A network of microvilli lined channels was seen on day 6. Development of canalicular structure was seen later in scaffolds (around day 9; Figure 4.5d) probably due to the slower compaction of the tissues. However multiple tight junctions and microvilli lined canalicular networks were observed on day 9 and 12 (Figure 4.5e

& f), respectively. The presence of a wide range of organelles typically found in most mammalian cells like mitochondria, nuclei, endoplasmic reticulum and Golgi complex were observed in both spheroids and scaffolds. Biliary excretion was also examined by the addition of fluorescein diacetate dye at various time intervals, including 72 (Figure 4.5a) and 120 h post-seeding. Viable cells in the spheroids will cleave FDA into fluorescein dye by intracellular esterases which then be excreted by MRP2 into the bile canaliculi. FDA staining in the spheroids showed an accumulation in the bile canaliculus between cells.

In order to quantify the effect of the three microenvironmental factors on the functionality of cells, albumin secretion from the different growth platforms was analyzed. Among the three spheroids, the 1000 cell spheroid was found to have the highest mean specific productivity ($4.38 \mu\text{g}/10^6 \text{cells/day}$) over the culture period and was significantly higher than 2D ($1.61 \mu\text{g}/10^6 \text{cells/day}$). Meanwhile the 2000 and 5000 cell spheroids, even though 3D had lower productivity than 2D. This might be due to the fact that their sizes were too big as discussed before (Figure 4.3 and 4.6a) and might have developed a hypoxic core reducing their productivity which points to the fact that spatial (size) factor is important for functionality.

Once the spatial parameter was optimized, the 1000 cell/spheroid was chosen to analyze the effect of exogenous ECM proteins on the functional CPR response elicited from the cells. Bovine Plasma Fibronectin was chosen as a representative as it has been shown that FN is major component required for compact spheroid formation and activation of fibroblasts²⁴. Cells lacking in FN expression (FN^{-/-}) or having mutated ligation site for integrin $\alpha_5\beta_1$ (FN^{RGE/RGE}) were found to be loosely adherent. Also, FN^{RGE/RGE} cells showed reduced accumulation of endogenous FN than the wild-type cells, but no such decrease in accumulation of FN was evident in 2D cultures, suggesting that the formation of compact spheroids and accumulation of FN was RGD-

dependent and is more dependent on RGD- $\alpha_5\beta_1$ integrin interaction in 3D than in monolayers. Moreover, adhesion in cell-derived matrices was found to be solely dependent on integrin $\alpha_5\beta_1$ ²⁵ (Cukierman et al, 2001), which is the major receptor for FN. Intuitively, it was predicted that the set of integrin involved in 3D matrix adhesions would be complex due to the presence of multiple molecules in the matrix, however that was not the case. Moreover, it has also been shown that a 3D matrix can promote $\alpha_5\beta_1$ integrin activation²⁶ and lead to transdominant inhibition of integrin $\alpha_v\beta_3$ (another FN receptor) which is a characteristic component of focal adhesions in 2D but is absent from the “3D matrix adhesions” formed on fibrillar cell derived 3D matrices⁸. No significant difference was observed between the albumin production in control 1000 cell/spheroid and the ones containing exogenous FN (Figure 4.6a). In spite of this result it is hard to conclude that exogenous FN does not have any effect on the function of the cells in 3D due to a few constraints in the study. Firstly, FN was added to the spheroid containing medium in soluble form and so its affect might be differed from when RGD peptides are cross-linked in the scaffold architecture or FN is adsorbed on a surface. Second, a fixed concentration of FN was used which had been calculated by normalizing against the number of cells present in spheroids (1000) to the scaffold (7×10^5) while coating the scaffold (1cm diameter) at $5 \mu\text{g}/\text{cm}^2$. It might be that this particular concentration is too low to cause a significant effect in the albumin productivity of the spheroids.

Finally, to determine the effect of the biophysical cues, the mean albumin productivity of the spheroid (no exogenous biophysical factors) was compared to scaffold B (“rigid” biophysical microenvironment). As discussed above the Young’s modulus of synthetic polymers is above the physiological range, therefore they intuitively do not provide the cells with an optimal environment. However, the mean albumin productivity was found to be not significantly

different between the two platforms over 8 days in culture (4.38 $\mu\text{g}/106\text{cells}/\text{day}$ for spheroid vs. 3.57 $\mu\text{g}/106\text{cells}/\text{day}$ for Scaffold B) while it was significantly higher for the scaffold compared to 2D (Figure 4.6b). This might be due to the fact that the scaffold is 89% porous and the Young's Modulus is considerably lower for porous substrates compared to the bulk state (Asthana and Kisaalita, 2013). Another possible explanation for the above lack of pliability effect comes from the "cell-on-cell" hypothesis²⁷, where cell to cell contacts appear to play a more pivotal role as neighboring cells provide a soft "stroma" for surrounding cells and produce responses similar to those seen when cells are grown in softer gels. When cells are seeded at a high density, as in the case of the scaffold, the cell-cell interactions might supersede the cell-substrate interaction leading to the formation of a cohesive microtissue such that only the outermost layer is in contact with the substrate while others are in contact with each other. Moreover, the surface of the scaffold and the pores is not flat, rather rough and porous and nanofibrous (image not shown). Therefore the engagement of cells with the surface should not result in the development of actin stress fibers as happens on a flat 2D TCPS. This is further substantiated by the fact that the cell matrix adhesions achieved in the scaffold are quite similar to the "3D matrix adhesions" (Cukierman et al, 2001) ergo, more physiologically relevant to in vivo as shown by downregulated FAK Y397 staining (Cheng et al., 2008). Finally, the deposition of endogenous ECM, which happens as early as day 3 in scaffold B (Figure 4.2e) can provide a pliable microenvironment for the cells irrespective of the modulus of the scaffold.

4.5 Conclusion

This study shows that the microenvironment plays a part in defining the functionality of the model. The size or the spatial factor is most important of the three and hypoxia should be

avoided as it decreases the hepatic functions. Also, the physical property of the substrate does not significantly alter the behavior of the cells. Exogenous chemical coatings are also rendered redundant as the tissue develops its own ECM with time. The ideal pore size for the scaffold was also established and its function was comparable to the spheroid. It can be a better suited liver model to HTS drug screening as it exerts a physical constraint on the size of the microtissue.

4.6 References

1. Friedman, S.E.; Grendel, J.H.; McQuaid, K.R. (2003) Current Diagnostics & Treatment in Gastroenterology. New York: Lang Medical Books/McGraw-Hill, p 664-679.
2. Wilkening S. *et al.* Comparison of primary hepatocytes and hepatoma cell line HepG2 with regard to their biotransformation properties. *Drug Metab. Disp.*, 31 (2003), 1035–1042.
3. Ek, M.; Soderdahl, T.; Kuppers-Munther, B.; Edsbagge, J.; Andersson, T.B.; Bjorquist, P.; Cotgreave, I.; Jernstrom, B.; Ingelman-Sundberg, M.; Johansson, I. (2007) Expression of drug metabolizing enzymes in hepatocyte-like cells. *Chemical Pharmacology* 74:496-503.
4. Morsiani, E.; Brogli, M.; Galavotti, D.; Bellini, T.; Ricci, D.; Pazzi, P.; Puviani, A.C. (2001) Long-term expression of highly differentiated functions by isolated porcine hepatocytes perfused in a radial-flow bioreactor. *Artificial Organs* 25(9):740-748.
5. Miyashita, T.; Enosawa, S.; Suzuki, S.; Tamura, H.; Amemiya, H.; Matsumura, T.; Omasa, T.; Suga, K.; Aoki, T.; Koyanagi, Y. (2000) Development of a bioartificial liver with glutamine synthetase-transduced recombinant human hepatoblastoma cell line, HepG2. *Transplant Proc.* 32(7):2355-2358.
6. Kisaalita WS. 3D Cell-Based Biosensors in Drug Discovery Programs: Microtissue Engineering for High Throughput Screening, Boca Raton (CRC Press, Taylor and Francis Group), 2010.
7. Griffith, L.G. and Swartz, M.A. Capturing complex 3D tissue physiology in vitro. *Nat. Rev. Mol. Cell Biol.* 7, 211, 2006.
8. Green JA and Yamada KM. Three-dimensional microenvironments moderate fibroblast signaling responses. *Advanced Drug Delivery Reviews* 2007, 59:1293-1289.
9. Asthana, A., & Kisaalita, W. S. (2013). Biophysical microenvironment and 3D culture physiological relevance. *Drug discovery today*, 18(11), 533-540.
10. Cheng, K.; Lai, Y.; Kisaalita, W.S. (2008) Three dimensional polymer scaffolds for high throughput cell-based assay systems. *Biomaterials* 29:2802-2812.
11. Zhang R, Ma PX. Poly(alpha-hydroxyl acids)/hydroxyapatite porous composites for bone-tissue engineering. I. Preparation and morphology. *Journal of Biomedical Materials Research*, 44 (1999), pp. 446–455.
12. Liu X, Lim JY, Donahue HJ, Dhurjati R, Mastro AM, Vogler EA. Influence of substratum surface chemistry/energy and topography on the human fetal osteoblastic cell line hFOB

- 1.19: Phenotypic and genotypic responses observed in vitro. *Biomaterials* 2007; 28: 4535–4550.
13. Freyman TM, Yannas IV, Gibson LJ. Cellular materials as porous scaffolds for tissue engineering. *Progress in Material Science*. 2001;46:273-282.
14. Asthana, A., & Kisaalita, W. S. (2012). Microtissue size and hypoxia in HTS with 3D cultures. *Drug discovery today*, 17(15), 810-817.
15. Chen, A.A., Khetani, S.R., Lee, S., Bhatia, S.N., Van Vliet, K.J. 2009. Modulation of hepatocyte phenotype in vitro via chemomechanical tuning of polyelectrolyte multilayers. *Biomaterials* 30:1113.
16. Lai, Y., Cheng, K., and Kisaalita, W.S. 2012. Porous polystyrene scaffolds for three-dimensional cell-based assays (accepted).
17. Wang Y-Q, Cai J-Y. Enhanced cell affinity of poly(L-lactic acid) modified by base hydrolysis: Wettability and surface roughness at nanometer scale. *Curr Appl Phys* 2007; 7S: e108–e111.
18. Curcio, E., Salerno, S., Barbieri, G., De Bartolo, L., Drioli, E., & Bader, A. (2007). Mass transfer and metabolic reactions in hepatocyte spheroids cultured in rotating wall gas-permeable membrane system. *Biomaterials*, 28(36), 5487-5497.
19. Liu H, Liu XM, Li SC, Wu BC, Ye LL and Wang QW et al. 2009. A high-yield and scaleable adenovirus vector production process based on high density perfusion culture of HEK 293 cells as suspended aggregates, *J Biosci Bioeng* **107**(5):524–529.
20. Hubbard, A.L., Barr, V. A., and Scott, L.J. 1994. Hepatocyte surface polarity. In “The Liver: Biology and Pathobiology” (I. M. Arias, J. L. Boyer, N. Fausto, W. B. Jakoby, D. Schachter, and D. A. Shafritz, Eds.), Raven Press, New York.
21. Maurice, M., Rogier, E., Cassio, D., and Feldmann, G. 1988. Formation of plasma membrane domains in rat hepatocytes and hepatoma cell lines in culture. *J. Cell Sci.* 90:79–92.
22. Moghe, P.V., Berthiaume, F., Ezzell, R.M., Toner, M., Tompkins, R.G., and Yarmush, M.L. 1996. Culture matrix configuration and composition in the maintenance of hepatocyte polarity and function. *Biomaterials* 17:373–385.

23. LeCluyse, E.L., Audus, K.L., and Hochman, J.H. 1994. Formation of extensive canalicular networks by rat hepatocytes cultured in collagen-sandwich configuration. *Am. J. Physiol.* 266:C1764–C1774.
24. Salmenperä P, Kankuri E, Bizik J, Sirén V, Virtanen I, Takahashi S, Leiss M, Fässler R and Vaheri A, Formation and activation of fibroblast spheroids depend on fibronectin–integrin interaction, *Exp. Cell Res.* 2008, 314:3444–3452.
25. Cukierman E, Pankov R, Stevens DR, Yamada KM. Taking cell-matrix adhesions to the third dimension. *Science* 2001, 294:1708-1712.
26. Mao Y, Schwarzbauer JE. Stimulatory effects of a three-dimensional microenvironment on cell-mediated fibronectin fibrillogenesis. *J Cell Sci.* 2005, 118:4427–4436.
27. Discher, D., Janmey, P. & Wang, Y. 2005. Tissue cells feel and respond to the stiffness of their substrate. *Science* 310:1139–1143.

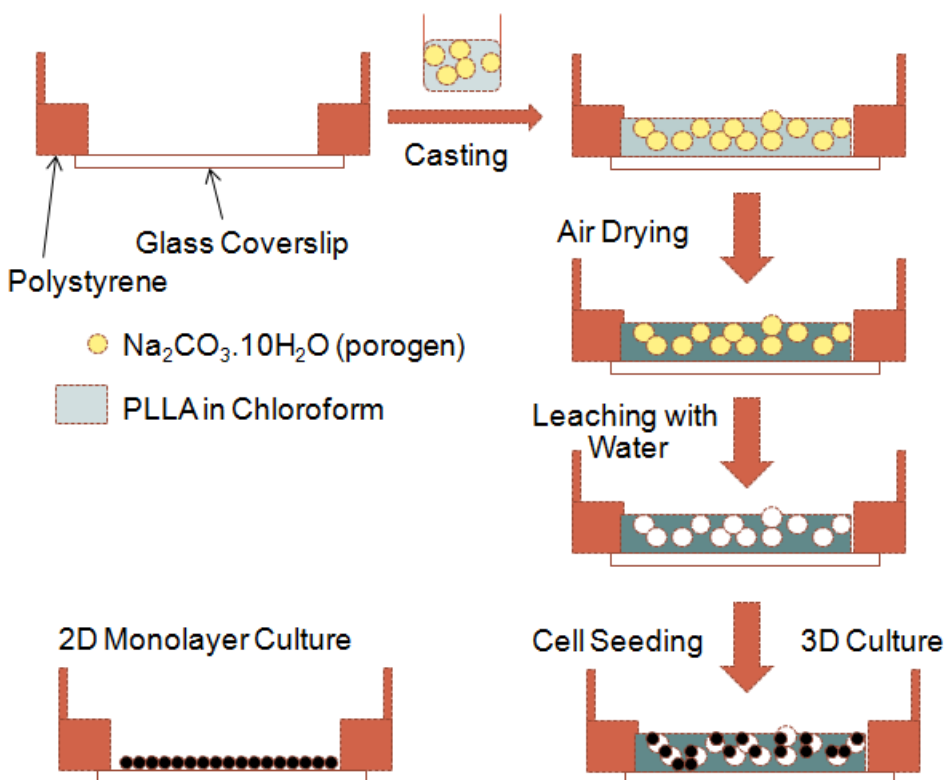


Figure 4.1. Schematic of the fabrication process for micro porous Poly L-lactic acid (PLLA) scaffold using salt leaching technique. PLLA was dissolved in chloroform and then sieved sodium carbonate decahydrate particles were added to the polymer solution and mixed thoroughly. The casting mixture was composed of 0.2 g PLLA, 2.5 g sodium carbonate decahydrate and 4 ml chloroform. The size of the salt particles used was in the range of 106-125 μm (Scaffold A) and 218-250 μm (Scaffold B). 140 μL of the solution was casted in MatTek® glass bottom Petri dishes (well diameter: 10 mm). After casting, the plate was immediately covered to control the evaporation rate of chloroform and also weld the scaffold by partially dissolving the polystyrene wall of the well. After chloroform was completely evaporated, the dishes were leached with water overnight.

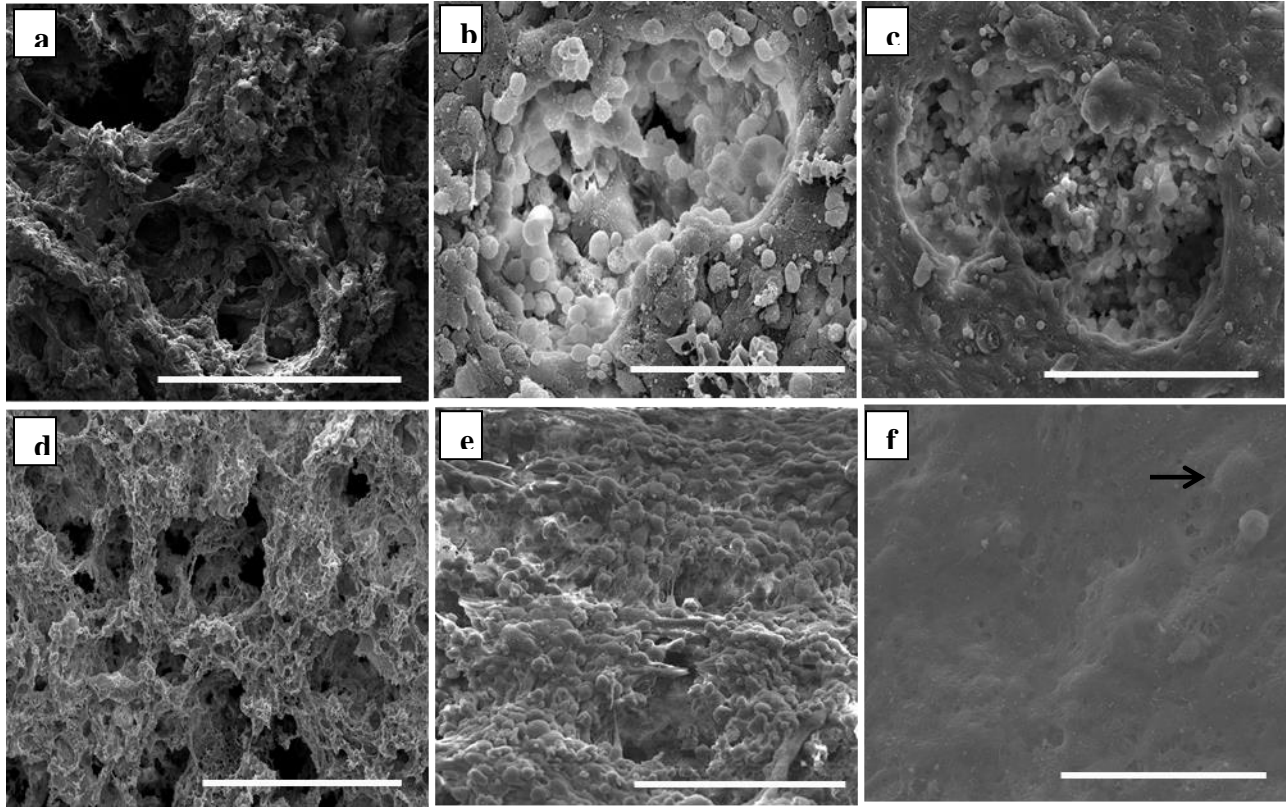


Figure 4.2. Progression of tissue formation in Scaffold A (a,b,c) and B (d,e,f). Part (a) shows unseeded SEM image of the scaffold A while (b) and (c) were taken on day 3 and 7 respectively. The round morphology of the cells which is a characteristic of 3D culture is visually evident in the pores. Single cell surfaces can be seen on day 3 but are less evident on day 7 signifying compaction of tissues and production of ECM. Part (d) shows unseeded SEM image of the scaffold B while (e) and (f) were taken on day 3 and 7, respectively, and show that the deposition of ECM is higher in Scaffold B. Arrow shows a cell embedded in ECM (f). Scale bars are 400 μm for (a,d), 100 μm for (b,e,f) and 200 μm (c).

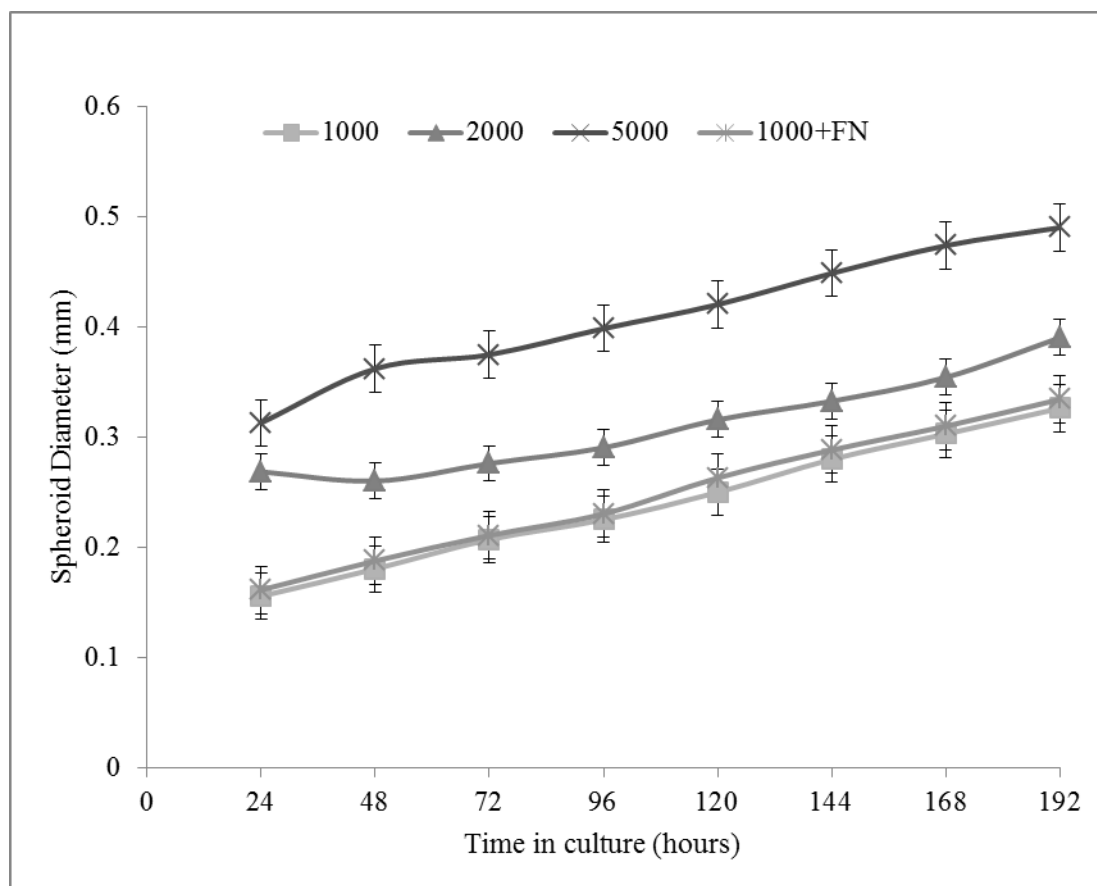


Figure 4.3. Size/Time/Cell number profile for spheroids. Phase contrast images of 3 spheroids were taken every day and analyzed to get the diameter. Each point shows the mean \pm SD (n=3).

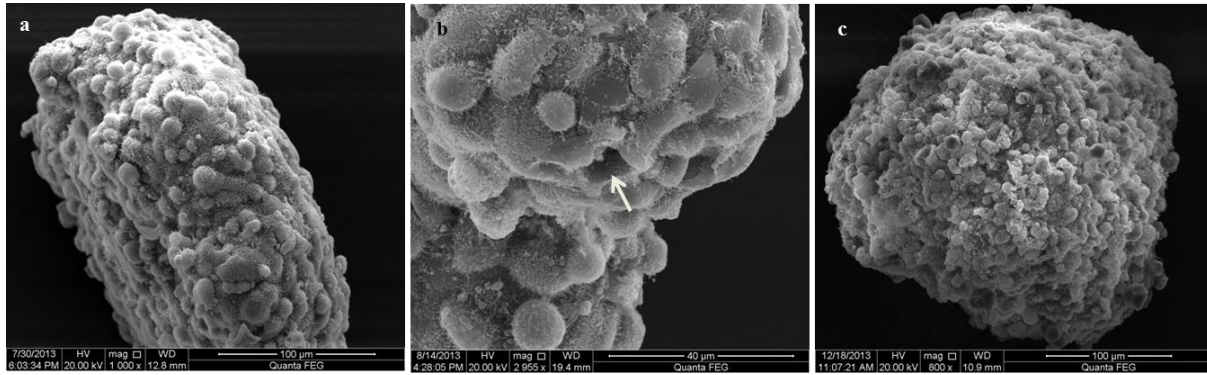


Figure 4.4. SEM images of the 1000 cell spheroid. Compact tissue-like spheroids, with a thin ECM layer were observed at day 3 (a). There is an extensive network of channels inside spheroids. Arrow indicates the opening pores of the channels on the surface of mature spheroids (b; day5). (c) Image taken on day 9.

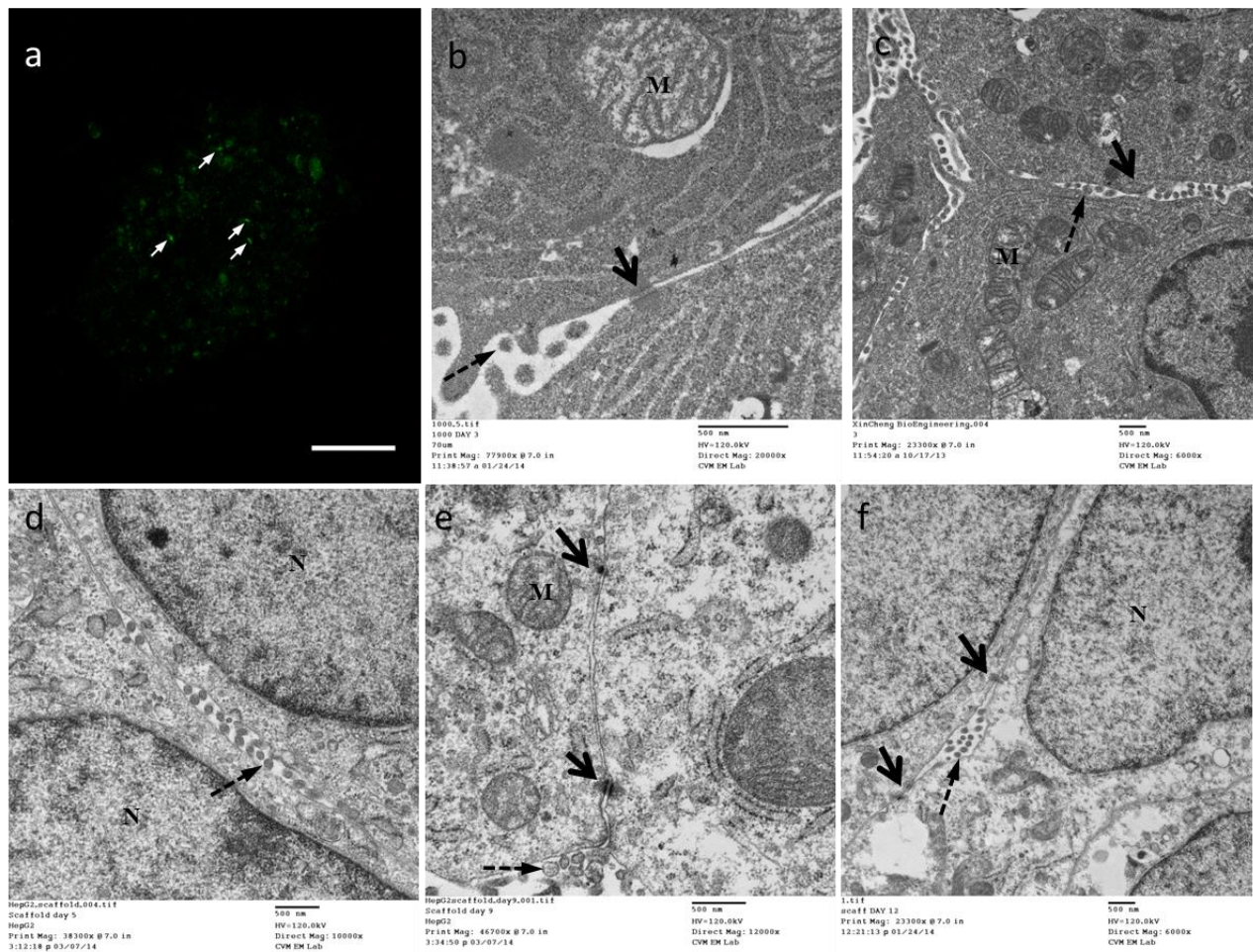


Figure 4.5. Confocal (a) and TEM (b-f) images of bile canaliculi-like structures. The first row (a-c) shows the progression of bile canaliculi formation in 1000 cell spheroid while the second row (d-f) shows the same in scaffold A. The spheroid had functional canaliculi on day 3 as shown by fluorescein excretion (a) micro villi lined canaliculi were formed as early as day3 in spheroids as confirmed by TEM (b). the formation started late in scaffolds (day 9; e). On day 12 multiple tight unctions and canicular network could be seen in scaffolds (f). black solid arrow – tight junction, black dashed arrow – micro villi, white arrow – excretion of cleaved fluorescein by the cell into bile canaliculi-lie structures, M – Mitochondria. Scale is 100 μ m in (a).

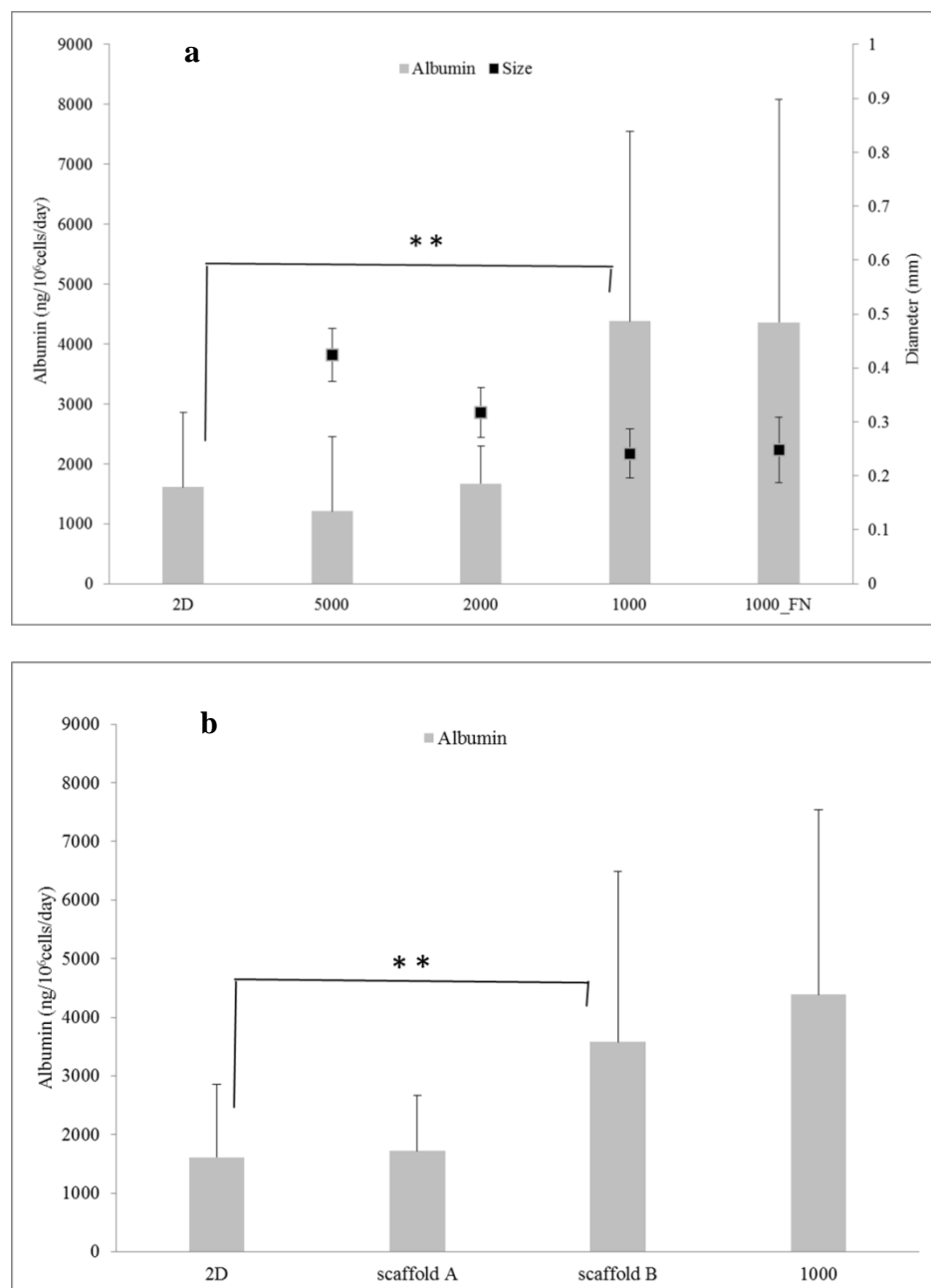


Figure 4.6. Mean albumin productivity (ng/10⁶ cells/day) from different growth platforms. Part (a) compares 2D with the spheroids while part (b) is a comparison between the ideal spheroid and the two scaffolds cultures. Mean diameter of spheroids over 8 days of culture is depicted as dot plot in (a). Each point shows the mean±SEM **($p < 0.05$)

CHAPTER 5

CYTOKINE UPREGULATION IN 3D HEPG2 CULTURES⁴

⁴Asthana A, White C and Kisaalita WS. To be submitted to Tissue Engineering: PartA

5.1 Abstract

There is need to find a biomarker that could act as an early indicator of the complex physiological relevance (CPR) of a tissue or a microtissue model. Physiological relevance is detected late in culture and requires different analytical techniques. A biomarker would bring this to a common detection platform. Cytokines have been explored for their 3D bio marking potential and three cytokines (VEGF-A, IL-8 and PDGF-AB/BB) were found to not just be upregulated in 3D compared to 2D at early time points (48 and 72 hours) but were also able to predict the most physiologically relevant 3D platforms. This upregulation is not just a 2D/3D differential event but is physiologically justified as these cytokines are involved in angiogenesis. Also, the upregulation of cytokines was determined to be Ras/Raf/ERK pathway dependent. However, in vivo validation of these cytokines is needed. Validated biomarkers of physiologically relevant three-dimensionality will lead to advances in tissue engineering, regenerative medicine, drug screening, tumor & developmental biology and also in the study of cell-cell and cell-material surface interactions and will take the field a step closer towards understanding and thus engineering 'in vivo-like' cell culture microenvironments.

5.2 Introduction

It has been proposed that three-dimensional (3D) cell-based assays may yield "physiologically more relevant" results and thus have the potential to save time and cost by reducing drug candidate attrition through early fidelity matching of drug candidates and targets¹. However, the problem with the many emerging 3D platforms is that whenever 2D/3D culture differences are observed, "more physiological relevance" is claimed with no "gold standard" to substantiate the claims. Apart from the concept of "three-dimensional matrix adhesion,"

originally proposed by Curkieman et al. (2001)² as a possible indication or “diagnosis” or marker for a culture state of three-dimensionality, the field of tissue engineering has not provided knowledge on the basis of which a consensus for three-dimensionality and the associated complex physiological relevance could be established. We are addressing this problem by establishing a basis for three-dimensionality biomarkers.

Traditionally, the meaning of three-dimensionality in cell culture has been simply associated with providing a 3D spatial microenvironment. In our recent work, the meaning has been extended to providing the total microenvironment that supports the formation of microtissue that exhibit “complex” physiological relevance (CPR) or better emulation of the in vivo microtissue functionality in a manner not possible in 2D cultures³. The three main categories or microenvironment factors (MEFs) or “three-dimensions” are: 1) chemical or biochemical composition, 2) spatial (geometric 3D) and temporal dimensions, and 3) force and substrate physical properties^{3,4}. Beyond the “more physiological relevance” substantiation, the concept of using combinatorial approaches to fabricate libraries of polymers or other material scaffolds⁵ for tissue engineering or cell-based drug discovery calls for a high throughput assay by which “hit materials” can be quickly identified for further development. The development of such assays or biosensors can potentially be guided by a cell-material interaction outcome⁶. An interaction with a material that yields cells that emulate in vivo conditions would be most desirable. Three-dimensionality biomarkers would provide the intellectual basis for material discovery platform development. Furthermore, in order to lower the costs associated with 3D platforms and make them more accessible for high throughput applications, simplification of the platform without giving up the physiologically relevant behavior of the cells is necessary. This simplification can be achieved easily if the physiologically relevant outcome can be measured in

terms of three-dimensionality biomarkers, as discussed in detail by Lai et al., 2011a⁷. As the platform architecture design is simplified, it will be possible, with such a marker, to know when the trajectory toward CPR outcomes is being compromised by the introduced simplification(s).

Taken together, the subfield or field of 3D culture needs validated biomarkers. Many 2D/3D comparative transcriptomic studies, with cells from the four main tissues types (nerve, muscle, connective, and epithelial) cultured in a wide variety of platforms, have reported up-regulation of cytokines and their receptors in 3D cultures. For example, Klapperich and Bertozzi (2004)⁸ reported up-regulation of seven cytokines (IL-8, CXCL1, CXCL2, CXCL3, CXCL5, VEGF, LIF) by a human fetal lung fibroblast (IMR-90) cultured in a collagen–glycosaminoglycan (collagen/GAG) 3D mesh. Also, Ghosh et al. (2005)⁹ reported upregulation of six cytokines (CXCL1-3, IL-8, MIP-3a, Angiopoietin like4) by a melanoma cell line (NA8) cultured on poly-2-hydroxyethyl methacrylate (polyHEMA) plates when compared to 2D surfaces. These transcriptomic findings have also been supported by studies at the protein level. For example, Enzerink et al (2009)¹⁰ has shown that clustering of fibroblasts induces chemokine (CCL2-5, CXCL1-3, CXCL8) secretion in five different fibroblast cell lines cultured in agarose. Also, Fischbach et al¹¹ cultured tumor cells in a 2D and 3D RGD-alginate system and reported a dramatic enhancement of IL-8 levels, however, no significant VEGF differences were reported between 2D and 3D cultures. These reports strongly point to cytokines and related chemical species as the most likely compounds to provide the badly needed biomarkers. We propose to conclusively confirm or rule out this possibility in this study. The long term goal in our laboratory is to identify and validate ubiquitous biomarkers of physiologically relevant three-dimensionality. As a first step, we are using cells of hepatic origin (HepG2) to confirm or rule out if cytokines can serve this purpose. Specific objectives are to establish cytokine production

time-profiles, in HepG2 cultures grown in 3D platforms providing different microenvironmental factors (spatial, chemical and biophysical) and to determine the molecular basis for the upregulation of cytokine production in 3D.

5.3 Materials and Methods

5.3.1 Scaffold fabrication

The microporous polymer scaffold was fabricated using the salt leaching method routinely used in our laboratory¹². Briefly, poly L-lactic acid (PLLA) was dissolved in chloroform and then sieved sodium carbonate decahydrate particles were added to the polymer solution and mixed thoroughly. The casting mixture was composed of 0.2 g PLLA, 2.5 g sodium carbonate decahydrate and 4 ml chloroform. The size of the salt particles used was in the range of 106-125 μm (Scaffold A) and 218-250 μm (Scaffold B). 140 μL of the solution was casted in MatTek® glass bottom Petri dishes (Cat#: P35G-0-10; well diameter: 10 mm). After chloroform was completely evaporated, the dishes were leached with water overnight. Then the scaffold was treated with 0.1 mM NaOH for 40 minutes at 40°C to make it hydrophilic. After washing with water thrice, the scaffold was sterilized in 70% ethanol (3 hours) and UV (30 mins). Finally, to increase cell adhesion, both the scaffolds (A and B) were coated with fibronectin (8 μg in 150 μL PBS).

5.3.2 HepG2 cell culture

HepG2 human hepatocellular carcinoma cells (HB-8065) (ATCC, VA) were routinely cultured in 75 cm^2 tissue culture flasks (Costar, Corning, NY) in Dulbecco's Modified Eagle Medium (DMEM) (Life Technologies) containing 10% heat inactivated fetal bovine serum (FBS), 2.2 g/L sodium bicarbonate, 2 mM l-glutamine and 1 mM sodium pyruvate in 5% CO_2 at

37 °C. At 75% confluence, the cells were detached by using 0.25% Trypsin-EDTA (Gibco®) and re-suspended in growth medium for plating. For seeding on scaffolds, cells were counted using Millipore Scepter 2.0 handheld automated cell counter and 7×10^5 cells (in 140 μ l medium) were seeded on each scaffold. After allowing 4 hours for attachment, the medium was removed and 2 ml fresh growth medium was added to each plate. Control 2D cultures were plated in 48 well tissue culture plates in 500 μ l of medium.

5.3.3 Spheroid culture

HepG2 spheroids (1000 cells/spheroid) were fabricated in AggreWell™400 plate according to the manufacturer's protocol. Briefly, the wells were first coated with 5% Pluronic F-127 to avoid attachment. Cells were counted using Millipore Scepter 2.0 handheld automated cell counter and 1.2×10^6 cells (in 2 ml medium) were seeded in each well followed by centrifugation at 355 x g for 5 minutes. After 24 hours of incubation the wells were triturated and the spheroids were resuspended in either 100mm dishes or 48 well plates (one spheroid in each well; 500 μ l medium) coated with 5mg/ml Poly(2-hydroxyethyl methacrylate) (poly HEMA) to avoid attachment. For pathway inhibition study, MAP Kinase inhibitor UO126 (Cell Signaling Technology, MA) was added to the spheroids on days 1 (5 μ M) and 2 (2 μ M).

5.3.4 Cytokine assay

The Milliplex MAP Human High Sensitivity Cytokine/Chemokine Panel Kit (measuring 21 analytes) was used to quantify cytokine concentrations in the supernatants collected from 2D, scaffold and spheroid cultures at 48 and 72 hour time points. Manufacturer's instructions were followed. A minimum of 50 beads of each targeted analyte were acquired on a Luminex 200

instrument (Biorad). The concentration of each analyte in an unknown sample was estimated from a five parameter log-logistic calibration curve (5PL) fit to standards of known concentration.

5.3.5 Flow cytometry

Rabbit anti- Erk1 (pT202/pY204) + Erk2 (pT185/pY187) primary and Alexa 488 goat anti-rabbit secondary antibodies were bought from Abcam (MA, USA) and Invitrogen, respectively. For flow cytometry, standard protocol was followed. Briefly, 1×10^6 cells were fixed with 100 μ l of 4% paraformaldehyde and 0.1% Triton-X at room temperature for 20 minutes. After removal of fixative, cell were incubated with ice cold methanol for 30 minutes at -20°C . After centrifugation washing with 3% BSA in PBS, primary antibody was added (10 $\mu\text{g}/\text{ml}$) and cells were incubated overnight at 4°C . After washing with the wash buffer, secondary antibody (1:500) was added and the cells were incubated for an hour at room temperature. After the final wash with wash buffer, cell were resuspended in 500 μ l PBS and taken for flow cytometry. The fluorescence was recorded by collecting 20,000 events on a Cyan flow cytometer. The median fluorescence intensity was used for comparisons.

5.3.6 Statistical analysis

Statistical comparisons were undertaken using paired two-tailed Student t tests. Results were expressed as mean \pm standard error of the mean.

5.4 Results and Discussion

5.4.1 Expression profile of cytokines in 3D HepG2 cultures

A 21-plex Human cytokine/chemokine kit (EGF, GM-CSF, GRO, IFN γ , IL-10, IL-13, IL1-B, IL-2, IL-6, IL-8, MCP-1, MDC, MIP-1a, MIP-1b, PDGF-AA, PDGF-AB/BB, RANTES, TGF α , TNF α , TNF β and VEGF) was used to analyze the cell culture supernatants from 2D, 1000 cells/spheroid, scaffold A and scaffold B at the 48 and 72 hour time points. These particular analytes were chosen because they have been shown to be upregulated in many different cell lines spanning various cell types including primary cells, fibroblasts, multi and pluripotent stem cells and cancer cells grown on different 3D platforms as shown in Table 2.1. The 3D constructs used in this study have been shown to exhibit the highest complex physiological outcome quantified in terms of albumin secretion as shown in Chapter 4. The mean specific albumin productivities for 1000 cells/spheroid, scaffold A and scaffold B over 8 days in culture were found to be 4.38, 3.57 and 1.71 $\mu\text{g}/10^6\text{cells}/\text{day}$, respectively, compared to 2D (1.61 $\mu\text{g}/10^6\text{cells}/\text{day}$). 2D was used as a control to determine if cytokines could differentiate between monolayer and CPR exhibiting 3D cultures. The analysis was performed on samples collected at the 48 and 72 hour time point as we wanted to establish cytokines as early indicators of CPR expression later in culture. A CPR outcome, especially a structural one can be considered as an end-point observation. This means that once it is expressed, the culture has already been on a trajectory, prior to this point, towards the desired in vivo emulation state. Therefore, the expression of cytokines at early time points in the culture can be used to predict the development of in vivo-like behavior of microtissues during later stages of the culture.

Out of the 21 analytes in the cytokine/chemokine panel only six were spontaneously expressed in HepG2 cells and their quantities at the two time points have been presented in Table

5.1. Three cytokines (VEGF-A, IL-8 and PDGF-AB/BB) were chosen for further discussion as potential biomarkers as they showed maximum difference between 2D and 3D (especially scaffolds A & B) cultures and their production profiles are shown in Figure 5.1. In fact there was no expression of PDGF-B in 2D at either time point. Even though the spheroid had been shown to be more physiologically relevant with respect to albumin production (Chapter 4) when compared to 2D, the difference between cytokine secretion in 2D and the spheroid was not found to be significantly different except for PDGF-AB/BB secretion at the 72 hour time point. However, at the 72 hour mark the expression of both VEGF and PDGF-AB/BB was not statistically different ($p > .05$) between the spheroid and Scaffold B (most physiologically relevant platforms), while the expression of IL-8 was lower in the spheroid compared to 2D at both time points ($p < 0.1$ and $p < 0.05$ for 48 and 72 hours, respectively). Each of the three cytokines has been significantly upregulated in at least one of the 3D platforms compared to 2D but their profiles are not consistent between the two 3D platforms that showed highest albumin productivity (CPR). As such, cytokine upregulation can be used to differentiate between 2D and 3D platforms but cannot conclusively predict complex physiological relevance of the platform. This can be due to the fact that albumin production was chosen as a single representative of complex functionality. A more comprehensive functional analysis of the platforms involving other hepatic functions such as urea production and cytochrome p450 expression might be required to determine the platform providing the most optimal microenvironmental cues to the cells.

However, the upregulation of these cytokines is in accordance with the transcriptomic results previously published from our lab, which showed upregulation in VEGF-A and PDGF-B gene expression in neuronal 3D cultures when compared to monolayers⁷. Moreover, these

particular cytokines have been shown to be upregulated in 3D cultures of various other cell and tissue types as shown in Table 2.1. For instance, both IL-8 and VEGF-A have been shown to be over expressed in 3D cultures of human fetal lung fibroblasts⁸, oral squamous cell carcinoma, glioblastoma, breast cancer^{11, 13} and melanoma¹⁴ which points towards their potential for ubiquitous expression spread across various cell types.

The functional classification of these cytokines suggests an underlying theme of angioadaptation and angiogenesis which is physiologically relevant as tumor cells in a 3D culture in vitro might relate to avascular tumor progression in vivo. VEGF promotes tumor angiogenesis through endothelial cell proliferation and survival¹⁵. Its expression also results in an increase in the migration and invasion of endothelial cells and the permeability of existing vessels. Further, it leads to the development of a lattice network for endothelial cell migration; and enhanced chemotaxis and homing of bone marrow derived vascular precursor cells^{16, 17}. It has also been shown to have autocrine effects on tumor cell survival, migration and invasion; immune suppression and also plays a role in tumor metastasis^{15, 18}.

IL-8 also plays an important role in the tumor microenvironment. Production of IL-8 from tumor cells can increase the proliferation and survival of cancer cells in an autocrine manner. Like VEGF, tumor-derived IL-8 leads to the activation of endothelial cells in the tumor vasculature to promote angiogenesis and induce a chemotactic infiltration of neutrophils into the tumor site¹⁹. Platelet-derived growth factor (PDGF) also plays a role in angiogenesis as it regulates the proliferation and migration of mesenchymal cells such as vascular smooth muscle cells, fibroblasts, glial cells, macrophages and chondrocytes²⁰.

5.4.2 ERK inhibition in spheroids

ERK might be the controller of cytokine production in 3D as discussed in Chapter 2 and illustrated in Figure 2.4. It has already been shown that there is an elevation in the steady state activity of Ras and ERK1/2 in 3D cultures. This activity is not dependent on the traditional autophosphorylation of FAK at Tyr397 as seen in 2D cultures but was found to be Src dependent²¹. In fact, FAK phosphorylation at Tyr397 is down regulated in 3D matrices as shown by Cukierman et al., 2001². Moreover, IL-8 signaling has been shown to induce the activation of this Ras/Raf/Erk signaling cascade in cancer cells²². IL-8 transactivates the epidermal growth factor receptor (EGFR) which leads to the downstream activation of MAPK signaling, via Grb2/SOS mediated activation of Ras-GTPase²² (Figure 2.4), resulting in cancer cell proliferation and survival in an autocrine manner. Furthermore, a compelling evidence of the involvement of the ERK pathway in cytokine production is given by the usage of phorbol esters, like PMA, that have been widely used to elicit an immunogenic response from cells. They generally act by activating PKC²³ which in turn activates Raf²⁴, whose activity might be aberrant in 2D cultures as it is controlled by integrin mediated adhesion²⁵ to the ECM assembly. Also, it has been reported that normally PKC is activated by extracellular matrix fibronectin but the 2D cells lack it and so the pathway might not be properly regulated in them²⁶. Phorbol esters, thus lead to the enhancement of the activity of transcription factors like AP-1²³, CREB and NF- κ B²⁷, which bind to the promoter region of various cytokine genes and lead to their expression. Taken together, this emphasizes the involvement of the ERK in the upregulation of cytokines in 3D cultures.

To test this hypothesis, we inhibited it using MEK1/2 inhibitor UO126. The inhibition of ERK1/2 was verified at the 72 hour time point using flow cytometry. Samples and controls

treated with UO126 and the vehicle (DMSO), respectively, were activated with PMA and subjected to flow cytometry analysis after fixation and permeabilization, using an anti phospho Erk1 (pT202/pY204) + Erk2 (pT185/pY187) antibody. The magnitude of ERK phosphorylation, in samples treated with UO126 only or with both UO126 and PMA, was comparable and about 2.5 fold lower than the samples treated with just PMA showing that the activation of ERK had indeed been inhibited (Figure 5.2). UO126 significantly affected the expression of all VEGF-A and IL-8 as shown in Figure 5.3. VEGF-A expression was significantly lower in the inhibitor treated culture compared to the control at the 48 hour time point but not at 72 hours. Its production increased in inhibitor containing cultures from 48 to 72 hours. This might be due to the fact that VEGF production is not solely dependent on the activation of ERK. It has been shown that STAT3 activity can also regulate the expression of VEGF in a “feed forward” manner^{28, 29} and after its initial expression its upregulation might be independent of ERK activity. The production of IL-8 completely ceased at the 72 hour time point in cultures containing the inhibitor which directly implicates ERK in its upregulation in 3D. However PDGF-AB/BB expression was not significantly inhibited by UO126. These results show that the role of ERK can be implicated in the upregulation of cytokines in 3D.

5.5 Conclusion

Three cytokines (VEGF-A, IL-8 and PDGF-AB/BB) were found to be significantly upregulated in 3D compared to 2D at early time points (48 and 72 hours). This upregulation is not just a 2D/3D differential event but is physiologically justified as these cytokines have been shown to be involved in tumor angiogenesis. However a more comprehensive functional analysis of the 3D platforms is required to determine their physiological relevance and its correlation with

cytokine upregulation. The upregulation of cytokines in 3D was found to be ERK dependent.

Finally, in vivo validation of these cytokines will be needed to establish them as biomarkers of three-dimensionality.

5.6 References

1. Kunz-Schughart LA, Freyer JP, Hofstaedter F, Ebner R. The use of 3-D cultures for high-throughput screening: the multicellular spheroid model. *J. Biomol. Screen.* 2004, 9:273-285.
2. Cukierman E, Pankov R, Stevens DR, Yamada KM. Taking cell-matrix adhesions to the third dimension. *Science* 2001, 294:1708-1712.
3. Kisaalita WS. *3D Cell-Based Biosensors in Drug Discovery Programs: Microtissue Engineering for High Throughput Screening*, Boca Raton, FL: Taylor and Francis, 2010.
4. Griffith, L.G. and Swartz, M.A. Capturing complex 3D tissue physiology in vitro. *Nat. Rev. Mol. Cell Biol.* **7**, 211, 2006.
5. Yang Y, Dorsey SM, Becker ML, Lin-Gibson S, Schumacher GE, Flaim GM, Kohn J, Simon Jr CG. X-ray imaging optimization of 3D tissue engineering scaffolds via combinatorial fabrication methods. *Biomaterials*, 2008b, 29:1901-1911.
6. Yang Y, Becker ML, Bolikal D, Kohn J, Zeiger DN, Simon Jr CG. Combinatorial polymer scaffold libraries for screening cell-biomaterial interactions in 3D. *Advanced Materials* 2008a, 20:2037-2043.
7. Lai Y, Asthana A and Kisaalita WS. Biomarkers for simplifying HTS 3D cell culture platforms for drug discovery: the case for cytokines. *Drug Discovery Today* 2011, 16(7-8):293-7.
8. Klapperich, C.M. and Bertozzi, C.R. Global gene expression of cells attached to a tissue engineering scaffold. *Biomaterials* **25**, 5631, 2004.
9. Ghosh, S. et al., Three-dimensional culture of melanoma cells profoundly affects gene expression profile: a high density oligonucleotide array study. *J. Cell Physiol.* 204, 522, 2005.
10. Enzerink A., Salmenperä, P., Kankuri, E. and Vaehri, A. Clustering of fibroblasts induces proinflammatory chemokine secretion promoting leukocyte migration. *Mol. Immunol.* 46, 1787, 2009.
11. Fischbach, C. et al. Cancer cell angiogenic capability is regulated by 3D culture and integrin engagement. *Proc. Natl. Acad. Sci. U S A* **106**(2), 399, 2009.
12. Cheng, K.; Lai, Y.; Kisaalita, W.S. (2008). Three dimensional polymer scaffolds for high throughput cell-based assay systems. *Biomaterials* 29:2802-2812.

13. Talukdar, S. and Kundu, S. C. A Non-Mulberry Silk Fibroin Protein Based 3D In Vitro Tumor Model for Evaluation of Anticancer Drug Activity. *Adv. Funct. Mater.* 22, 4778, 2012.
14. Ghosh S, Josh MB, Ivanov D, Federengus C, Spagnoli GC, Martin I, Erne P, Resink TJ. Use of multicellular tumor spheroids to dissect endothelial cell-tumor cell interactions: A role for T-cadherin in tumor angiogenesis. *FEBS Lett* 581, 4523, 2007.
15. Ellis, L. M., & Hicklin, D. J. (2008). VEGF-targeted therapy: mechanisms of anti-tumour activity. *Nature Reviews Cancer*, 8(8), 579-591.
16. Gimbrone, M.A. Jr, Leapman, S.B., Cotran, R.S. & Folkman, J. Tumor angiogenesis: iris neovascularization at a distance from experimental intraocular tumors. *J. Natl Cancer Inst.* 50, 219–228 (1973).
17. Rafii, S., Lyden, D., Benezra, R., Hattori, K. & Heissig, B. Vascular and haematopoietic stem cells: novel targets for anti-angiogenesis therapy? *Nature Rev. Cancer* 2, 826–835 (2002).
18. Kaplan, R.N. et al. VEGFR1-positive haematopoietic bone marrow progenitors initiate the pre-metastatic niche. *Nature* 438, 820–827 (2005).
19. Waugh, D. J., & Wilson, C. (2008). The interleukin-8 pathway in cancer. *Clinical cancer research*, 14(21), 6735-6741.
20. Yu, J., Ustach, C., & Kim, H. R. C. (2003). Platelet-derived growth factor signaling and human cancer. *Journal of biochemistry and molecular biology*, 36(1), 49-59.
21. Damianova, R., Stefanova, N., Cukierman, E., Momchilova, A., & Pankov, R. (2008). Three-dimensional matrix induces sustained activation of ERK1/2 via Src/Ras/Raf signaling pathway. *Cell biology international*, 32, 229-234.
22. Venkatakrisnan G, Salgia R, Groopman JE. Chemokine receptors CXCR-1/2 activate mitogen-activated protein kinase via the epidermal growth factor receptor in ovarian cancer cells. *J Biol Chem* 2000;275:6868–75.
23. Nishijima K, Fujiki T, Kojima H & Iijima S. The effects of cell adhesion on the growth and protein productivity of animal cells. *Cytotechnology* 2000, 33:147–155.
24. Corbit KC, Trakul N, Eves EM, Diaz B, Marshall M and Rosner MR. Activation of Raf-1 Signaling by Protein Kinase C through a Mechanism Involving Raf Kinase Inhibitory Protein. *The Journal of Biological Chemistry* 2003, 278(15):13061–13068.

25. Lin TH, Chen Q, Howe A and Juliano RL. Cell Anchorage Permits Efficient Signal Transduction Between Ras and Its Downstream Kinases. *The Journal of Biological Chemistry* 1997, 272(14):8849-8852.
26. Vuori K and Ruoslahti E. Activation of protein kinase C precedes $\alpha 5\beta 1$ integrin-mediated cell spreading on fibronectin. *J. Biol. Chem.* 1993, 268:21459–21462.
27. Jiang X, Norman M and Li X. Use of an array technology for profiling and comparing transcription factors activated by $TNF\alpha$ and PMA in HeLa cells. *Biochimica et Biophysica Acta (BBA) - Molecular Cell Research* 2003, 1642(1-2):1-8.
28. Niu, G. et al. Constitutive Stat3 activity up-regulates VEGF expression and tumor angiogenesis. *Oncogene* 21, 2000–2008 (2002).
29. Sumimoto, H., Imabayashi, F., Iwata, T. & Kawakami, Y. The BRAF–MAPK signaling pathway is essential for cancer-immune evasion in human melanoma cells. *J. Exp. Med.* 203, 1651–1656 (2006).

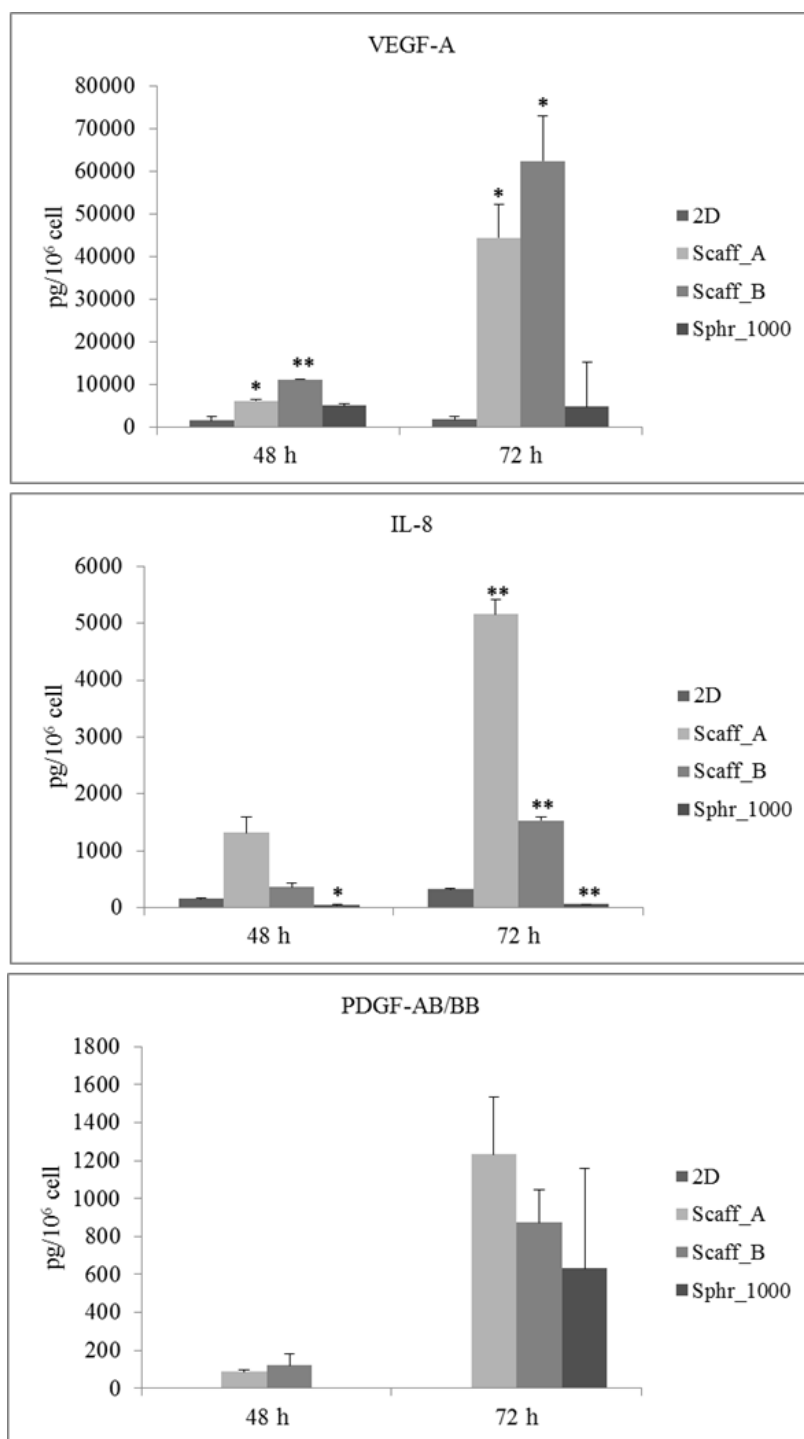


Figure 5.1. VEGF-A, IL-8 and PDGF-AB/BB production profile for 2D, spheroid, Scaffold A and Scaffold B at 48 and 72 hours. Data expressed in terms of mean+S.E.M. (Comparison between 2D culture and all 3D cultures *($p < 0.1$), **($p < 0.05$))

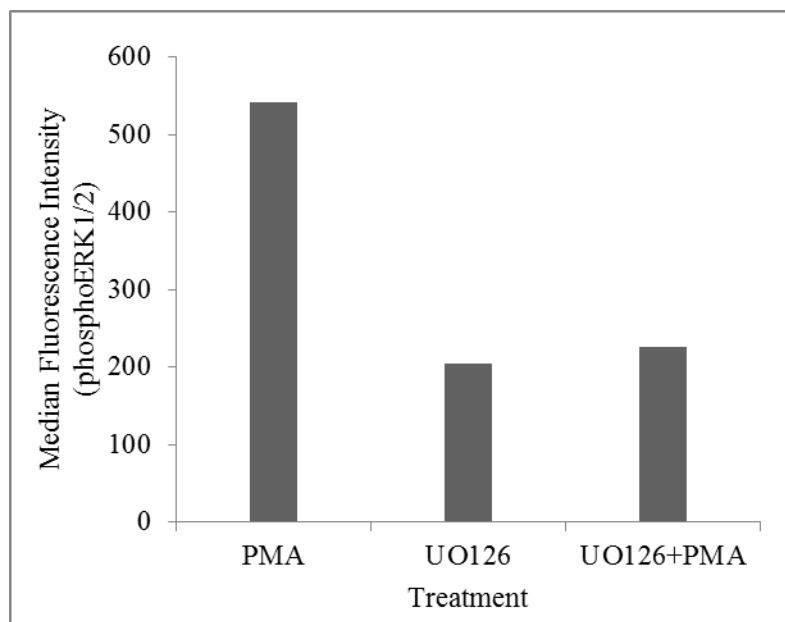


Figure 5.2. Flow cytometric analysis of HepG2 for Erk1 (pT202/pY204) + Erk2 (pT185/pY187) activation. The magnitude of ERK phosphorylation, in samples treated with UO126 only or with both UO126 and PMA, was comparable and about 2.5 fold lower than the samples treated with just PMA showing that the activation of ERK had been inhibited. Phosphorylation is expressed in terms of median fluorescence intensity. The medians were calculated from the events versus log fluorescence intensity graphs obtained after flow cytometry.

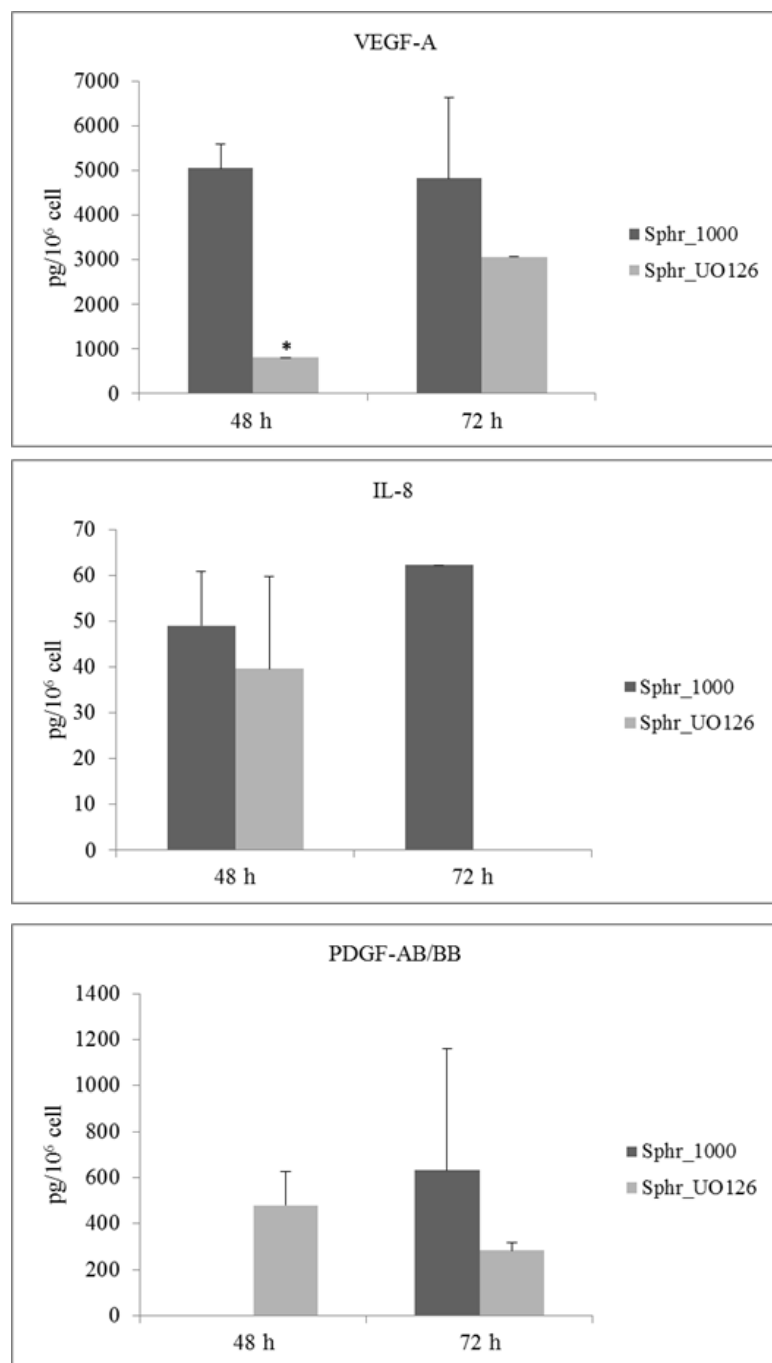


Figure 5.3. Cytokine production time profile of VEGF-A, IL-8 and PDGF-AB/BB production profile for UO126 treated spheroids and control at 48 and 72 hours. Data expressed in terms of mean+S.E.M. (Comparison between spheroid and UO126 treated spheroids *($p < 0.1$)).

Table 5.1. Cytokine production profile for 2D, spheroid, Scaffold A and Scaffold B at 48 and 72 hours.

	VEGF-A		IL-8		PDGF-B	
	48 h	72 h	48 h	72 h	48 h	72 h
2D	1628.317	1892.901	152.3571	329.0603	0	0
Scaff_A	6155.207	44390.41	1322.31	5154.005	85.36008	1231.592
Scaff_B	11213.5	62438.03	364.2693	1533.574	120.3453	872.0178
Sphr_1000	5052.464	4823.353	49.01284	62.27545	0	632.3353
	GRO		RANTES		PDGF-A	
	48 h	72 h	48 h	72 h	48 h	72 h
2D	0	962.5283	0	18.98719	79.14105	160.1662
Scaff_A	188.6312	815.468	6.303647	39.85839	322.5946	1166.971
Scaff_B	115.9056	312.5137	8.645778	23.15344	81.46921	274.4948
Sphr_1000	0	2150.898	70.41281	86.82635	0	35.92814

(Data expressed in terms of mean productivity (pg/ml))

CHAPTER 6

CONCLUDING REMARKS AND FUTURE STUDIES

The overall aim of this study was to establish the potential of cytokines as biomarkers of three-dimensionality and associated physiological relevance. As a first step, we tried to determine the optimal 3D microenvironmental composition that cells need to be provided with so that they can exhibit in vivo-like characteristics. In order to engineer a physiologically relevant 3D tissue model, the microenvironment was first deconstructed and the effect of each individual factor on cell behavior was determined. Using HepG2 cells as a representative for hepatic model, we analyzed the effect of each factor on albumin secretion and bile canalicular network development which served as a representative of complex physiologically relevant (CPR) outcomes. It was found that size or the spatial factor is most important of the three. If the size is too small, the tissue might not be complex enough to emulate in-vivo and if it is too large then hypoxia can manifest itself in the core of the tissue thereby decreasing the hepatic functions. Also, the physical property of the substrate does not significantly alter the behavior of the cells. Instead, it provides a physical constraint on the size of the tissue preventing it from getting hypoxic over time due to uncontrolled proliferation. Exogenous chemical coatings are also rendered redundant as the tissue develops its own ECM with time. Therefore the microenvironment provided by the PLLA micro porous scaffold developed in this study is optimal for developing a hepatic model with structural integrity and complex functionality.

The next step was to find a biomarker that could act as an early indicator of the complex physiological relevance of the model. Physiological relevance is developed late in culture and

requires different analysis techniques for determination. A biomarker would bring this to a common detection platform. Three cytokines (VEGF-A, IL-8 and PDGF-B) were found to not just upregulated in 3D compared to 2D but were also able to predict the most relevant out of the various 3D platforms. The early production of cytokines (48-72 hours) coupled with their secretion in cell culture supernatant made prediction of later development of CPR feasible. Also, the underlying mechanism for the upregulation of cytokines was determined in it was found that the Ras/Raf/ERK pathway is responsible.

Finally, a neuroblastoma based 3D model for neurodegenerative disease drug discovery was developed. Neural tissues lack a well-developed CPR outcome and so the first step was to determine a phenomenon that would happen in 3D and in vivo but not in 2D. It was found that calcium oscillation frequency is upregulated in traditional 2D cultures while it was found to be comparable to in vivo in our SH-SY5Y based spheroid 3D model. It was also found that cells in 3D proceeded towards a more differentiated state with time without the need for an exogenous differentiating agent.

Future aims should be as follows:

1. To adapt the PLLA based microporous scaffold to a HTS 96 and 384 well plate format using automated liquid handlers.
2. To generate in vivo cytokine profiles of HepG2 cells implanted in SCID mice and comparing them to those found in this study. This will finally validate them as biomarkers of three dimensionality and associated complex physiological relevance.
3. To extend the study to other tissue types to find out if these particular cytokines can serve as ubiquitous biomarkers or are just limited to hepatic tissues.

APPENDIX
PUBLISHED WORK

BIOMARKERS FOR SIMPLIFYING HTS 3D CELL CULTURE PLATFORMS FOR DRUG
DISCOVERY: THE CASE FOR CYTOKINES⁵

Abstract

In this review, we discuss the microenvironmental cues that modulate the status of cells to yield physiologically more relevant three-dimensional (3D) cell-based high throughput drug screening (HTS) platforms for drug discovery. Evidence is provided to support the view that simplifying 3D cell culture platforms for HTS applications calls for identifying and validating ubiquitous three-dimensionality biomarkers. Published results from avascular tumorigenesis and early stages of inflammatory wound healing, where cells transition from a two-dimensional (2D) to 3D microenvironment, conclusively report regulation by cytokines, providing the physiological basis for focusing on cytokines as potential three-dimensionality biomarkers. We discuss additional support for cytokines that comes from numerous 2D and 3D comparative transcriptomic and proteomic studies, which generally report upregulation of cytokines in 3D compared with 2D culture counterparts.

⁵ Lai, Y., Asthana, A., & Kisaalita, W. S. (2011). *Drug discovery today*, 16(7), 293-297.

NEURAL CELL 3D MICROTISSUE FORMATION IS MARKED BY CYTOKINES' UP-REGULATION⁶

Abstract

Cells cultured in three dimensional (3D) scaffolds as opposed to traditional two-dimensional (2D) substrates have been considered more physiologically relevant based on their superior ability to emulate the in vivo environment. Combined with stem cell technology, 3D cell cultures can provide a promising alternative for use in cell-based assays or biosensors in non-clinical drug discovery studies. To advance 3D culture technology, a case has been made for identifying and validating three-dimensionality biomarkers. With this goal in mind, we conducted a transcriptomic expression comparison among neural progenitor cells cultured on 2D substrates, 3D porous polystyrene scaffolds, and as 3D neurospheres (in vivo surrogate). Up-regulation of cytokines as a group in 3D and neurospheres was observed. A group of 13 cytokines were commonly up-regulated in cells cultured in polystyrene scaffolds and neurospheres, suggesting potential for any or a combination from this list to serve as three-dimensionality biomarkers. These results are supportive of further cytokine identification and validation studies with cells from non-neural tissue.

⁶ Lai, Y., Asthana, A., Cheng, K., & Kisaalita, W. S. (2011). *PloS one*, 6(10), e26821.

MICROTISSUE SIZE AND HYPOXIA IN HTS WITH 3D CULTURES⁷**Abstract**

The three microenvironmental factors that characterize 3D cultures include: 1) chemical or biochemical composition, 2) spatial (geometric 3D) and temporal dimensions, and 3) force and substrate physical properties. Even though these factors have individually been studied, their interdependence and synergistic interactions have not been well appreciated by bioscientists and tissue engineers. We make this case by illustrating how microtissue size (spatial) and hypoxia (chemical) can be used in the formation of physiologically more relevant constructs (or not) for cell-based high throughput screening (HTS) in preclinical drug discovery. We further show how transcriptomic/proteomic results from heterogeneously sized microtissues and scaffold architectures that deliberately control hypoxia can misrepresent and represent *in vivo* conditions, respectively. Finally, we offer guidance, depending on HTS objectives, for rational 3D culture platform choice for better emulation of *in vivo* conditions.

⁷ Asthana, A., & Kisaalita, W. S. (2012). *Drug discovery today*, 17(15), 810-817.

BIOPHYSICAL MICROENVIRONMENT AND 3D CULTURE PHYSIOLOGICAL RELEVANCE⁸

Abstract

Force and substrate physical property (pliability) is one of three well established microenvironmental factors (MEFs) that may contribute to the formation of physiologically more relevant constructs (or not) for cell-based high-throughput screening (HTS) in preclinical drug discovery. In 3D cultures, studies of the physiological relevance dependence on material pliability are inconclusive, raising questions regarding the need to design platforms with materials whose pliability lies within the physiological range. To provide more insight into this question, we examine the factors that may underlie the studies inconclusiveness and suggest the elimination of redundant physical cues, where applicable, to better control other MEFs, make it easier to incorporate 3D cultures into state of the art HTS instrumentation, and reduce screening costs per compound.

⁸Asthana, A., & Kisaalita, W. S. (2013). *Drug discovery today*, 18(11), 533-540.